PRACA DOKTORSKA

Jakub Sielewiesiuk

IChF PAN

Warszawa, czerwiec 2002

http://rcin.org.pl

PhD Dissertation

On Applications of Nonlinear Chemical Systems to Direct Information Processing.

by Jakub Sielewiesiuk

Under supervision of Doc. dr hab. Jerzy Górecki

Department of Chemical Dynamics

Institute of Physical Chemistry

Polish Academy of Sciences

Kasprzaka 44-52

01-224 Warsaw, Poland

Warsaw, June 2002

http://rcin.org.pl

Instytut Chemii Fizycznej
Biblioteka
P. A. N.
B 347/02

http://rcin.org.pl

To my wife, Anna.

http://rcin.org.pl

Acknowledgments.

I am very grateful to my supervisor, Doc. dr hab. Jerzy Górecki, for his friendly attitude, kind cooperation, developing discussions and remarkable help in my PhD studies. The work was proceeding fast mainly because of fresh ideas and constant motivation that I was receiving from him.

I would like to thank Dr. Bartlomiej Legawiec for the time he spent teaching me an effective implicit algorithm for numerical integration of reaction - diffusion equations. This algorithm was used extensively for the purpose of this work.

In September 1999 I visited the laboratory of Prof. Kenichi Yoshikawa at the Department of Physics, Kyoto University, Kyoto, Japan. This is where I found out about processing information with chemical reactors. I am thankful to Prof. Yoshikawa for inviting me there and supporting my visit financially.

Due to courtesy of Dr. Arno Muenster from the Institute of Physical Chemistry of the Wuerzburg University, Wuerzburg, Germany, I had the opportunity to make real (not numerical!) experiments with chemical waves in the Belousov - Zhabotinsky reaction and a unique chance to check some of the numerical results described in this work in a real system. Thank you, Arno. During my visit in Wuerzburg, Michael Seipel helped me a lot with all kinds of the laboratory equipment. Thanks, Michael!

Last but not least, I want to express my thankfulness to my wife, parents and parents-in-law, who were always supporting me, even if they had to tolerate me writing articles late at night or going away for conferences (and especially then).

http://rcin.org.pl

Yet More Acknowledgments (Financial).

This work was partially supported by KBN grant no. 4 T09A 062 22.

During my visit in Wuerzburg, Germany, in March 2002, I made some experiments on chemical signal frequency transforming on a passive barrier. The visit was fully supported by the European Science Foundation. I am especially grateful to Prof. F. W. Schneider and Prof. S. K. Scott for supporting my application and granting the money for this visit.

http://rcin.org.pl

Contents

http://rcin.org.pl

http://rcin.org.pl

Chapter 1

Introduction.

In the introductory section the author would like to convince the Reader that nonlinear chemical systems are interesting and worth studying, because they play a very important role in numerous phenomena occuring in living and nonliving nature. Moreover, this chapter contains examples of applications of nonlinear chemical systems to information processing of various types. Further, the basic facts about chemical excitable systems are given and possible ways of experimental realizations of such systems are described. This information enables to specify the aims of this work and determines the background and motivation for the research described in Chapter 2.

1.1 Why are nonlinear chemical systems important?

Nonlinear chemical reactions are of vital importance for all living creatures as well as for numerous events occurring in the nonliving world. If the reactions proceed in far from equilibrium conditions, they may lead to a variety of phenomena (for example oscillations, trigger waves, excitable pulses etc.),

http://rcin.org.pl

which contribute to and reveal in processes like morphogenesis ([1], p. 593), formation of static and dynamical spatial patterns ([1], p. 327-590) and the cycles, observed on all levels of organization of the living matter, from single cells to whole organisms ([1], p. 140). In particular, the existence of cycles can be explained by the oscillatory character of the underlying chemical reactions [1]-[4]. Together with the cyclic external perturbations (for example by the day/night cycle) they give grounds to so called "biological clocks" [1], ie. the mechanisms which control rhythms of different activities of the living creatures. Thus, the biological and biochemical systems provide a "natural" environment for nonlinear chemical reactions. Lots of examples can be found in any textbook on biochemistry (eg. [5]) or review reports on oscillations in chemical reactions (eg. [6, 7]). The majority of the biochemical cycles are very complicated, as there are thousands of complex reactions proceeding inside the living cells, most of which are catalyzed by enzymes and contain autocatalytic/nonlinear steps. Still, they provide a very attractive subject of research, because of their fundamental importance.

Oscillations have also been discovered in chemical reactions proceeding outside living organisms. Historically first well described example is known as the Bray reaction [8] (catalytic decomposition of H_2O_2, during which the rate of O_2 production oscillates). In early 1950s periodical changes of concentrations of reagents were observed by B. P. Belousov [9] in the reaction of oxidation of citric acid with bromate, catalyzed with cerium. This observation surprised the community of "orthodox" chemists. Further studies confirmed that the oscillations were really the result of the chemical reaction. Moreover, other examples of catalytic oxidation of organic substances with bromate were found [10, 11]. This group of reactions, called the Belousov - Zhabotinsky (BZ) reactions, became probably the most famous and most

http://rcin.org.pl

intensively studied type of oscillatory chemical reactions in the last 30 years. In the meantime, oscillations of concentrations of reagents were found in numerous catalyzed or non-catalyzed reactions (the references [2, 3, 4] give many examples of such systems).

All these reactions have attracted a lot of scientific interest and there are at least two reasons for that. First, these reactions are usually far simpler than enzymatic biochemical processes and yet qualitatively similar to them, as they reveal oscillations, excitability etc. Consequently, their cognition and description is much easier, but it gives grounds for better understanding of complex mechanisms of biochemical cycles. Second, in systems where chemical reactions appear together with the process of diffusion, a diversity of phenomena have been observed, which are interesting themselves, as a separate subject of studies. They include: chemical waves [10, 11], travelling fronts and excitable pulses (examples further in this work), Turing structures [12, 13, 14], pattern formation [1], [15]-[31], synchronization [32, 33, 34] and resonances [35, 36, 37], to name only a few. The patterns and structures appearing in such systems are not only beautiful [15], but they also influence processes of practical use, for example chemical reactions catalyzed by surfaces [38]-[41].

Experimental investigations of these phenomena are (in most cases) very complicated. To make them easier and - first of all - to understand them better, their proper theoretical (and mathematical) description is necessary. Thus, much effort was devoted to finding the models of the known nonlinear reactions and processes. As a remarkable part of my thesis concerns the phenomena occuring in systems based on the Belousov - Zhabotinsky reaction, it is worth mentioning that a commonly accepted mechanism of this particular type of reaction was proposed in 1972 by R. J. Field, E. Körös and R. M.

http://rcin.org.pl

Noyes [42]. It is known as the FKN mechanism of the BZ reaction. The FKN mechanism gave grounds for mathematical description of the system. Two simplified mathematical models, which are derived on the basis of the FKN mechanism, are the Oregonator model [43] and the Rovinsky - Zhabotinsky model [44, 45, 46]. They are very popular and frequently used in numerical studies of the BZ reaction.

The results obtained within mathematical models are characterized by a high level of generality. They can be applied to any systems, to which a given model is applicable. In particular, the oscillatory or excitable systems appear in a variety of fields apart from chemistry. Investigations of thermochemical, electrochemical or biochemical systems [47], pulses in heart tissues [48]-[52], optical systems [53], or even ecosystems (population growth, [1], p. 1-107, disease spread [1], p. 610) or economics are only a few examples.

On the other hand, models invented in other fields were adapted by chemists. A good example is the well known FitzHugh - Nagumo model (FH-N), originally developed to describe the propagation of pulses of excitation in nerve tissues [54, 55], as a simplification of the Hodgkin - Huxley model [56]. The FH-N model has been used for investigations of chemical systems for many years [57, 58].

Interesting applications of oscillatory or excitable chemical reactions include information processing (this area of research is briefly introduced in Section 1.3) or self-oscillating polymer gels [59]-[63], which may be used to construct artificial muscles.

Undoubtedly, the investigations of nonlinear chemical systems have become a fast developing field of science, with interdisciplinary character. In this field theoretical studies and computer simulations are equally important as experimental works and both approaches are complementary.

http://rcin.org.pl

1.2 Excitable systems.

This section contains basic information about chemical excitable systems. It includes the definitions of excitability, refractory time and explains how travelling excitable pulses may appear in spatially distributed systems. Further the response of an excitable system to periodic perturbations is discussed, using a very general and simple model. It is shown that the dependency of the frequency of excitations of the system on the parameters of perturbations may have a devil's-staircase-like form, due to non-zero refractory time of the excitable medium.

1.2.1 What is an excitable system?

A chemical system is called excitable if it has a stable stationary state of a special kind. The amplitude of a small perturbation of this state decays exponentially in time. However, if the amplitude of a perturbation exceeds a certain critical value, then during the evolution towards the stable state, the distance on the phase space between the time dependent state of the system and the stable state may become a few orders of magnitude larger than the distance between the stable state and the initial perturbation. Thus, perturbations with sufficiently large amplitude are amplified and the system returns to its steady state after much longer time than in the case of a small perturbation. The evolution after such perturbation forms a closed trajectory (so called excitation cycle) in the phase space. For a given type of perturbation one can introduce s_{min} as the minimum strength of perturbation which leads to systems excitation.

The excitable systems have another important and interesting feature: just after an excitation they become refractory with respect to consecutive

http://rcin.org.pl

perturbations. The minimal time after which the system can be re-excited is called refractory time (t_r). Of course, t_r depends on the strength of the system's perturbation s.

As far as the mathematical description of such systems is concerned, excitability means that the nullclines of equations describing the system, as well as the vector fields driving the variables, are qualitatively similar to those presented in Figures 1 and 2 (Section 2.1; the figures contain also examples of excitation cycles). Of course, any translations, rotations and mirror images of the presented nullclines together with the vector field are allowed. What is important is that the nullclines have only one common point, located near the extreme of the S-shaped curve, as well as the orientation of the vector field. If the nullclines intersect in three or more points (a system has two or more stable stationary states), then the excitable (non-monotonic) switching between the stable states may be observed ([1], p. 335). To describe an excitable system a set of minimum two autonomous differential equations (two-variable system) is necessary.

If the system is distributed in space and locally perturbed, then a local excitation may propagate (by diffusion) to the neighboring areas, while the points initially excited relax to the stationary state. Thus, for the proper choice of parameters travelling pulses may appear in the system (one pulse per one supercritical perturbation). The pulses are stable. After initiation they develop into stationary forms, which do not depend on the method of initiation.

The refractory time of the medium limits from above the frequency at which excitable pulses may appear at a certain point of a spatially distributed system. Once a pulse has passed through a part of the system, then at least the time t_r is necessary before another pulse would be able to propagate

http://rcin.org.pl

in this region. If the next pulse arrives earlier it cannot propagate and disappears. The situation here is similar to burning the grass: once the grass has been burnt it needs some time to grow again before it can be burnt.

1.2.2 Devil's-staircase-like response in a "naive" model of a periodically perturbed excitable system.

Let us consider an excitable system which is periodically perturbed. Observing consecutive excitations of the system and comparing their frequency with the frequency of perturbations one may see that the frequency of excitations is equal to the frequency of perturbations, or lower. The difference between the frequencies of perturbations and of successful excitations can emerge in every excitable system, just because of the non-zero refractory time. If the time shift between consecutive perturbations is shorter than the refractory time of the perturbed medium (for a given strength of perturbations), then some of the perturbations have to occur at moments, when the system is in the refractory state and cannot be excited. Thus, for a high frequency of perturbations, not all of them lead to excitation of the system.

Let us consider an excitable system characterized by the refractory time t_r, schematically shown in Figure 0A. The horizontal axis of Fig. 0A presents the strength of the perturbation, given in s_{min} units (s_{min} is the minimum strength of perturbation which leads to system's excitation). The vertical axis gives the refractory time (in arbitrary units). Let us take into account two successive perturbations, occurring at times *0* and *t*. Let us fix the strength s of these perturbations. At time 0 every perturbation characterized by s ($s/s_{min}>1$) excites the system. A successful excitation by the second perturbation depends on the values of t and s. The line $t_r(s)$ in Fig. 0A corresponds to the minimal time shift after which the second perturba-

http://rcin.org.pl

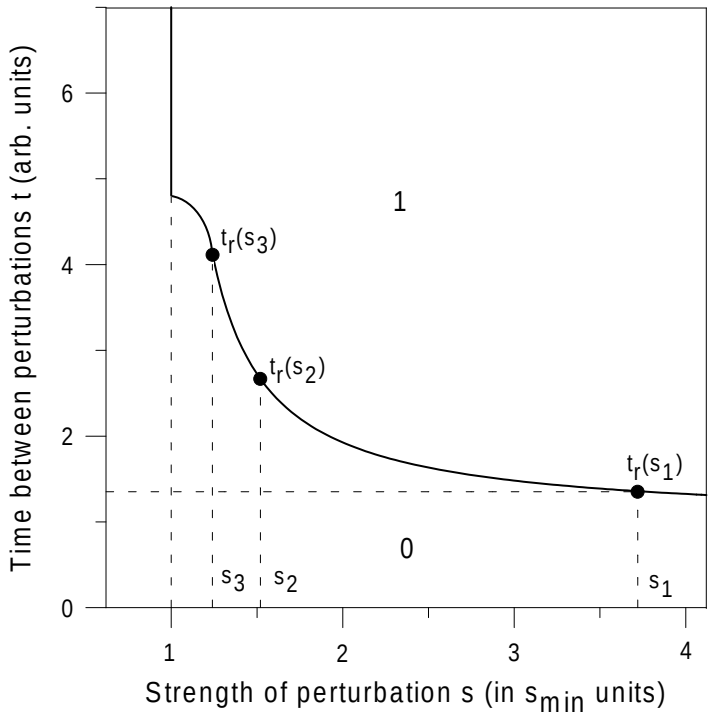

Figure 0A. The "naive" model of a perturbed excitable system. The probability that the second perturbation excites the system is shown as a function of the strength of perturbation s in s_{min} units (x - axis) and the time separating perturbations t (arbitrary units, y - axis). The set of parameters for which the second perturbation excites the system is located above the line. For a given s the line separating excited by the second perturbation from unexcited ones shows $t_r(s)$. Note that for times $t<t_r$ and for $s/s_{min}<1$ the system cannot be excited.

http://rcin.org.pl

tion of the strength s is able to excite the system. Thus, if the perturbation is strong enough, then re-excitation occurs when $t>t_r$. The shape of the $t_r(s)$ dependency shown in Fig. 0A seems quite natural, for the following reasons: First, if s is too small ($s/s_{min}<1$), the system is not excited by the second perturbation, nor by the first one, no matter how large is the time shift between them. Second, after a successful excitation the system relaxes towards the steady state. It can be excited again if it has reached the appropriate neighborhood of the steady state before the second perturbation occurs. This neighborhood is larger (and reached faster) for stronger perturbations. Consequently, for $s/s_{min}>1$ one should expect that t_r gets smaller when perturbation's strength increases. Third, even if the perturbations are very strong, the system cannot be excited if it is too far from the steady state. As a consequence, the curve $t_r(s)$ becomes less and less steep for larger s.

For a simplified analysis let us assume that a state of the system is not significantly changed after an unsuccessful perturbation and the probability of excitation shown in Fig. 0A remains valid if a periodic sequence of perturbations is considered. Now t denotes the time from the last perturbation which excited the system. Let us consider a periodic sequence of perturbations at times $k\cdot t_p$, $k\in N$, characterized by a fixed strength s. It is easy to see that if $t_p>t_r(s)$, then each perturbation excites the system. If $t_r(s)/2\leq t_p<t_r(s)$ then every second of them excites the system, if $t_r(s)/3\leq t_p<t_r(s)/2$, then every third perturbation does it and so on. Plotting the firing number f (ie. the ratio between the frequencies of excitations and perturbations) as a function of t_p (Figure 0B), one obtains a plot similar to devil's staircase [64]. Another staircase-like plot can be obtained by representing the firing number as a function of s for a fixed t_p (cf. Figure 0C).

Of course, the "naive" model that has just been discussed is extremely

http://rcin.org.pl

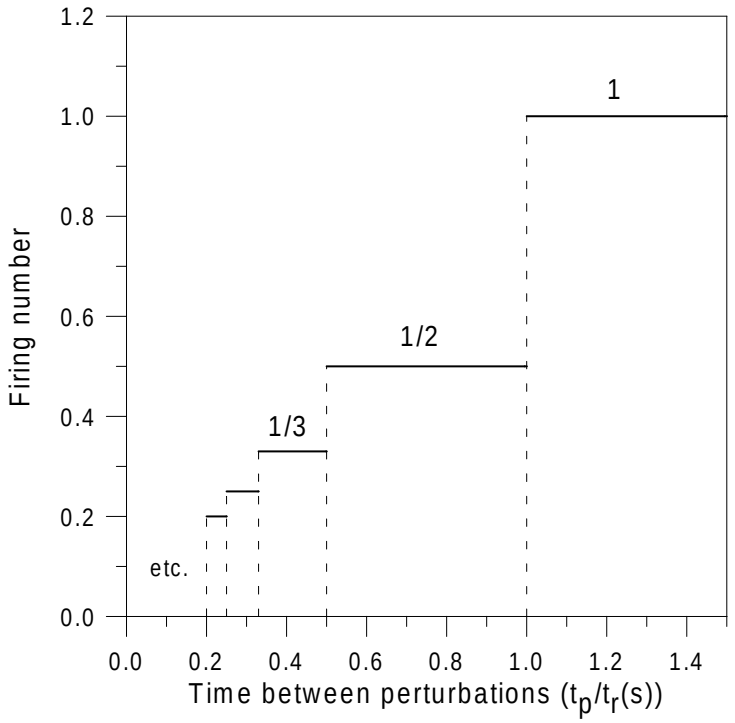

Figure 0B. The firing number as the function of the time interval between consecutive perturbations of the system (in $t_p/t_r(s)$ units), for a fixed strength of perturbation s. This result has been obtained for the "naive" model of a perturbed excitable system.

http://rcin.org.pl

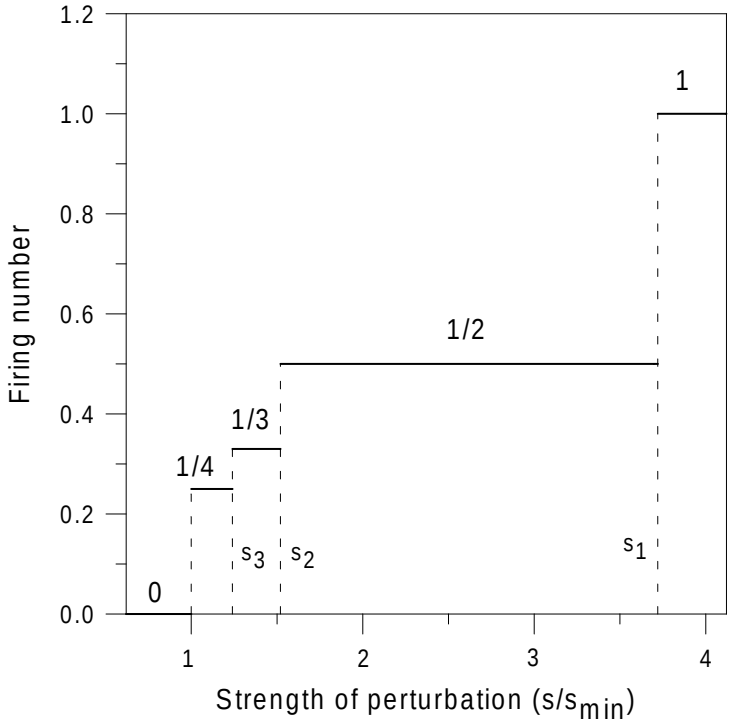

Figure 0C. The firing number as the function of the strength of perturbation s, for a fixed t_p. This result has been obtained for the "naive" model of a perturbed excitable system.

Instytut Chemii Fizycznej PAN BIBLIOTEKA

http://rcin.org.pl

crude, but it predicts that devil's-staircase-like dependence of firing number on the period of perturbations should be widely observed in excitable systems. It is true indeed. Such dependence can be found in a number of experiments concerned with periodic perturbations of a homogeneous excitable system, the results of which were published by M. Marek and collaborators [65]-[68]. Another staircase-like dependence of the firing number was observed by A. Toth, V. Gaspar and K. Showalter in spatially distributed excitable systems linked with a capillary tube [69]. The excitable waves were generated in one system and they might excite the other one via reagents' transport in the capillary. In this experiment the diameter of the capillary controlled the strength of perturbation. If it was small, the refractory time of the perturbed system was much longer than the refractory time in the system where waves were originally generated. As the result only a fraction of generated waves excited the system after passing through the capillary and the firing number as the function of entering wave period had a devil's-staircase-like dependence (cf. Fig. 6 in [69]). Similar phenomenon was observed by K. Suzuki, T. Yoshinobu and H. Iwasaki [70] in the ferroin catalyzed BZ system. In their experiment a train of excitable pulses, travelling on a ferroin covered membrane, arrived at a gap (a narrow stripe of area without ferroin). The frequency of pulses on the other side of the gap depended on the gap's width and was a certain fraction of the frequency of the arriving train of pulses. Moreover, recent studies indicate that it is possible to excite a spatially distributed excitable system by a local periodic modulation of one of its parameters [71]. Although all the perturbations are subcritical (ie. a single perturbation of that kind never leads to an excitation cycle), an appropriately tuned frequency of periodic perturbations goes in resonance with the damped oscillations around the stable fixed point and leads to regular

http://rcin.org.pl

excitations of the system [71]. Also in this case the firing number (the ratio: number of excitations to number of perturbations in the same time interval) as a function of the modulation frequency reveals a devil's-staircase-like structure.

http://rcin.org.pl

1.3 Information processing by chemical systems.

The idea of information processing with purely chemical devices is attractive for both scientific community and leading hi-tech companies. Two most promising ways of constructing such devices come from the molecular chemistry approach (the information is processed by individual molecules) [72] and from the nonlinear chemical reactions.

Logical functions and other kinds of information processing tasks were implemented in homogeneous (stirred) reactors, in which a reaction possessing two or more stable stationary states proceeds. Once a logical value is assigned to all of these states, the reactors can be applied to processing information [73]. A good example is the idea of Okamoto and collaborators [74], who proposed to use a cyclic enzyme system, in which two reactions are coupled by a shared reagent. Such system can be controlled (or stimulated) by the supply of the substrate precursors of the two main reactions (considered as the two "input signals"). The level of the shared reagent, which has two stable stationary states, corresponds to the "output signal". This system behaves like a neural cell and because of that it is called a "biochemical neuron". The homogeneous reactors coupled by diffusion can be arranged in networks, and used eg. for pattern recognition [75] or building multilayer biochemical neuron networks, which may perform tasks of a high complexity [74, 76].

Two dimensional photosensitive BZ systems are also suitable for direct image processing. The BZ system should be prepared in the oscillatory regime. In this regime the color of the BZ solution depends on the point of the limit cycle and changes periodically in time. The period of oscillations can

http://rcin.org.pl

be influenced by external illumination. In particular, if an image is projected onto such system, then a chemical "representation" of the image is produced in the system, as the period changes from point to point, according to the light intensity. Once the light is switched off, different areas of the system start to evolve towards the new limit cycle with different initial conditions. Because of that the initial variances in illumination of neighboring areas may be increased (contrast enhancement) or decreased (contrast reduction) during the evolution. When the phase of the limit cycle changes by π, then the negative image is obtained. Alternatively, if a high intensity of light is used, then in some regions (the brightest parts of the image) the system may be switched from the oscillatory to excitable regime. This regime may be applied to determining or smoothing contours of the originally projected picture [77, 78, 79].

Another interesting application of a photosensitive BZ system, presented by Rambidi and Yakovenchuk [80], is finding the shortest path in a labyrinth. The authors of [80] project the picture of the labyrinth onto a properly prepared Ru catalyzed system and then register the consecutive stages of chemical wave spreading throughout the image of the labyrinth's pathway with a video camera. The images are processed by a computer, using a special iterative procedure which enables to establish the shortest path between given starting and target points.

Another class of chemical devices which process information utilize the fact that a chemical pulse, which can be produced in excitable or oscillatory media, carries information. The area of a high concentration of a particular reagent may be considered as corresponding to the logical "true" state, while the area of a low concentration - to the logical "false". Alternatively, a pulse present in a selected part of a system may corresponds to the logical "1"

http://rcin.org.pl

state and if it is not there - it implies the logical "0". The travelling pulses or regular trains of such pulses are called "chemical signals". On such signals one can perform operations analogical to electronic ones. Using this idea the chemical reactors which work as the basic logical gates (AND, OR, NOT) were invented and constructed in real experiments [81, 82]. They utilize the BZ reaction proceeding in capillary tubes [81] or on a catalyst loaded membrane [82].

It has been found that a chemical system may perform more complex logical operations if it is inhomogeneous and composed of "active" regions, in which reactions occur, and "passive" areas, where some of the reagents are absent and so only a part of reactions proceed there. In practice it means that an immobilized catalyst is inhomogeneously distributed in space. The passive areas are those which do not contain catalyst. In such systems a "chemical diode", which conducts travelling pulses only in one direction was constructed [83]-[86] (the structure and functioning of the chemical diode is presented in Section 2.4.7). The chemical diode was then used as a vital component of successively proposed logical gates, coincidence detectors [86] and memory cells, which can be written, read and erased [86, 87]. Most of the studies concerning such reactors present theoretical (numerical) results [84]-[87], but there are also a few experimental works [83, 87]. Of course, information processing devices of this kind are far slower than silicon ones. However, they may be competitive to traditional "chips" in different fields, such as new kinds of "intelligent" materials or medicaments.

http://rcin.org.pl

1.4 Experimental methods.

The numerical results presented in this thesis concern two dimensional reactors, in which BZ-type reactions proceed. The considered reactors consist of active areas, containing the catalyst and passive areas, without catalyst. This section provides basic information about obtaining such systems in real chemical experiments.

Typical reactions used in such experiments include the ferroin catalyzed BZ reaction ([19, 70, 81, 82, 83], [87]-[95]) or several types of photosensitive BZ reactions (catalyzed with Ce, Ru or Mn [78], [96]-[100]).

The active areas of the system, where the reaction can proceed, are covered with an immobilized catalyst. In case of ferroin, it may be fixed on thin cellulose nitrate or polysulfone membranes just by pouring the membranes into appropriate solutions (the "classical" description of ferroin's fixation on membranes can be found in [89]). Other cation-exchange membranes [70, 82, 88, 90, 91, 93, 94], [101]-[105] or mesoporous glass [83] may also be used. The important question is how to obtain catalyst-free pattern on an otherwise catalyst-covered membrane. In simplest cases the solution containing ferroin can be put on desired areas of a membrane with a fiber-pen [89] or printed with an ink-jet computer printer [82, 101, 102, 106], which provides better accuracy.[1] The most accurate technique of fabrication of catalyst micropatterns has been recently developed by K. Suzuki, T. Yoshinobu and H. Iwasaki [70, 103, 104]. In their method a membrane is first covered with a photoresist layer on which a mask containing the desired pattern is printed. After exposure to light the membrane is developed and immersed in a ferroin solution. The ferroin molecules can then stick only to the parts of

[1] Printing the catalyst with an ink-jet printer is also used in completely different systems, eg. when desired patterns for metal deposition on a surface are needed [107].

http://rcin.org.pl

the membrane that were previously exposed to light. As the last step of the process the photoresist is removed by ethanol. The photolitographic technique enables to obtain catalyst-free (passive) stripes of the width of $50\mu m$ [70]. On the other hand, it enables to control catalyst-filled areas with $20\mu m$ precision [103]. If a photosensitive BZ reaction is used, the desired pattern can be just projected onto the system by using a proper mask [78, 87]. In this case the reaction proceeds in the dark areas and it is inhibited in the illuminated ones (so they become passive).

Travelling waves or pulses of excitation in such systems may be initiated very easy by touching the membrane with a silver wire [70, 82, 89, 91, 93], with a glass tip [105] or just by dropping the activator from a micropipet at the desired point of the system [108]. More sophisticated methods include the electrochemical method, in which a silver wire electrode present in a system is positively biased for a short moment (eg. $100msec$), thus producing a chemical pulse or a wave [69, 70]. The pulses may also be initiated with an external electric field [109] or with a laser [94, 98]. In order to obtain a train of pulses with a constant frequency it is also common to use a rotating spiral, located in the appropriate part of the system [70, 99].

http://rcin.org.pl

1.5 The aims of this work.

The methods of direct information processing by means of chemical reactors are intensively investigated, as they seem very promising. High hopes are associated with two dimensional reactors composed of active and passive areas, in which the information is carried by travelling pulses of excitation. Quite a large number of such reactors have already been proposed, but most of them come as the result of purely theoretical/numerical studies and only a few have been tested experimentally. Consequently, the aims of this work are the following:

1. Numerical calculations oriented on finding the new geometries of reactors (ie. distribution of active and passive areas in space), which might be applied to direct processing of chemical signals. The structures of the cross junction (Section 2.3) and the simple passive barrier (Section 2.4) have been proposed.

2. Theoretical investigation of the phenomena which occur in proposed signal processing reactors. It has been found that the cross junction may work as a logical AND gate, a time coincidence detector of two pulses and a switch of the direction of propagation of a pulse (Section 2.3). The passive barrier has the ability of systematical elimination of pulses from a train. Consequently, it can be used as a transformer of frequency of regular trains of pulses (Section 2.4).

3. Suggesting the experiments, in which these structures and phenomena would be tested, thus proving the correctness or revealing the incorrectness of models used in numerical studies. Experiments on frequency transforming by a passive barrier have been made (Section 2.7).

http://rcin.org.pl

Their results confirm the numerical predictions and the correctness of the Rovinsky - Zhabotinsky model of the ferroin catalyzed Belousov - Zhabotinsky reaction used here (the model is described in Section 2.1.2).

4. Using the simple signal processing elements the properties of which are already known, I can suggest more complex information processing reactors, like for example a reactor that is able to add two given numbers together (Chapter 3).

http://rcin.org.pl

Chapter 2

Results.

2.1 The models.

The major part of my work has been dedicated to theoretical studies of propagation of excitable pulses in two dimensional reactors, whose geometry enables processing of chemical signals in the form of single travelling pulses or regular trains of such pulses. The investigations have been carried out by numerical integration of reaction - diffusion equations describing the time evolution of variables appearing in selected models. Most of the results have been obtained for the FitzHugh - Nagumo type model (FH-N) or the Rovinsky - Zhabotinsky model (R-Z). The variables of the latter model are directly related to concentrations of chemical spices in the ferroin catalyzed Belousov - Zhabotinsky reaction. Both models are presented below.

2.1.1 The FitzHugh - Nagumo model.

The FitzHugh-Nagumo type model used in this work [54, 55, 86] consists of two variables: u and v. The time evolution of their values is given by the

http://rcin.org.pl

following set of equations:

$$\tau \frac{\partial u}{\partial t} = -\gamma[ku(u-\alpha)(u-1)+v] + D_u \nabla^2 u \tag{2.1}$$

$$\frac{\partial v}{\partial t} = \gamma u \tag{2.2}$$

This model is relatively easy for theoretical and numerical analysis, as it contains only the polynomials of the third order. It was originally developed to describe the propagation of pulses of excitation in nerve tissues [54, 55], as a simplification of the Hodgkin - Huxley model [56]. The FH-N model has a very good biochemical background (presented in a clear way eg. in [110]). The crucial disadvantage of this model is that its variables do not represent directly concentrations of a known reaction scheme, so the results obtained within this model cannot be regarded as a quantitative basis for a chemical experiment.[1] Nevertheless, the model has been used as generic model for nonlinear chemical phenomena [57], because its dynamics reflects the basic features of an excitable system.

The variables u and v in Eqs. (2.1-2.2) can be either negative or positive. One may say that Eqs. (2.1-2.2) describe the time evolution of a "chemical" system with two components. One of them (described by u) is the "activator" (because it may speed up its own production) and the other (described by v) is the "inhibitor" (because it slows down the production of u). In this sense the values of u and v are related to the "concentrations" of the corresponding "reagents". In the spatially distributed system it is assumed that the "inhibitor" is always immobilized (it never diffuses). The system (2.1-2.2) is excitable for the following parameters describing reactions: γ=1, τ=0.03, k=3.0, α=0.02 [86]. The nullclines of Eq. (2.1) without the diffu-

[1] Although there was a successful attempt to propose a microscopic reaction scheme corresponding to this model [58].

http://rcin.org.pl

sion term (solid line) and Eq. (2.2) (dashed vertical line identical with the v axis) for these values of parameters are shown in Figure 1. Solid and dashed arrows indicate the vector fields driving u and v respectively. The nullclines have only one common point u=v=0, indicating the stationary homogeneous solution of Eqs. (2.1-2.2). The dotted line with symbols shows a possible evolution of the system in the phase space after a sufficiently large perturbation. This is where the excitability of the system can be observed (note, that the initial perturbation does not decrease, but at first it increases).[2] The diffusion coefficient of the "activator" D_u equals 0.00045 because for this value well defined pulses propagate in the system [111, 112]. Areas of the studied FH-N systems where Eqs. (2.1-2.2) hold are called excitable or active areas.

In some parts of considered structures the "inhibitor" v is absent, no reactions occur and only diffusion of the "activator" u is possible. These areas of the FH-N systems are called diffusion or passive areas. Within them the time evolution of u and v is described by the following set of equations [86]:

$$\tau \frac{\partial u}{\partial t} = D_u \nabla^2 u \tag{2.3}$$

$$v = 0 = const. \tag{2.4}$$

where k=0.03 and D_u=0.00045 [111, 112], as previously. In all the studied structures free diffusion of the "activator" u between active and passive areas is assumed.

[2]The response of the system described by Eqs. (2.1-2.2) without the diffusion term to a perturbation of v_i=-0.2 is illustrated in Fig_01a.htm on the CD-ROM (folder *Figures*). Response of the same system to two consecutive perturbations is presented in Fig_01b.htm and Fig_01c.htm. In the case of Fig_01b.htm the second perturbation comes too early after the initial one and consequently is disappears almost instantly. In Fig_01c.htm the second perturbation occurs a moment later and the system is excited again. In both cases the second perturbation has the same amplitude of (Δu=0.4, Δv=0.0)

http://rcin.org.pl

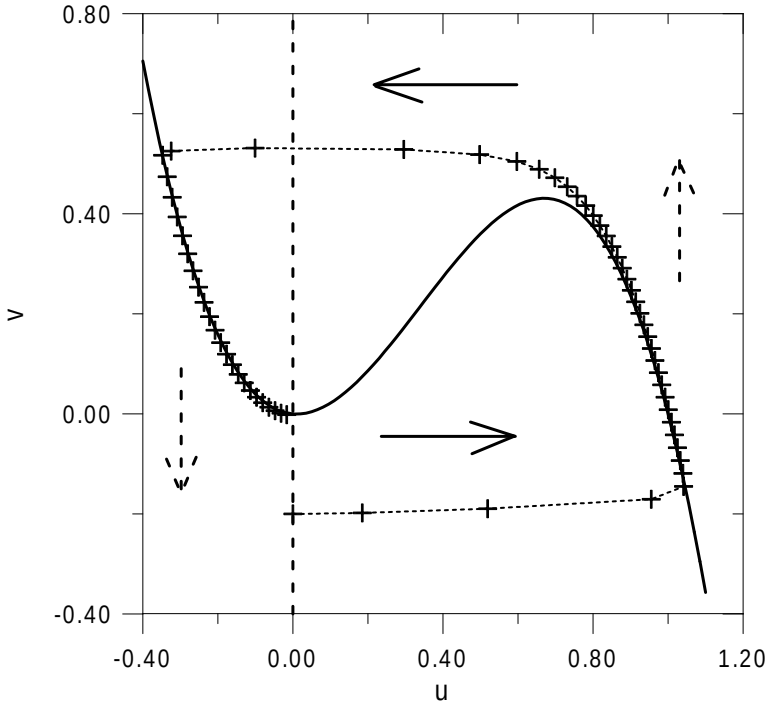

Figure 1. The nullclines of Eq. (2.1) without the diffusion term (solid line) and Eq. (2.2) (dashed vertical line identical with the v axis) for the values of parameters given in Section 2.1.1. Solid and dashed arrows indicate the vector fields driving u and v respectively. The nullclines have only one common point u=v=0, indicating the stationary homogeneous solution of Eqs. (2.1-2.2). The dotted line with symbols shows the evolution of the system in the phase space after a sufficiently large perturbation (v_{ini}=-0.2).

http://rcin.org.pl

One may notice that the number of parameters used in Eqs. (2.1-2.4) may be reduced without losing generality, which is true, as Eq. (2.1) can be divided by τ and then only four independent parameters remain in the model. On the other hand, the form of the equations presented above is very convenient for manipulations, because k and α influence the threshold value of perturbation exciting the system, D_u controls the propagation of excitable pulses, τ corresponds to different time scales of the dynamics of "activator" and "inhibitor" and γ is just a "switch" between active and passive areas (γ=1 for the active medium and 0 for the passive one).

2.1.2 The Rovinsky - Zhabotinsky model.

Another important model used in my calculations is the Rovinsky - Zhabotinsky model [44, 45] of the ferroin catalyzed Belousov - Zhabotinsky reaction [10]. This model is based on the Field - Körös - Noyes mechanism [42]. To avoid duplicating information, only the most important facts about this model are included in this section, because the variables, coefficients and details about scaling can be found in Appendix A, together with the detailed step-by-step derivation of the reaction - diffusion equations from the chemical reaction scheme.

The model consists of two variables: x and z, which correspond to dimensionless concentrations of the activator x ($HBrO_2$) and of the oxidized form of catalyst z ($Fe(phen)_3^{3+}$), where the scaling is given by Eqs. (A24-A25) in Appendix A. In the active regions, which contain the catalyst, the time evolution of the concentrations of x and z is described by Eqs. (2.5-2.6):

$$\frac{\partial x}{\partial \tau} = \frac{1}{\epsilon}[x(1-x) - (2q\alpha\frac{z}{1-z} + \beta)\frac{x-\mu}{x+\mu}] + \nabla_\rho^2 x \tag{2.5}$$

$$\frac{\partial z}{\partial \tau} = x - \alpha\frac{z}{1-z} \tag{2.6}$$

http://rcin.org.pl

In the passive regions, without catalyst, the concentrations of x and z evolve according to Eqs. (2.7-2.8):

$$\frac{\partial x}{\partial \tau} = -\frac{1}{\epsilon}[x^2 + \beta\frac{x-\mu}{x+\mu}] + \nabla^2_\rho x \tag{2.7}$$

$$z = 0 = const. \tag{2.8}$$

α, β, μ and ϵ are scaled coefficients defined by Eqs. (A28-A31) in Appendix A. τ and ρ are dimensionless variables describing time and distance respectively. Their connection with physical time and distance is given by Eqs. (A26-A27), Appendix A.

Eqs. (2.5-2.8) correspond to a typical experimental situation in which the catalyst is immobilized on a membrane, whereas the activator is in the solution and it can diffuse (compare eg. [19, 70, 81, 82], [87]-[91], [93, 94, 95, 102, 113, 114]).

In numerical calculations for the BZ system the following values of parameters (the same as considered in [44, 45, 112], [115]-[118]) have been used: A=0.02 M, B=0.2 M, C=0.001 M, k_1=$100M^{-2}/sec$, k_4=$1.7\cdot10^4 M^{-2}/sec$, k_5=$10^7 M^{-2}/sec$, k_7=$15M^{-2}/sec$, K_8=$2\cdot10^{-5}M/sec$, k_{13}=$10^{-6}sec^{-1}$, q=0.5. The corresponding values of scaled parameters α, β, ϵ, μ are $0.017\cdot$ h_0^{-2}, $0.0017\cdot$ h_0^{-1}, 0.1176 and 0.00051 respectively, where h_0 denotes the Hammett acidity function, describing the effective proton concentration [46, 119, 120] and it is expressed in *mol/l*. For these values of parameters the system becomes excitable if h_0<0.9899 [118]. Here h_0=0.5 has been used.

For these values of parameters Eqs. (A26-A27) give the following constants which transform dimensionless time (τ) and distance (ρ) into physical units:

$$t[sec] = 8.5 \cdot \tau \tag{2.9}$$

$$r[cm] = 2.915 \cdot \sqrt{D_X/[cm^2/sec]} \cdot \rho \tag{2.10}$$

http://rcin.org.pl

where t and r are physical time and distance. Consequently, similar transformation constant connecting the dimensionless (ν) and physical (v) velocities of a pulse can be calculated:

$$v[cm/min] = 20.58 \cdot \sqrt{D_X/[cm^2/sec]} \cdot \nu \tag{2.11}$$

In the last two equations D_X is the diffusion constant of the activator X. However, this constant strongly depends on the medium the reactions proceed in. In the aqueous solution it is of the order of $10^{-5} cm^2/sec$ [45, 46, 84, 118, 119] whereas for a reaction in a gel it may be reduced by two orders of magnitude [61, 84]. In order to make the results more general, all distances and velocities concerning the R-Z model are presented in double form: dimensionless and as the function of the ratio of diffusion constants $\frac{D_X}{D_{X_0}}$, where the value of D_{X_0} corresponds to a particular choice of the diffusion constant: D_{X_0}=$1 \cdot 10^{-5} cm^2/sec$ [45, 118]. The second number allows to see more clearly the real spatial and temporal scale of the considered processes.

The nullclines of Eq. (2.5) without the diffusion term (solid line) and Eq. (2.6) (dashed line) for these values of parameters are shown in Figure 2. The dotted line with symbols shows a possible evolution of the system in the phase space after a sufficiently large perturbation.[3]

The coordinates of intersection of nullclines in Fig. 2 give the stationary

[3]Like in the case of the FH-N model, there are additional animated figures illustrating nullclines of the system described by Eqs. (2.5-2.6) without the diffusion term (CD-ROM, folder *Figures*). The response of such a system to a perturbation of x_i=0.1 is illustrated in Fig_02a.htm Response of the same system two consecutive perturbations is presented in Fig_02b.htm and Fig_02c.htm. In the case of Fig_02b.htm the second perturbation comes too early after the initial one and consequently is disappears almost instantly. In Fig_02c.htm the second perturbation occurs a moment later and the system is excited again. In both cases the second perturbation has the same amplitude of (Δx=0.1, Δz=0.0)

http://rcin.org.pl

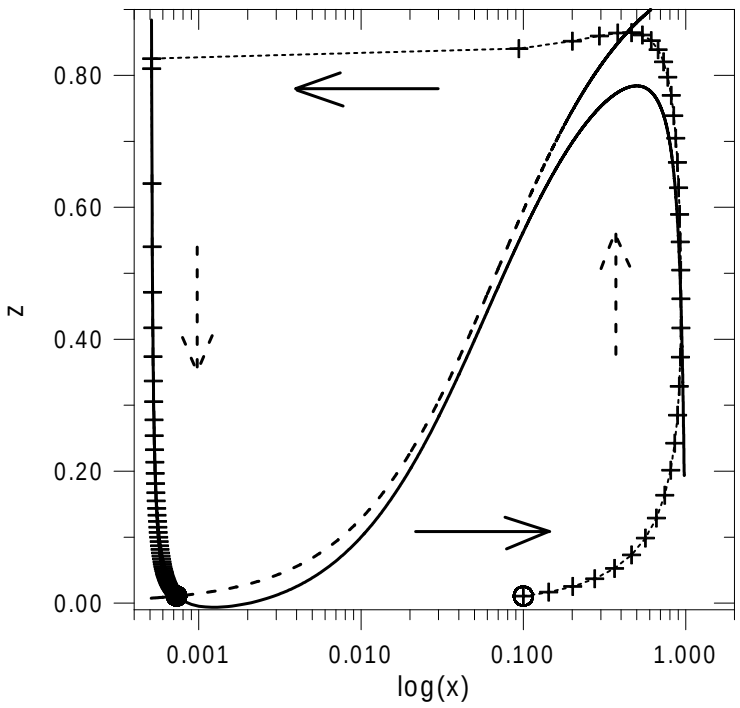

Figure 2. The nullclines of Eq. (2.5) without the diffusion term (solid line) and Eq. (2.6) (dashed line) for the values of parameters given in Section 2.1.2. Solid and dashed arrows indicate the vector fields driving x and z respectively. The nullclines have only one common point (x_{sa}=7.283·10^{-4}, z_{sa}=1.060·10^{-2}) indicating the stationary homogeneous solution of Eqs. (2.5-2.6). The dotted line with symbols shows the evolution of the system in the phase space after a sufficiently large perturbation (x_{ini}=0.1).

http://rcin.org.pl

values of x and z in the active (excitable) area. They read:

$$x_{sa} = 7.283 \cdot 10^{-4} \tag{2.12}$$

$$z_{sa} = 1.060 \cdot 10^{-2} \tag{2.13}$$

(which is the stationary solution of Eqs. (2.5-2.6)). The stationary concentrations in the passive area (the stationary solution of Eqs. (2.7-2.8)) are given by:

$$x_{sp} = 5.099 \cdot 10^{-4} \tag{2.14}$$

$$z_{sp} \equiv 0 \tag{2.15}$$

Free diffusion of the activator x is assumed between active and passive areas.

http://rcin.org.pl

2.2 Propagation of single pulses of excitation through a passive gap.

I. Motoike and K. Yoshikawa considered two active areas separated by a stripe of the passive one [86]. A pulse of excitation propagating in one of these areas may excite the other active area if the passive stripe is narrow. The maximum width of the passive stripe for which such excitation still occurs is called the penetration depth. They found [86] that the penetration depth depends on the geometry of the junction and on the direction of propagation of incident pulses and it is maximal for plain pulses travelling in the direction perpendicular to the barrier. In [86] Motoike and Yoshikawa describe their results obtained with an Euler explicit method for the FitzHugh - Nagumo model, the same and with the same values of parameters as considered here. According to [86], if the penetration depth for a single pulse with the wave vector perpendicular to the barrier is denoted by $d_{c,FH-N}$, then for a pulse travelling parallel to the barrier it is only $0.94 \cdot d_{c,FH-N}$. This result has been confirmed for the purpose of this study with an implicit method based on the Crank - Nicolson discretization of the Laplace operator [121].[4] It has been found [86, 116] that $d_{c,FH-N} \approx 0.163$.

Similar calculations have been carried out for the Rovinsky - Zhabotinsky model [115, 116]. The penetration depth for a single pulse travelling in the direction perpendicular to the barrier is $d_{c,R-Z} \approx 3.295$ $(0.03037 \cdot \sqrt{\frac{D_X}{D_{X_0}}} cm)$, while for a pulse travelling parallel to the barrier it is about 3.287 $(0.03029 \cdot \sqrt{\frac{D_X}{D_{X_0}}} cm)$, which is $0.995 \cdot d_{c,R-Z}$. Note, that this result implies, that the penetration

[4] This method has been used to obtain most of the results presented in this work; if other algorithms have been applied, it is indicated in the text. The formulas corresponding to implicit integration schemes mentioned here as well as the explicit Euler method can be found in Appendix B.

http://rcin.org.pl

depth for "perpendicular" and "parallel" pulses differ by 0.5% only, while for the FitzHugh - Nagumo model it is 6%. Creating a stripe of passive field with higher than 0.5% accuracy in its width is a hard, but achievable task from the experimental point of view. One may apply for example the photolithographic methods for the introduction of catalyst [70, 103, 104].[5]

[5]At first the BZ system was studied for h_0=0.97. The penetration depths for pulses travelling perpendicularly or parallel to the passive stripe for this value of h_0 are almost the same, as they differ by less than 0.05%. Therefore it seems to be very difficult to make a passive stripe impenetrable for a "parallel pulse" and penetrable for a "perpendicular" one in the laboratory. Decrement of h_0 stabilizes the stationary solution of Eqs. (2.5-2.6) [115]. This results in a faster relaxation of the active medium and remarkably increases the asymmetry in the penetration depth. From the chemical point of view smaller h_0 corresponds to lower concentration of H^+ in the system. The results given in text have been obtained for h_0=0.5.

http://rcin.org.pl

2.3 The cross junction and its properties.

Having in mind the results of the previous section (Section 2.2) concerning the FH-N model one may notice that a layer of the width d_{FH-N} ($0.94 \cdot d_{c,FH-N} < d_{FH-N} < d_{c,FH-N}$) is transparent for a pulse propagating perpendicularly, but impenetrable for a pulse propagating parallel to it.[6] This observation opens the way to construct a simple coincidence detector of chemical signals.

Let us consider a plain (two dimensional) system with geometry shown in Figure 3, where the brighter areas correspond to the active (excitable) medium and the dark stripes - to the passive (diffusion) one. The excitable and diffusion areas in the device shown in Fig. 3 form two perpendicular "channels", in which travelling pulses can propagate. To simplify the description that follows let us assume that the excitable areas of our cross junction are numbered as in Fig. 3.

If the width of the stripes of the diffusion field d_{FH-N} is between $0.94 \cdot d_{c,FH-N}$ and d_c then the cross junction presented in Fig. 3 may have interesting properties. It can be expected that:

i A single pulse propagating in one of the channels is able to propagate along its own channel, but it cannot move "sideways" (because it cannot cross the stripe of the diffusion field parallel to the direction of its motion, as $d_{FH-N} > 0.94 \cdot d_{c,FH-N}$);

[6] The asymmetry of the penetration depth within the FH-N model is nicely illustrated in Fig_03a.htm and Fig_03b.htm on the CD-ROM (folder *Figures*). Brighter colors correspond to higher concentration of the "activator" u. The passive stripe is blue and the active areas are red. The same color coding is used for all the other animations mentioned later in text. In Fig_03a.htm a plain pulse of excitation gets through a barrier perpendicular to the direction of its motion, while the same barrier cannot be crossed by a pulse travelling parallel to it (Fig_03b.htm).

http://rcin.org.pl

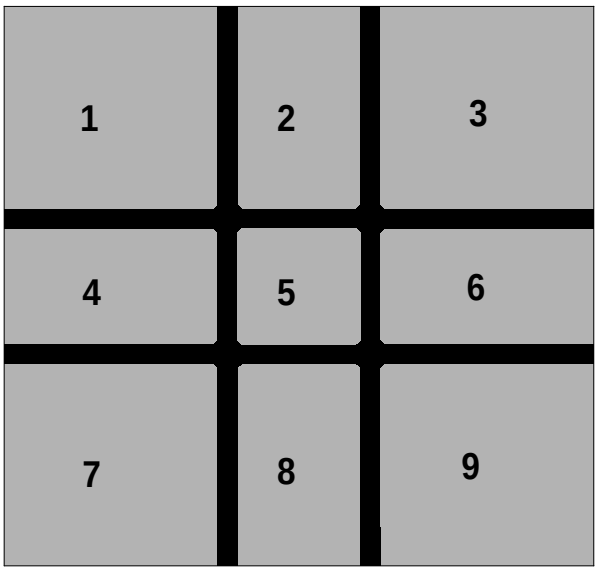

Figure 3. Geometry of the cross junction: brighter areas correspond to the excitable field and the dark stripes - to the diffusion one. The excitable areas are numbered to simplify the description in text.

http://rcin.org.pl

ii The pulse is able to propagate through the junction of two channels (because it is able to cross the stripe of the diffusion field perpendicular to the direction of its motion, as $d_{FH-N} < d_{c,FH-N}$).

Of course, properties (i) and (ii) are formulated for the FitzHugh - Nagumo model, but analogical construction and explanations are valid for the Rovinsky - Zhabotinsky model.[7]

If there are two pulses of excitation propagating in perpendicular channels of the cross junction presented in Fig. 3, they may coincide and interact in the common central part of the device (area 5 in Fig. 3). This interaction may be different, depending on the time difference between the incoming signals. Thus, the detection of coincidence of signals from individual channels should occur in the central area of the cross junction. It is interesting and useful to obtain the full characteristics of the behavior of the cross junction with respect to the time difference between the incoming pulses.

2.3.1 Results for the FH-N model.

The properties of the cross junction within the FH-N model have been thoroughly studied for passive stripes of the width d_{FH-N}=0.16 [111]. The pulses have been initiated on the border by decreasing the value of the inhibitor v inside the channel to v_i=-0.2. The answer of a homogeneous system with respect to such excitation is shown in Fig. 1 (Section 2.1.1). The stationary shape of a pulse is obtained after $t_{s,FH-N} \approx$2.50 and the velocity of free propagation of the pulse is $v_{s,FH-N} \approx$0.77. Thus after covering the distance of 2 units the pulse retains its stationary form.

[7]Properties (i) and (ii) for the FH-N model are presented in Fig_03c.htm on the CD-ROM (folder *Figures*). All passive stripes in Fig_03c.htm have the same width of about $0.96 \cdot d_{c,FH-N}$

http://rcin.org.pl

Figure 4 presents a typical stationary shape of a travelling pulse in terms of the variable u. Brighter areas correspond to the higher values of u. Thin stripes of the diffusion field are located between the pairs of dashed lines (the stripes are not filled black, so that the picture is more legible). One can see characteristic "whiskers" of the pulse, slightly sticking outside the stripes of the diffusion field. The collision of these "whiskers" explains part of the characteristics of the cross junction given below (points A and C). Such stationary shape of a pulse does not depend on the mechanism of initialization.

If the width of the excitable field inside the channel ($d_{e,FH-N}$) is large enough ($d_{e,FH-N}$>0.40) we do not observe its influence on the amplitude and velocity of a pulse. In very narrow channels ($d_{e,FH-N}$<0.10) both amplitude and velocity are remarkably smaller than those characterizing a pulse in a wide channel. In particular, in a channel characterized by $d_{e,FH-N}$=0.10 the amplitude of the pulse of u ("activator") is by 2% smaller than for a pulse propagating in a wide channel (u_{max}=0.93 has been observed instead of 0.95 seen in wide channels). The velocity of such a pulse drops by 13%, from 0.77 to 0.67. In the narrowest channels studied ($d_{e,FH-N}$=0.02) the amplitude of the pulses of u is u_{max}=0.75 and their velocity is only 0.39, but the pulses still propagate.

The features of a pulse mentioned above are important for its propagation through the junction. The data concerning penetration of diffusion filed given by I. Motoike and K. Yoshikawa in [86] applies to pulses propagating in wide channels. If the width of the channel is smaller than 0.70, then the penetration depth for transverse propagation decreases. The width of the excitable field inside each channel is also important for a pulse to propagate through the junction, because the pulse needs enough space between the two stripes of the diffusion field on its way to cross both of them. In other words:

http://rcin.org.pl

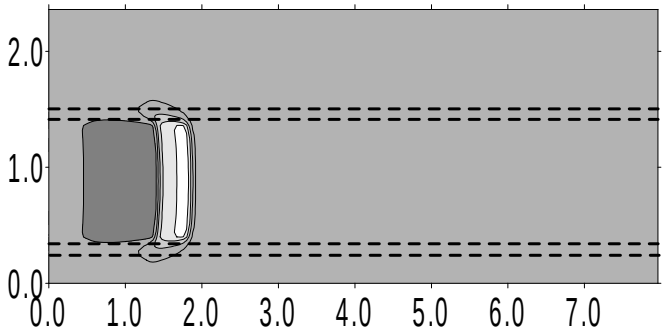

Figure 4. Typical stationary shape of a travelling pulse in terms of the variable u. Brighter colors correspond to higher values of u. Thin stripes of the diffusion field are located between the pairs of dashed lines (the stripes are not filled black, so that the picture is more legible).

http://rcin.org.pl

to obtain the propagation of a pulse from the area 4 to the area 6 in Fig. 3 - the area 5 cannot be too small. It has been found [111] that in order to obtain the junction with features (i) and (ii) the inner diameter of the channel $d_{e,FH-N}$ should not be lower than ca. 0.80.

All the results presented below are obtained by integrating Eqs. (2.1-2.4) numerically. The calculations have been carried out with the implicit method [121]. The values of parameters given in Section 2.1.1 have been used, as well as $d_{e,FH-N}$=1.02. The time step of the integration dt=0.005. Three sizes of the square the junction is built on have been considered (5x5, 7x7 and 8x8), covered with square lattices of 250x250, 350x350 or 400x400 points respectively. Thus, the space step in all those calculations dx=dy=0.02 remains constant. The results for different system's sizes are consistent. No flux boundary conditions have been used at the border of the square.

To find the time characteristics of the cross junction the following technique has been applied. In each of the input channels (areas 4 and 8) one input signal (a pulse) is initiated. The pulses are produced on the border of the square. For various experiments the channels are located in different parts of the square, so that the pulses travel over various distances before reaching the cross junction. This way, due to their constant velocity ($v_{s,FH-N}$ ≈0.77), one is able to adjust the time difference Δt between their arrival at the junction.[8] Depending on Δt seven types of the junction's response have been obtained. They are presented in Figures 5-11.[9] The figures marked as a)-f)

[8]Note, that Δt can be specified only with finite resolution of $dx/v_{s,FH-N}$=0.02/0.77≈0.026, as the distance between the place of initiation of a pulse and the cross junction is controlled up to the space step of the grid used (0.02). This makes the "spectrum" of Δt discontineous (see points A.-G. below).

[9]Each of Figs. 5-11 has its color, animated version under the name like Fig_05a.htm, Fig_06a.htm, ... Fig_11a.htm (CD-ROM, folder *Figures*).

http://rcin.org.pl

show the time evolution of the activator in the junction (the exact timing of snapshots a)-f) is given in figure captions).

Due to the symmetry of the system it is enough to restrict the analysis to the case in which the first pulse is initiated in the area 4 and the second - in the area 8. The behavior of the cross junction may be classified in the following way:

A. For a very small time difference between incoming signals ($\Delta t \leq 0.26$) the cross junction acts as the "AND" logical gate. The output signal is produced in the area 7 between the two input channels (4 and 8) if and only if there are two input signals arriving at the junction within the given time difference. The output signal probably appears when the "whiskers" of the two travelling pulses meet (cf. Fig. 5).

B. For the time difference in the range $0.28 \leq \Delta t \leq 3.45$ only the earlier signal survives and propagates within its own channel - area 6. Here the cross junction works (as expected) as a coincidence detector in which the earlier pulse switches the central field into the refractory regime and blocks the propagation of the second signal (cf. Fig. 6).

C. When $3.48 \leq \Delta t \leq 3.79$ the earlier signal survives in its own channel (area 6) and in addition a new output signal is produced in the lower right hand side corner of the device (area 9). The new output signal appears due to the same mechanism as in the case A, ie. due to the coincidence of the "whiskers" (cf. Fig. 7).

D. For $3.81 \leq \Delta t \leq 4.22$ the evolution is the same as in the case B: only the earlier incoming signal survives and propagates in the area 6 (cf. Fig. 8).

http://rcin.org.pl

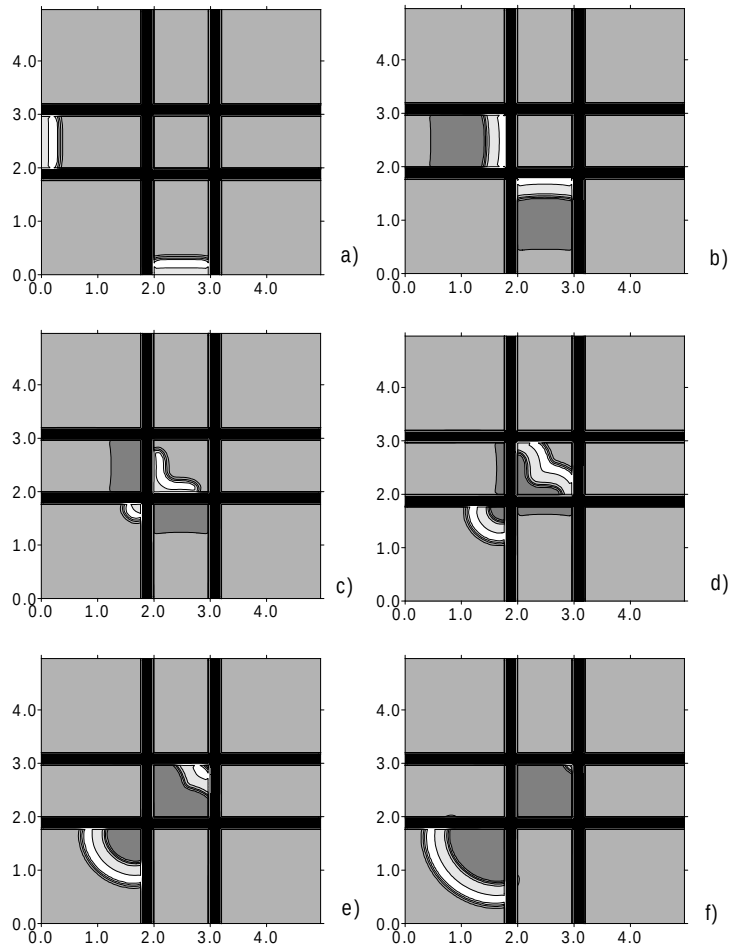

Figure 5. The "AND" logical gate for Δt=0.00. The output signal is produced in the area 7 between the two input channels (4 and 8). The consecutive snapshots correspond to a) t=0.5, b) t=2.5, c) t=3.5, d) t=4.0, e) t=4.5, f) t=5.0. Such behavior is observed for $\Delta t \in$[0.00, 0.26].

http://rcin.org.pl

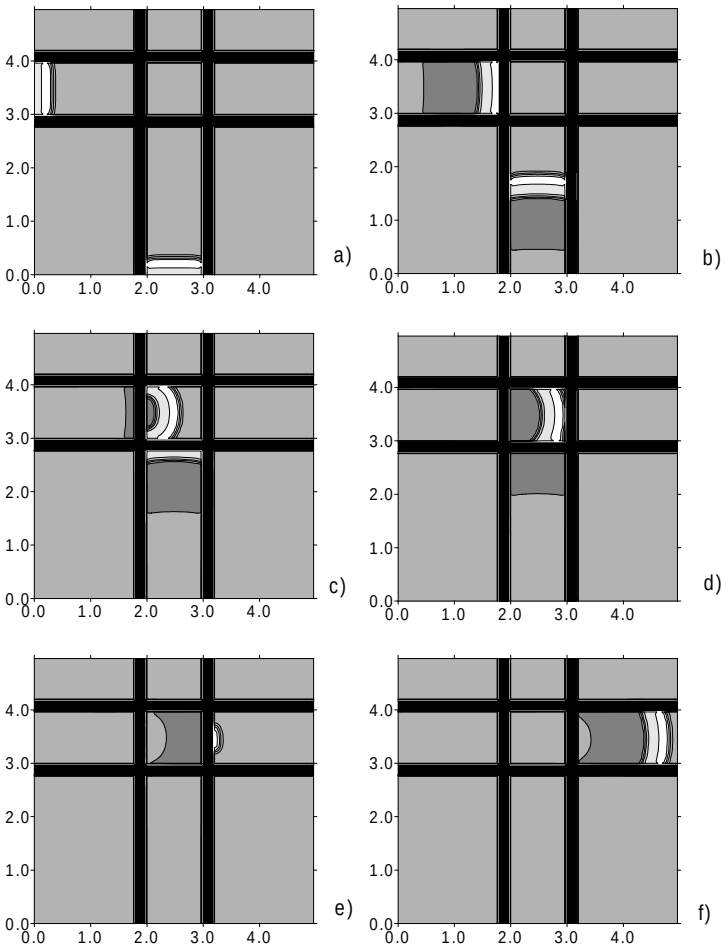

Figure 6. Only the earlier signal survives (within its own channel - area 6) for Δt=1.29. The consecutive snapshots correspond to a) t=0.5, b) t=2.5, c) t=4.0, d) t=4.5, e) t=5.5, f) t=7.5. Such behavior is observed for $\Delta t \in$[0.28, 3.45].

http://rcin.org.pl

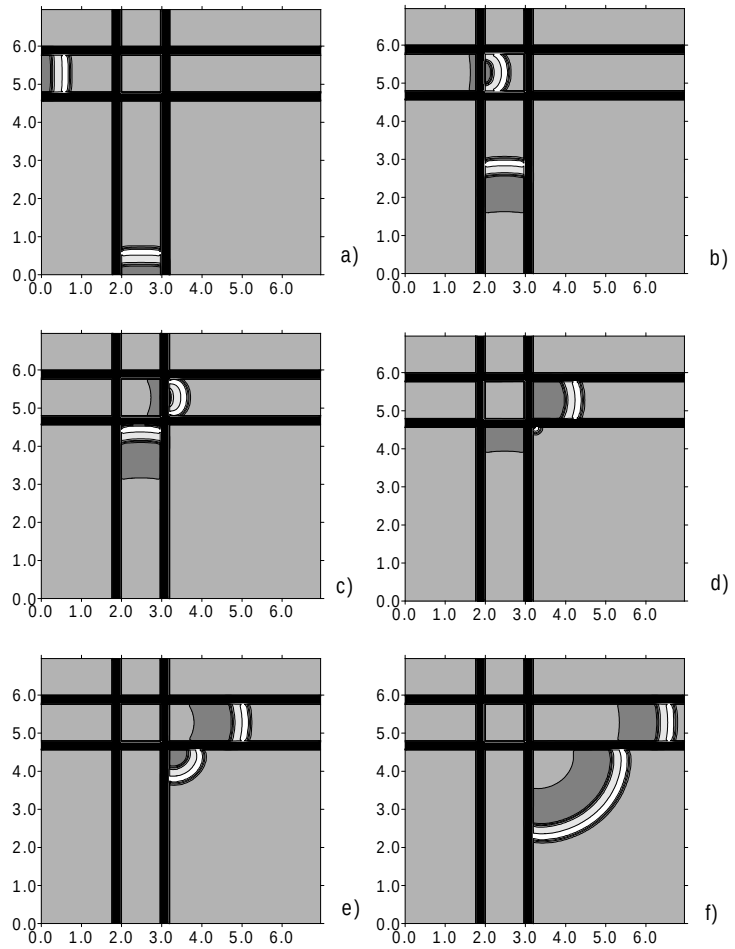

Figure 7. The earlier signal survives in its own channel (area 6) and in addition a new output signal is produced in the area 9 for Δt=3.61. The consecutive snapshots correspond to a) t=1.0, b) t=4.0, c) t=6.0, d) t=7.0, e) t=8.0, f) t=10.0. Such behavior is observed for $\Delta t \in$[3.48, 3.79].

http://rcin.org.pl

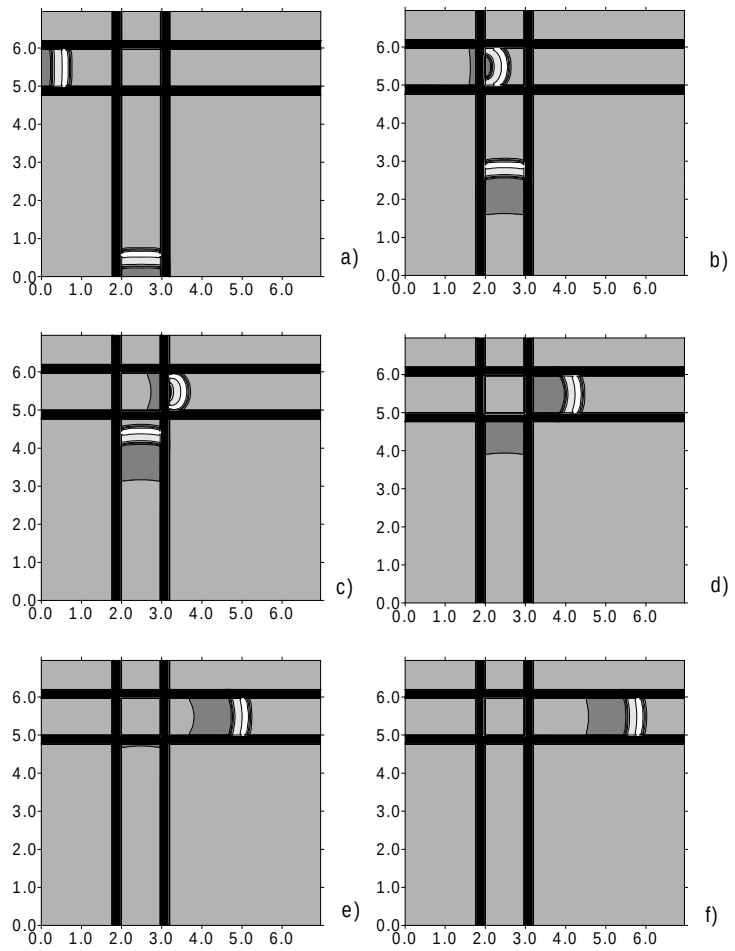

Figure 8. For Δt=3.87 only the earlier incoming signal survives (area 6). The consecutive snapshots correspond to a) t=1.0, b) t=4.0, c) t=6.0, d) t=7.0 e) t=8.0 f) t=9.0. Such behavior is observed for $\Delta t \in$[3.81, 4.22].

http://rcin.org.pl

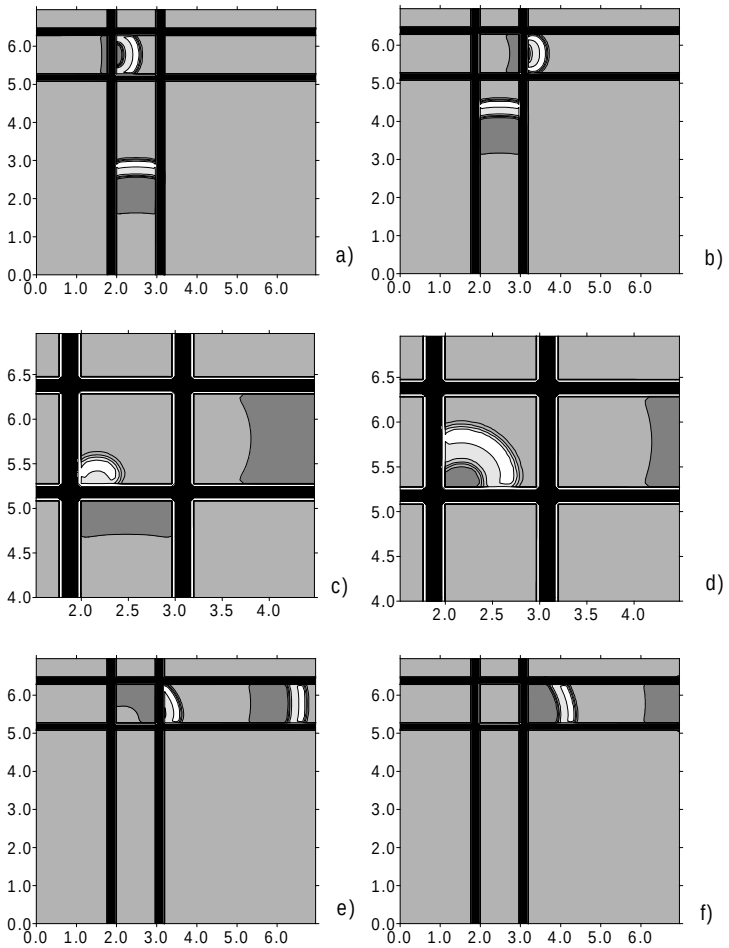

Figure 9. For Δt=4.25 the earlier incoming signal follows the way within its own channel (area 6) while the other signal is switched from the original path and follows the first signal (area 6). The consecutive snapshots correspond to a) t=4.0, b) t=6.0, c) t=8.0, d) t=8.5, e) t=10.0, f) t=11.0. Slides c) and d) present "zoomed" images of the central field of the junction, in order to show in details the most interesting part of the evolution in this area.

http://rcin.org.pl

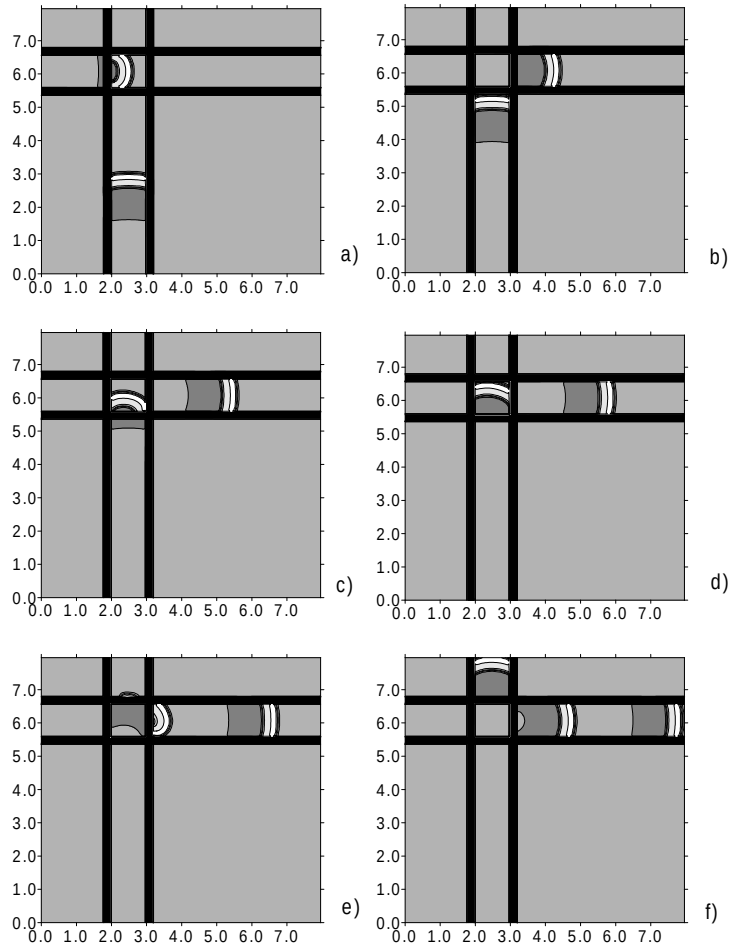

Figure 10. For Δt=4.64 the earlier signal goes unchanged through the junction, while the other signal initiates output pulses both within its own channel (area 2) and in the horizontal channel (area 6). The consecutive snapshots correspond to a) t=4.0, b) t=7.0, c) t=8.5, d) t=9.0, e) t=10.0, f) t=11.5. Such behavior is observed for $\Delta t \in$[4.28, 5.41].

http://rcin.org.pl

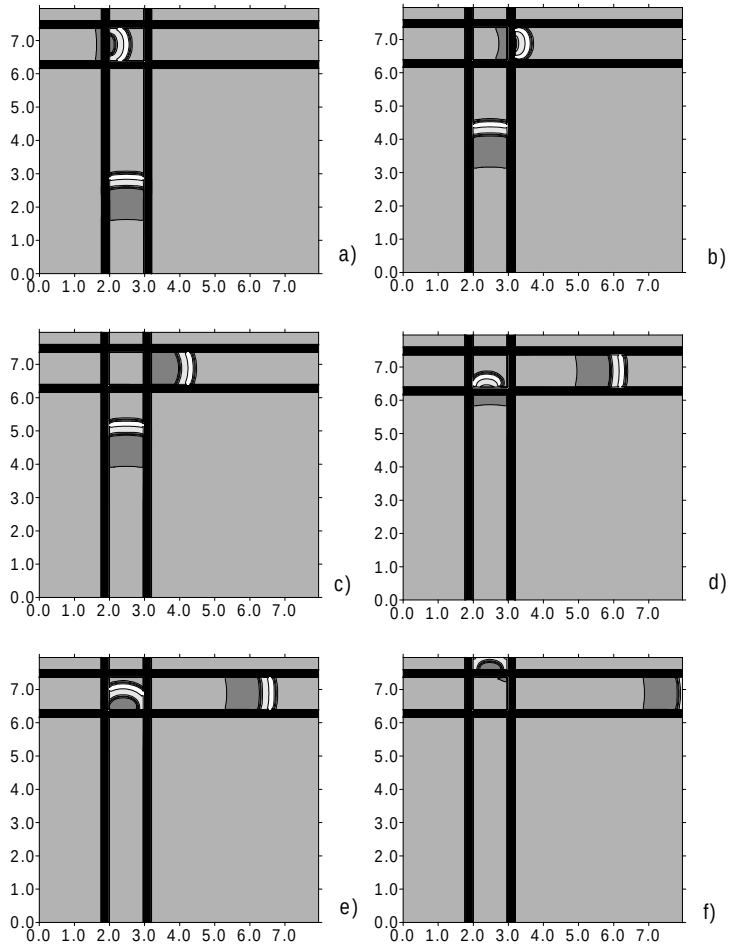

Figure 11. For Δt=5.67 the pulses do not "feel" each other any more. Each of them simply propagates in the channel it was initialized in (areas 6 and 2 respectively). The consecutive snapshots correspond to a) t=4.0, b) t=6.0, c) t=7.0, d) t=9.5, e) t=10.0, f) t=12.0. Such behavior is observed for $\Delta t \geq 5.43$.

http://rcin.org.pl

E. For $\Delta t \approx 4.25$ the earlier incoming signal propagates within its own channel (area 6), while the other signal is switched from the original path and follows the first signal (cf. Fig. 9). This behavior is caused by the fact that the second pulse finds the central area of the junction relaxed only on the left hand side. Consequently, further propagation of the pulse within the junction starts there and the geometry of the reactor makes the pulse switch its original direction. It can be seen in Figs. 9c) and 9d), which present the "zoom" of the central filed of the junction.

F. For $4.28 \leq \Delta t \leq 5.41$ the earlier signal passes unchanged through the junction, while the later signal initiates output pulses both within its own channel (area 2) and in the horizontal channel (area 6). The explanation of this case is similar to the one given it the previous point. The only difference is that here the second pulse enters the central area of the junction a bit closer to the right than in the case E, due to a better relaxation of the active medium in the central area (cf. Fig. 10).

G. For $\Delta t \geq 5.43$ the pulses do not "feel" each other any more. Each of them simply propagates in the channel it was initialized in (areas 6 and 2 respectively). This is because the central area of the junction is fully relaxed when the second pulse appears (cf. Fig. 11).

2.3.2 Results for the R-Z model.

Interesting results obtained within the FitzHugh-Nagumo model motivated me to study the propagation of excitable pulses in the cross junction geometry, but using a model which can be directly linked with chemical reactions, in order to give grounds to verify the results experimentally. For this purpose the Rovinsky - Zhabotinsky model has been applied.

http://rcin.org.pl

The system of partial differential equations (2.5-2.8) has been solved numerically using the explicit Euler technique with a constant time step $d\tau$=0.001. The pulses have been initialized at the boundaries of the square, inside the channels (areas 4 and 8 in Fig. 3) by increasing the concentration of x to 0.1. In the majority of calculations the square has been covered with a grid of 320x320 points. At the beginning the concentrations of x and z in all active and passive areas correspond to their stationary states x_{sa}, z_{sa} and x_{sp}, z_{sp} respectively (Eqs. (2.12-2.15)). On the lower and left hand side borders of the system no flux boundary conditions have been used. On the other hand the values of x and z have been fixed as equal to the corresponding stationary states (x_{sa}, z_{sa} and x_{sp}, z_{sp} respectively) at the upper and right hand side borders. This way the pulses arriving there may freely "leak out" of the system (they do not accumulate in the neighborhood of the borders) and any influence of the system's boundaries on the time evolution can be avoided.

Passive stripes which are d_{R-Z}=3.291 ($0.03034 \cdot \sqrt{\frac{D_X}{D_{X_0}}} cm$) wide have been considered (this value is between $0.995 \cdot d_{c,R-Z}$ and $d_{c,R-Z}$ given in Section 2.2). From the calculations the minimum width of a signal channel has been found. For the selected width of the passive stripes the pulse initiated (for example) in the area 8 always arrives to the central area 5. However, if the central field is too small then the amplitude of the activator is not high enough to excite the opposite area 2. It has been found that the minimum inner width of the signal channel for which pulses can propagate through the junction is about 10.526 ($0.097029 \cdot \sqrt{\frac{D_X}{D_{X_0}}} cm$).

The typical velocity of the pulse in our system is about 4.128 ($0.2686 \cdot \sqrt{\frac{D_X}{D_{X_0}}} cm/min$), which is a reasonable value for a chemical wave in the BZ reaction [46, 102, 113, 119, 122, 123].

http://rcin.org.pl

Knowing the width of a semitransparent passive barrier and the width of an active channel one can build a cross junction of the excitable BZ system which should work similarly to that for the FitzHugh - Nagumo dynamics. The pulses initiated in the horizontal channel (in the area 4 in Fig. 3) should be able to get through the junction (area 5 in Fig. 3) and arrive at the other side of the device (area 6 in Fig. 3) without escaping from the channel (to the areas 1-3 and 7-9 in Fig. 3) and due to the symmetry of the device the pulses in the vertical channel should behave in the same way. What is the interaction between pulses coming from perpendicular directions? At the beginning the system is in its stationary state. In calculations two sizes of the square on which the junction is built have been considered: 198.13x198.13 and 263.3x263.3 (corresponding to $1.8264 \cdot \sqrt{\frac{D_X}{D_{X_0}}} cm$ and $2.427 \cdot \sqrt{\frac{D_X}{D_{X_0}}} cm$), for which square lattices of 240x240 or 320x320 points respectively have been used. Thus, the space step in all those calculations $d\rho$=0.82 remains constant. Two channels of the width of 66.648 ($0.61436 \cdot \sqrt{\frac{D_X}{D_{X_0}}} cm$) or 132.473 ($1.22114 \cdot \sqrt{\frac{D_X}{D_{X_0}}} cm$) for smaller and larger systems respectively are placed symmetrically on the square. The results obtained for different grids are consistent. The first pulse is initiated on the left hand side border of the area 4 in Fig. 3. After a time $\Delta\tau$ another pulse is initiated on the lower border of the area 8. Because the distance from both borders to the junction is the same, the time difference between the arrival of the first and the second pulse at the junction is also $\Delta\tau$.

It has been observed that if the second pulse arrives at the central field earlier than $\Delta\tau_{min}$=107 ($910 sec$) after the first one, it is stopped at the central field. On the other hand, if $\Delta\tau > \Delta\tau_{max}$=115 ($978 sec$) both pulses follow their original signal paths without interaction.

Although it is apparently possible to build a coincidence detector based

http://rcin.org.pl

on the cross junction of excitable BZ systems with the dynamics given by the Rovinsky - Zhabotinsky model, the other interesting features of the junction, described in Section 2.3.1, do not occur in the R-Z model. In particular, the "AND" logical gate behavior, when two pulses coincide, producing an output pulse between the channels (in the areas 7 or 9 in Fig. 3) has never been observed. Neither the "chemical switch", when the second pulse changes the direction of propagation and follows the first one [111].

In order to see more clearly why the "chemical switch" does not work for the BZ system, calculations for the asymmetric junction presented in Figure 12 have been performed.[10] Here a square of 263.3x263.3 ($2.427 \cdot \sqrt{\frac{D_X}{D_{X_0}}} cm$), covered with the grid of 320x320 points has been used. The first pulse is initiated in the horizontal channel (area 4 in Fig. 3). The channel is located at the distance 56.363 ($0.51956 \cdot \sqrt{\frac{D_X}{D_{X_0}}} cm$) from the lower boundary; its width is 99.560 ($0.91775 \cdot \sqrt{\frac{D_X}{D_{X_0}}} cm$). After the time $\Delta\tau$=109.0 ($927 sec$) another pulse is initiated in the vertical channel (area 8 in Fig. 3). This channel is located at the distance 56.363 ($0.51956 \cdot \sqrt{\frac{D_X}{D_{X_0}}} cm$) from the left hand side boundary; its width is 152.220 ($1.40317 \cdot \sqrt{\frac{D_X}{D_{X_0}}} cm$). One can see that when the second pulse gets to the central area of the junction, it propagates in both vertical and horizontal directions. The propagation to the right fails, while the propagation upwards continues and, what is very important, the pulse is able to pass from its own channel (area 2 in Fig. 3) to the upper right hand side part of the system (area 3 in Fig. 3). Comparison of Figs. 12d) and 12e) shows that the pulses trying to get from the area 5 to the area 6 and from the area 2 to the area 3 "attack" the stripe of the diffusion field both at the same angle, so the geometrical factor is not the reason for the propagation

[10] Animated version of this Figure (Fig_12a.htm) can be found on the CD-ROM (folder *Figures*).

http://rcin.org.pl

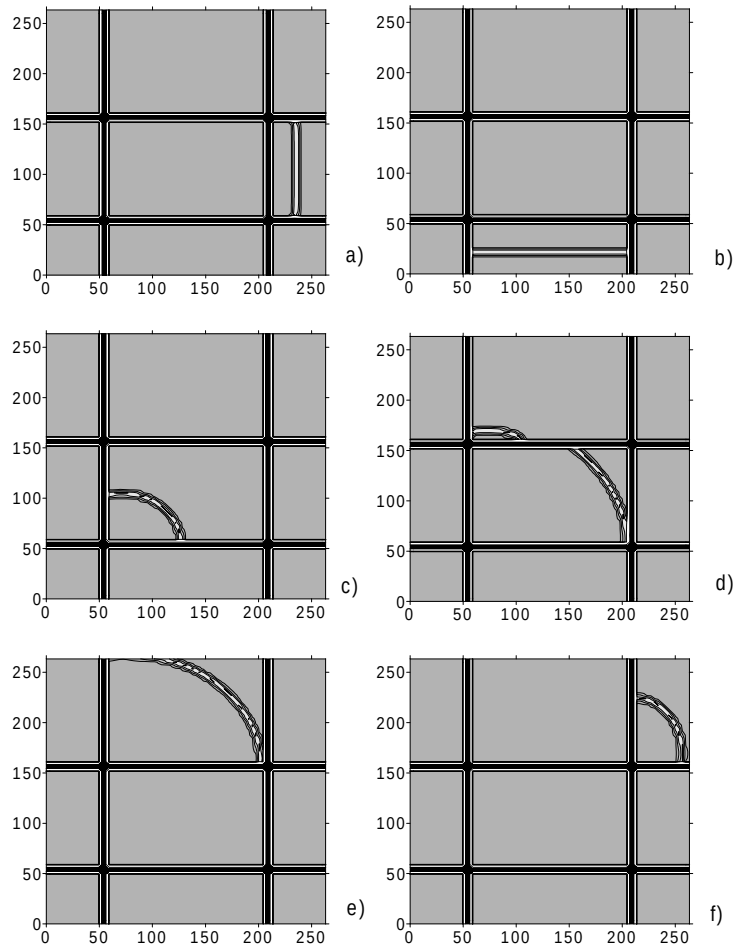

Figure 12. Two pulses in an asymmetric cross junction of systems with the Rovinsky - Zhabotinsky dynamics. Figures show the concentration of activator for a few selected moments in the case the second pulse of excitation arrives $\Delta\tau$=109 after the first one. The brighter areas correspond to higher values of x. a) τ=54 - the first pulse passes through the horizontal channel; b) τ=114 - the second pulse approaches in the vertical channel; c) τ=134 - the second pulse propagates asymmetrically in the central area; d) τ=150 - although the geometrical condition is fulfilled, the pulse cannot pass into the area 6, but it gets into the area 2; e) τ=170 - asymmetric propagation of the second pulse in the area 2; f) τ=184 - the pulse gets into the area 3. Such behavior is observed for $\Delta\tau\in$(107, 115).

http://rcin.org.pl

failure. The failure occurs apparently because the active medium in the area 6 is still not relaxed behind the first pulse. A number of calculations for a set of smaller time shifts $\Delta\tau$ has been performed (until the second signal is not able to enter the junction at all for $\Delta\tau$=$\Delta\tau_{min}$=107 ($910sec$)) as well as for the larger ones (until the second signal propagates through the junction and does not "feel" the influence of the first signal at all for $\Delta\tau$=$\Delta\tau_{max}$=115 ($978sec$)) and the second signal turning right from the area 5 to the area 6 has never been observed. Consequently, the "chemical switch" behavior in the Rovinsky - Zhabotinsky model has not been found, despite the favorable geometry of the system.

The difference with respect to the FitzHugh - Nagumo model may be explained as follows: in the Rovinsky - Zhabotinsky model the distance at which the catalyst (z) relaxes is by order of magnitude larger than the one for the activator (x), whereas in the FitzHugh - Nagumo both u and v relax at the same spatial scale.

Looking at Figs. 12e) and 12f) one can see that the simplest idea how to make the second pulse turn right is to direct the pulse excited in the upper right hand side corner of the system (area 3 in Fig. 3) into an additional channel.

This has been done in the computer experiment illustrated in Figure 13.[11] The size of the square, grid size, width of the diffusion stripes and the time shift between the signals are the same as in Fig. 12. The main channels of identical width of 132.473 ($1.22114\cdot\sqrt{\frac{D_X}{D_{X_0}}}cm$) are placed symmetrically in the middle of the square (at the distance 66.236 ($0.61057\cdot\sqrt{\frac{D_X}{D_{X_0}}}cm$) from each border). An extra channel of the diameter 33.735 ($0.31097\cdot\sqrt{\frac{D_X}{D_{X_0}}}cm$) is

[11] Animated version of this Figure (Fig_13a.htm) can be found on the CD-ROM (folder *Figures*).

http://rcin.org.pl

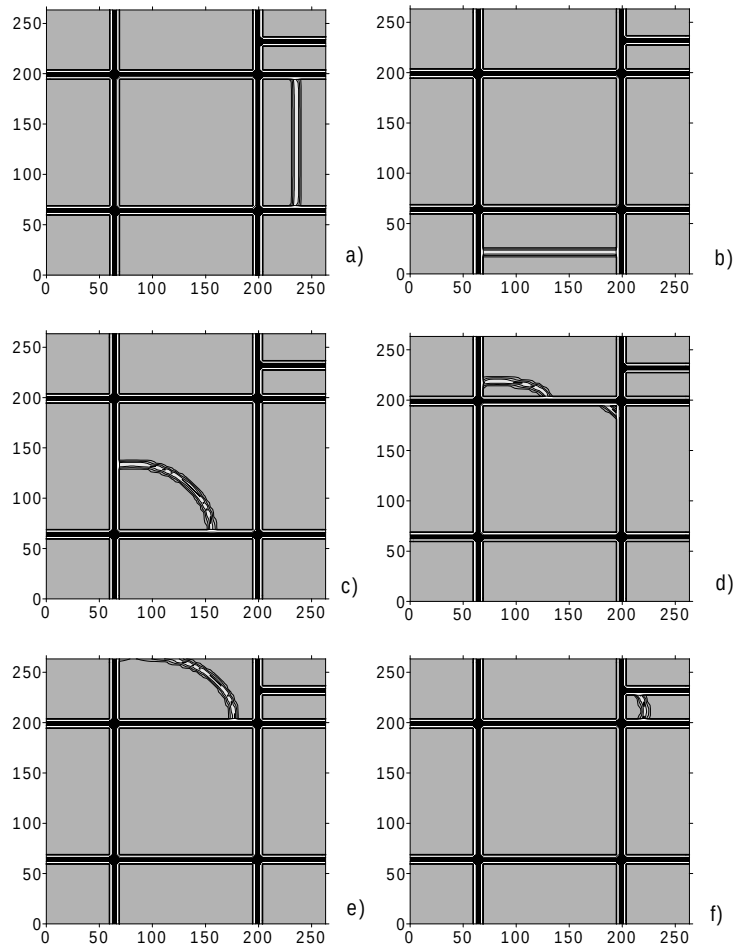

Figure 13. Two pulses in a symmetrical cross junction of systems with the Rovinsky - Zhabotinsky dynamics with an additional channel. Figures show concentration of activator for a few selected moments in the case the second pulse of excitation arrives $\Delta\tau$=109 after the first one. The brighter areas correspond to higher values of x. a) τ=54 - the first pulse passes through the horizontal channel; b) τ=114 - the second pulse approaches in the vertical channel; c) τ=140 - the second pulse propagates asymmetrically in the central area; d) τ=160 - the pulse is stopped on the right hand side boundary of the vertical channel; e) τ=170 - asymmetric propagation of the second pulse in the area 2; f) τ=182 - the pulse gets into the area 3 (as in Fig. 12f), but also generates a pulse in the extra channel.

http://rcin.org.pl

located in the upper right hand side corner of the system. In Fig. 13f) one can see that the pulse is in fact excited in that extra channel. The results obtained suggest that this type of behavior can be observed (at least) for $\Delta\tau \in [108, 111]$ [$918sec$, $944sec$].

Another way of building a "chemical switch" is to speed up the relaxation of the active chemical medium in the area 6 (Fig. 3) behind the first pulse. One can do it easily by increasing the diffusion coefficient in the area 6. Now pulses propagate here faster and the refractory time of the medium is shorter. The idea is demonstrated by results of another calculations presented in Figure 14.[12] The geometry is the same as in Fig. 13, except there is no the extra channel. Instead, the diffusion coefficient of the activator is doubled in the area 6, comparing to the rest of the system. The first pulse travels in the horizontal channel (areas 4-6 in Fig. 3) and speeds up remarkably after crossing the junction (in the area 6 in Fig. 3). After $\Delta\tau$=109.0 ($927sec$) a pulse in the vertical channel is initiated. This second pulse gets through the junction (within its own channel - area 2 in Fig. 3), but it also follows the first pulse, as desired. As in the previous calculations (Fig. 13) this behavior can be observed (at least) for $\Delta\tau \in [108, 111]$ [$918sec$, $944sec$].

The calculations have shown that the width of signal channels does not have significant influence on the behavior of the cross junction of the Rovinsky - Zhabotinsky systems (if only the channels are wider than the minimum $0.9703mm$). The system for which the signal paths are three times wider than those shown in Figs. 13 and 14 has been investigated (thus, the signal channels have been $3.66cm$ wide). It has been found that for this system the

[12] Animated version of this figure (Fig_14a.htm) can be found on the CD-ROM (folder *Figures*). In addition, Fig_14b.htm proves that in the last case a pulse propagating in the vertical channel does not "leak out" of it, despite the doubled diffusion coefficient in the area 6.

http://rcin.org.pl

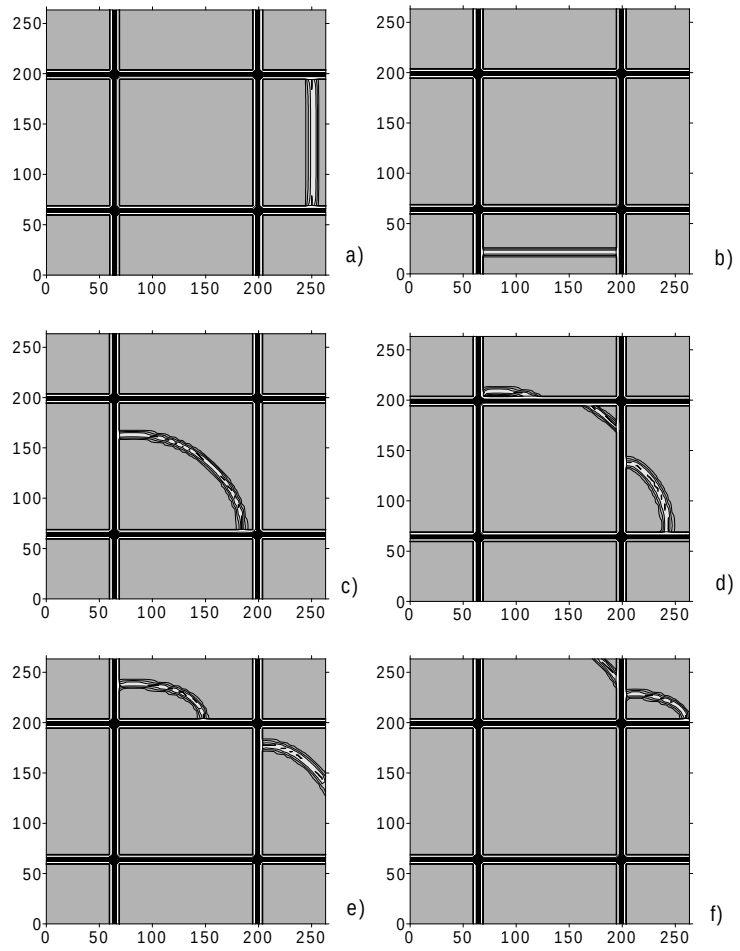

Figure 14. Two pulses in an asymmetric cross junction of systems with the Rovinsky - Zhabotinsky dynamics, in the case of faster diffusion in the area 6. Figures show concentration of activator for a few selected moments in the case the second pulse of excitation arrives $\Delta\tau$=109 after the first one. The brighter areas correspond to higher values of x. a) τ=54 - the first pulse passes through the horizontal channel; b) τ=114 - the second pulse approaches in the vertical channel; c) τ=146 - the second pulse propagates asymmetrically in the central area; d) τ=158 - the pulse is doubled: it turns right into the area 6 and follows its original path (area 2); e) τ=164 - asymmetric propagation of the second pulse in the areas 2 and 6; f) τ=176 - the pulse from the area 6 excites a pulse in area 3.

http://rcin.org.pl

pulses which arrive earlier than $\Delta\tau$=100 after the first one are stopped. Such result might have been expected as the "transparency" of the central field is related to the time the system spends in the refractory regime, which hardly changes with size. On the other hand, the interval of times for which the system works as a signal switch becomes slightly longer for larger systems. This is related to the direction of propagation of the second pulse in the central area. It has been observed that for three times wider signal channels ($3.66cm$) the junction works as shown in Fig. 12, even if the second pulse arrives $\Delta\tau$=120 after the first one.

2.3.3 Discussion.

It has been demonstrated that a cross junction of active and passive fields reveals interesting properties. These properties include coincidence detection (the pulses coming within times shorter than a characteristic one are stopped) and switching the direction of propagation of a chemical pulse. The features of the cross junction have been studied for the FitzHugh - Nagumo and the Rovinsky - Zhabotinsky dynamics. They can be realized in a junction of excitable systems of Belousov - Zhabotinsky reaction.

It has been found that in order to construct a working cross junction based on the Belousov - Zhabotinsky system it is necessary to create passive stripes with a very high accuracy. If the diffusion constant of the activator corresponds to the value characteristic for an aqueous system (D_{X_0}=$1\cdot 10^{-5}cm^2/sec$) then the stripe without catalyst should be $0.3034mm$ wide with only 1% of tolerance. Such a high precision can be achieved with newly developed photolithographic technique of introducing catalyst on the surface [70, 103, 104].

The most interesting feature of the cross junction is its ability to switch

http://rcin.org.pl

the direction of an incoming signal. The effect has been discovered for a symmetrical cross junction (the signal channels are of equal width) and the FitzHugh - Nagumo dynamics. Similar effect for the BZ system has not been observed, which seems to be connected to its slower relaxation. It has been found that a switch of a chemical signal can be constructed if the cross junction of excitable BZ systems is not symmetrical. Two working schemes, in which the asymmetry is related to the diffusion coefficient or to the existence of another output channel have been studied.

It is worth noticing that in the case of Belousov - Zhabotinsky reaction such properties as the penetration depth strongly depend on the parameters of the model. Therefore the comparison between calculations and carefully prepared experiments for a junction of passive and active areas may be a good verification of the model and the values of parameters used.

http://rcin.org.pl

2.4 Propagation of regular trains of pulses through a passive barrier.

This section is concerned with a simple two dimensional reactor consisting of an infinite plane of the active (excitable) medium with a stripe of the passive medium (a passive barrier). Unlike in the previous section, instead of single pulses of excitation - regular trains of such pulses arriving at the barrier with a certain frequency are now considered. Such a train of pulses is called a chemical signal. Pulses in the form of planar waves, travelling perpendicularly to the stripe are considered. Such a problem is symmetrical in the direction perpendicular to the stripe, so it can be described as one dimensional. Therefore in the calculations the system's evolution has been modelled on a (one dimensional) interval.

A scheme of the investigated system is shown in Figure 15. In the bottom part of Fig. 15 the black lines correspond to the active areas, which are separated by a passive barrier (the gray line). There are free flow boundary conditions between passive and active media and no flux boundary conditions at both ends of the interval. Initially both active and passive areas are in their stationary states. Pulses of excitation are initiated at the left end of the interval and they travel to the right, coming across the passive barrier on their way. Initiation of pulses is performed regularly at times $k \cdot t_p$, for selected $t_p > 0$ and k=1, 2, 3,...,k_{max}. In the following the "input signal" (a train of pulses arriving at the barrier) and the "output signal" (a train of pulses going away after crossing the barrier) are distinguished. The input signal frequency is defined as $f_p = 1/t_p$. If the passive barrier is narrow, it is transparent to all the incoming pulses; if it is wide - it is impenetrable for any of them. However, it turns out [116, 117, 124] that for a certain range

http://rcin.org.pl

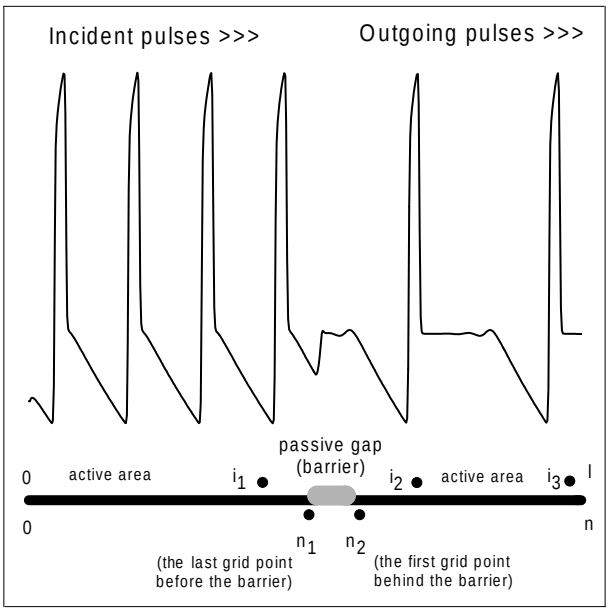

Figure 15. A scheme of the system studied. It is represented by one dimensional interval, shown in the bottom part of the figure; the active areas are black and the passive barrier is gray. The barrier is located between grid points n_1 and n_2. Concentrations of reagents are observed at grid points i_1 (before the barrier), i_2 (just behind the barrier) and i_3 (far behind the barrier). The upper part shows a snapshot of a train of pulses propagating in the system (incoming signal, on the left hand side and outgoing signal, on the right hand side). Note that the signals have different frequencies.

http://rcin.org.pl

of f_p and barrier's width d the passive gap transforms the frequency of the input signal. It means that the frequency of the output signal f_o (observed behind the barrier) is a fraction of f_p, because some of the incoming pulses are stopped at the barrier, while the others get through ($f_o/f_p \in [0,1]$). This fact is schematically shown in the upper part of Fig. 15.

2.4.1 The numerical technique.

The time evolution of the signal is studied by numerical integration of the reaction-diffusion equations in the active areas and within the barrier (Eqs. (2.1 - 2.4) for the FH-N model or (2.5 - 2.8) for the R-Z model). The system, represented by an interval of the length l, is divided into n parts by $n+1$ points of a grid, including both ends (cf. the bottom part of Fig. 15). The distances between the grid points dl may be different; by selecting a fine grid around the barrier it is possible to increase the accuracy of calculations, while a crude grid far away from the barrier saves computer time without affecting the accuracy. The barrier is located between grid points n_1 and n_2 ($1 \ll n_1 < n_2 \ll n$, cf. Fig. 15). It means that the evolution of the system at all grid points $j \in [0,n_1] \cup [n_2,n]$ is given by the set of reaction-diffusion equations corresponding to the active medium (Eqs. (2.1 - 2.2) for FH-N model or Eqs. (2.5 - 2.6) for FH-N model), and the equations describing the passive medium (Eqs. (2.3 - 2.4) or (2.7 - 2.8) respectively) give the evolution at all grid points $i \in (n_1,n_2)$. The barrier's width is estimated as:

$$d \cong (n_2 - n_1 - 1) \cdot dl_b \tag{2.16}$$

where dl_b is the distance between neighboring grid points (in the calculations dl_b is constant in the barrier and around it).

The concentrations of reagents of interest have been calculated using the

http://rcin.org.pl

implicit method already mentioned with the distance between neighboring grid points (dl) as the space step of numerical integration. In the computations two types of the space grids have been applied . In case of equally spaced (uniform) grids, used in part of calculations, the whole interval l has been divided into n equal parts (in this case $dl=l/n$).

In the other calculations adaptive grids have been used, for which the passive barrier and its neighborhood (so the part of the system which has the most influence on signal's transformation) has been covered with a fine grid and at both ends of the interval a longer distance between grid points has been used.[13] Two kinds of adaptive grids have been applied. One of such grids is formed by n=800 grid points and 30 of them are placed within the barrier (the barrier is located between n_1=400 and n_2=431). The time evolution in the active areas surrounding the barrier is also calculated using the same fine grid as for the barrier $dl_b=dl/8$. 40 grid points on each side of the barrier, with the distance dl_b between them are considered. Next there are 40 grid points of each side with the distance $2\cdot dl_b$ and yet another 40 points with the distance $4\cdot dl_b$. The reaction-diffusion equations in the remaining part of the system are solved with a crude grid of dl (cf. Figure 16). In order to test the numerical stability, another adaptive grid has also been used, for which the total number of grid points is n=870 and in this case the passive barrier, located between n_1=420 and n_2=481, is covered with 60 points of $dl_b=dl/16$. In the active areas located on both sides of the barrier the grid is fine ($dl/16$, 40 points) and next it increases as follows: $dl/8$ - 20 points, $dl/4$ - 40 points and $dl/2$ - 40 points. The rest of the system is covered with the space step dl.

[13]The formulas corresponding to the implicit method of numerical integration on adaptive grids are given in Appendix B.

http://rcin.org.pl

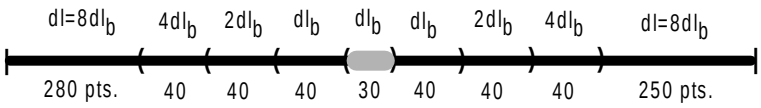

Figure 16. A scheme of the adaptive grid for n=800. Black intervals correspond to active areas, the gray one marks the barrier. The distance between grid points is given above the line, the number of grid points separated by a particular dl is given below the line.

http://rcin.org.pl

The values of activator and inhibitor are recorded at indicators located at the grid points i_1 (before the barrier), i_2 (just behind the barrier) and i_3, located far behind the barrier, as shown in the bottom part of Fig. 15. By comparing the time evolutions at i_1, i_2 and i_3 one can tell whether a pulse which arrives at the barrier is able to cross it. Moreover, by counting the number of maxima of activator within a certain time interval one can measure the frequency of the input and output signals (f_p and f_o respectively). When calculating f_p and f_o a few initial pulses (usually 10 or 20) are neglected in order to eliminate a transient behavior at the beginning of evolution. To describe quantitatively the passive barrier as a device which transforms chemical signal frequency, the filtering ratio defined as f_o/f_p is introduced. It corresponds to the firing number, if notation of [65]-[69] is used.

Calculations have been performed for different values of t_p (or f_p) and different values of the barrier's width d. The diagrams in the space of parameters (d,t_p) showing "phases" in which the barrier transforms the chemical signal in a given way are shown in figures presenting results obtained for particular models.

The parameters d and t_p (or f_p) seem to be proper variables to describe how a passive barrier works as a transformer of the signal frequency. The interval of t_p (or f_p) is limited by the fact that once the excitable medium has been excited it needs some minimal amount of time (called the refractory period) in order to relax, before it may be excited again. Thus, there exists a minimal time pace $t_{p,min}$ at which the pulses can be successfully initiated. The time $t_{p,min}$ depends on the strength of excitation and it fixes the upper frequency of the signal. On the other hand, making t_p very long reduces the problem to propagation of single pulses. The range of d is also finite as there always exists a barrier of width d_{min}, narrow enough to be transparent to

http://rcin.org.pl

all pulses in a train and another one, impenetrable for any of them (of the width of d_{max}). Thus, the nontrivial transforming properties of the passive barrier may be observed only in some finite range of t_p and d, which depends on the selected model and values of its parameters.

2.4.2 Results for the FH-N model.

In calculations for the FH-N model the following parameters of a uniform grid have been used: n=251, n_1=150, n_2=160, i_1=148, i_2=162, i_3=248. In order to produce a pulse the value of v has been decreased to v_{ini}=-0.8 on the left end of the interval.

For the considered values of parameters the minimum time after which the second pulse may be re-excited is $t_{p,min,FH-N}\approx$2.4. However, for such a short time of consecutive excitations it is not possible to obtain a regular, stable train of pulses, because it happens that the medium at the initiation point is not well relaxed and an attempt to re-excite it by the assumed v_{ini} fails. For the FitzHugh - Nagumo system the value of $t_{p,min,FH-N}$ strongly depends on v_{ini} (the strength of excitation) and also on dl, which describes the spatial size of excitation. Here in order to create a stable train of pulses $t_p\in$[2.90, 4.04] has been used .

The maximum time within which the evolution is studied (t_{max}) is fixed in the calculations. The system is excited approximately $p=t_{max}/t_p$ times, so it is expected that such number of pulses is produced. The time shift between individual pulses within a regular train equals t_p and $f_p=1/t_p$ gives the frequency of incident pulses at the first indicator (i_1).

To investigate the effect of the barrier t_{max}=500 and the time integration step $dt_1=5\cdot10^{-3}$ have been used to study a range of t_p from 2.98 to 4.04 with increment 0.02 ($f_p\in$[0.248, 0.336]) and the barrier's widths $d\in$[0.126, 0.172].

http://rcin.org.pl

For the selected t_{max} and t_p, from 120 to 160 pulses have been observed in the system for each combination of t_p and d.

Figure 17 presents a sample signal (concentration of u) observed at the grid points i_1, i_2 and i_3 for dl=0.0175 (uniform grid) and f_p=0.294. For all the results shown in Fig. 17 n_1=150, while n_2 is changed to obtain barriers of various width d. The upper curve (1) corresponds to incident pulses (reference signal at indicator i_1). In case of n_2=151 (no passive barrier) the same signal is observed at indicator i_2 with only a small time shift, which the signal needs to cover the distance between indicators i_1 and i_2 (signal at i_2 - curve 2). The result is the same for n_2=155, which corresponds to a thin, fully transparent passive barrier (curve 3 presents the signal at i_2). All incident pulses observed at indicator i_1 get through the barrier and are also observed at indicator i_2. However, for a properly chosen width the barrier becomes selective. For n_2=160 (the barrier's width is then d=0.158) exactly every second of the incident pulses is transmitted through the barrier and observed at indicator i_2 (curve 4) or indicator i_3 (curve 5).

Figure 18 summarizes the signal transforming properties of a passive barrier as a function of the barrier's width d and the time shift between consecutive incident pulses t_p. The white, labeled regions correspond to the given filtering ratio (f_o/f_p). The area labeled as "1" indicates the ratio equal to 1, which means that every incident pulse is able to get through the passive barrier (the barrier is transparent to all pulses). When t_p decreases - one arrives at the area (labeled as "1/2" in Fig. 18) where only every second of the incident pulses is transmitted. With increasing d the filtering ratio decreases, which means that the pulses are less and less frequently transmitted (see area "1/3" in Fig. 18, where only one out of three of incident pulses gets through the barrier). Finally the barrier becomes too wide and no pulse

http://rcin.org.pl

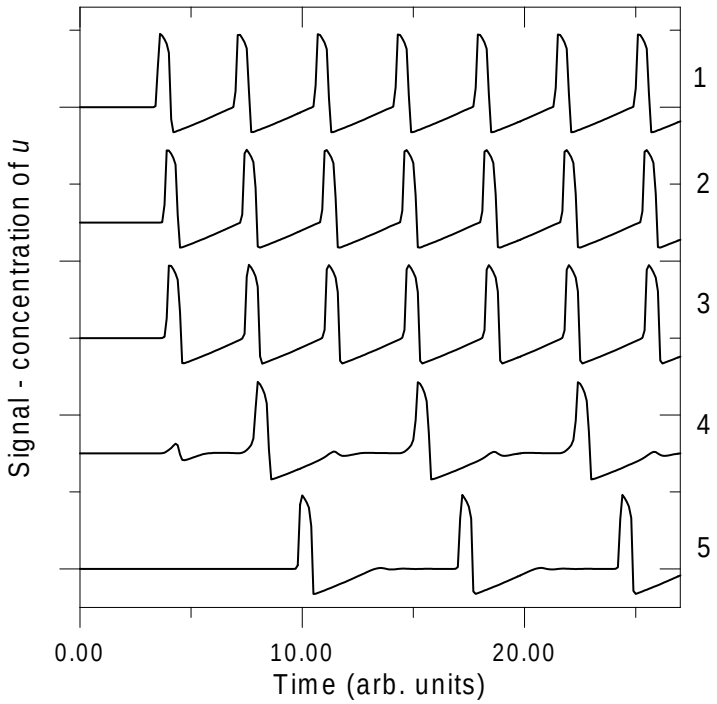

Figure 17. The time evolution of activator's concentration at the grid point i_1 (the upper curve 1), at the grid point i_2 (curves 2-4) and at the grid point i_3 far behind the barrier (curve 5). The evolutions at i_2 correspond to no barrier (curve 2), a narrow transparent barrier (curve 3) and to a barrier for which frequency transformation occurs (curve 4). In the last case the evolution at i_3 is also shown (curve 5). Results for the FitzHugh - Nagumo model (Eqs. (2.1-2.4)), t_p=3.40 (f_p=0.294), d=0.070 (curve 3), d=0.158 (curves 4 and 5).

http://rcin.org.pl

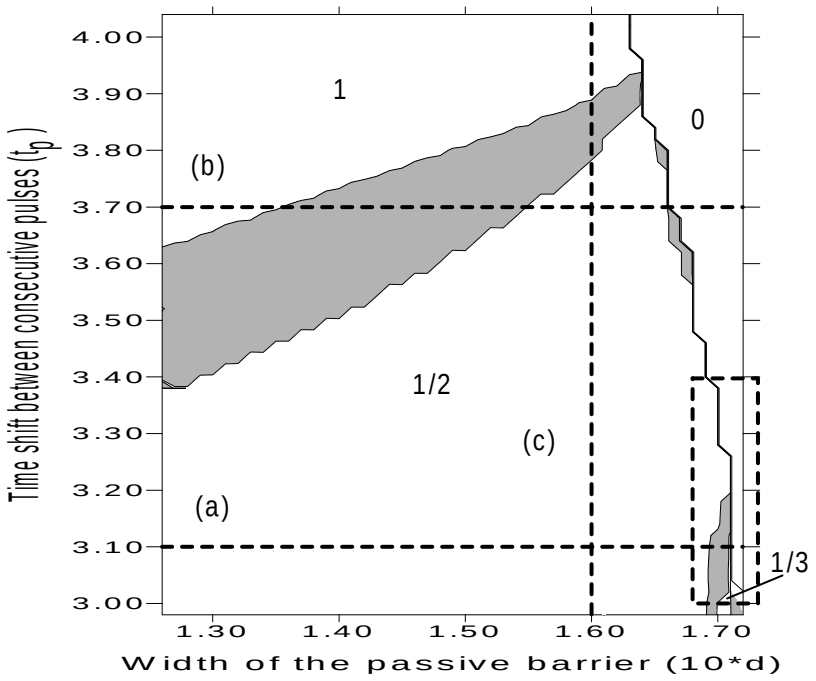

Figure 18. Filtering ratio (f_o/f_p) for the FitzHugh - Nagumo model as a function of the barrier's width (d) and the time shift between consecutive pulses (t_p). The white, labeled areas correspond to the situation when f_o is the fraction of f_p given in the picture. Gray color marks more complicated transformations of frequency. The dashed lines correspond to: (a) t_p=3.10 (f_p=0.323), (b) t_p=3.70 (f_p=0.270), (c) d=0.160. The rectangular area in the bottom right hand side corner of the picture has been studied more carefully and the results are illustrated in Fig. 19.

http://rcin.org.pl

can cross it (thus f_o=0). This corresponds to the area labeled as "0" in Fig. 18.[14] The dashed lines in Fig. 18 mark t_p=3.10 (f_p=0.323) - line (a), t_p=3.70 (f_p=0.270) - line (b), and d=0.160 - line (c). The filtering ratios as functions of parameters from the dashed lines (a), (b) and (c) are discussed in Sections 2.4.3 and 2.4.4. It is worth noticing that for the FitzHugh - Nagumo model the frequency transforming (corresponding to elimination of some of the incoming pulses by the barrier) may appear for barriers which are narrower or wider than the penetration depth for a single pulse ($d_{c,FH-N}$=0.163). In fact, in Fig. 18 there is a hidden line, corresponding to d=0.163, which divides the "1/2" area into two qualitatively different sub-areas. For d<0.163 the barrier is transparent for the first of incoming pulses, impenetrable for the second one etc. For d>0.163 the first of incoming pulses is stopped at the barrier, the second one gets through etc. In both cases the overall effect is the same (f_o/f_p=1/2). Thus, the described change occuring sharply for d=0.163 can be considered as phase shift of the outgoing signal.

The part of the parameter space for which the filtering ratio is smaller than 1 has been studied more carefully with t_{max}=500 and dt_2=$2\cdot10^{-3}$. The range of t_p from 3.00 to 3.40 with increment of 0.01 and the range of d from 0.168 to 0.173 with increment of 0.00018 have been investigated (this is the rectangular area marked with dashed line in the bottom right hand side corner of Fig. 18). The results are presented in Figure 19, for which the

[14]Various modes of the frequency transformation occurring in the FH-N model are presented on animated figures containing 6 incoming pulses each. The animations can be found on the CD-ROM (folder *Figures*). Fig_18a.htm presents the case of a fully transparent barrier, for which f_o/f_p=1. The width of the barrier is then increased. Fig_18b.htm shows f_o/f_p=2/3, Fig_18c.htm corresponds to f_o/f_p=1/2 and finally Fig_18d.htm presents an impenetrable barrier for which f_o/f_p=0. The frequency of the input signal f_p=0.270 (f_p=3.70) is the same for all the figures mentioned here.

http://rcin.org.pl

meaning of the colors and labels is the same as in Fig. 18.

The gray regions in Figs. 18 and 19, which separate the areas labeled as "1", "1/2", "1/3", correspond to more complex (periodic or non-periodic) transmission patterns described later in text. One of such patterns, corresponding to the filtering ratio f_o/f_p=2/5, is presented in Figure 20. Results presented in Fig. 20 have been obtained for n=251 (uniform grid), dl=0.01896, n_1=150 and n_2=160 (so the barrier's width is d=0.1707). Indicators have been located at grid points i_1=148, i_2=162 and i_3=248. Curves 1, 2 and 3 show the signal at indicators i_1, i_2 and i_3 respectively, for f_p=0.318 (t_p=3.14). Just after crossing the barrier the signal has the period of $5{\cdot}t_p$ with two maxima of concentration per period (Fig. 20, curve 2). The signal far behind the barrier is shown as the curve 3. One can see that the small maxima have not developed into regular pulses and the signal is composed of peaks separated by $2{\cdot}t_p$ and $3{\cdot}t_p$. Such form of a signal has a transient character. The numerical experiments with pulses in the FH-N system have indicated that the velocity of a pulse increases with the distance separating it from the preceding ones [125]. Thus, a pulse which propagates $3{\cdot}t_p$ after the preceding one is faster than that propagating $2{\cdot}t_p$ after the preceding one. In the long time limit one obtains a periodic signal, the frequency of which is 2/5 of the original one. The stability of the 2/5 transforming mode described here has been confirmed by calculations carried out up to t_{max}=10000.

2.4.3 Numerical difficulties.

The solutions which correspond to the filtering ratio 1/2 or 1/3 are quite stable numerically and they cover a large part of the parameter space. In order to learn more about what happens in the gray areas of Figs. 18 and 19 a series of calculations has been performed with one of the parameters (the

http://rcin.org.pl

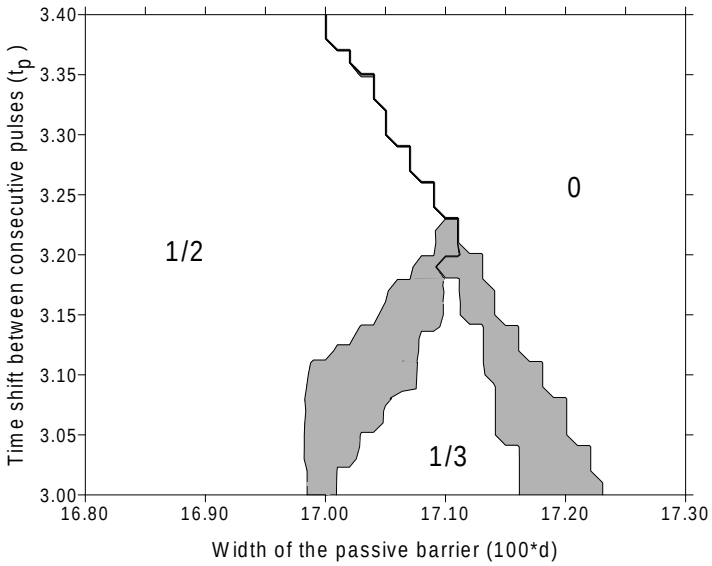

Figure 19. Filtering ratio (f_o/f_p) for the FitzHugh - Nagumo model as a function of the barrier's width (d) and the time shift between consecutive pulses (t_p). The white, labeled areas correspond to the situation when f_o is the fraction of f_p given in the picture. Gray color marks more complicated transformations of frequency.

http://rcin.org.pl

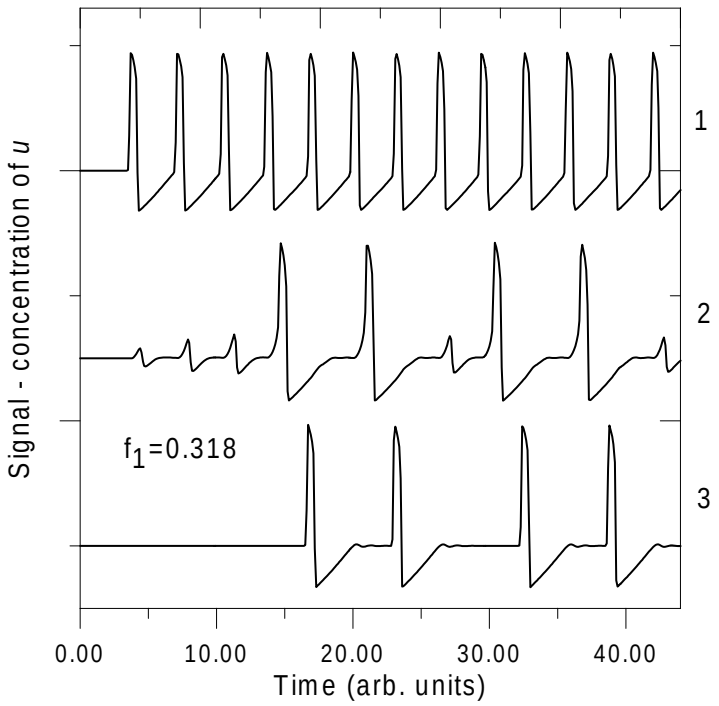

Figure 20. The time evolution of activator's concentration in the FitzHugh - Nagumo model at the grid point i_1 (curve 1), at the grid point i_2 (curve 2), and at the grid point i_3 (curve 3) for d=0.1707. Curves 1, 2 and 3 correspond to f_p=0.318 and illustrate the frequency transforming ratio equal to 2/5.

http://rcin.org.pl

width of the passive barrier d or the time shift between consecutive incident pulses t_p) fixed and the other changing within a certain range. By monitoring the input and output signals (similar to those presented in Fig. 17) one is not only able to calculate the filtering ratio for the given combination of d and t_p, but also describe the sequence of transmitted/stopped pulses in the input signal, which leads to a particular value of f_o/f_p. The calculations have been done for parameters on the lines of constant d or t_p shown in Fig. 18. The computations have to be performed for a period of time long enough to observe many full cycles of signal transformation. However, it has been discovered that the results of calculations are quite sensitive with respect to the size of the grid and the time integration step (dt) used in computations.

Figure 21 presents a set of curves showing the filtering ratio for t_p=3.10 (f_p=0.323) as a function of d. The considered values of parameters line on the horizontal dashed line (a) in Fig. 18. All results have been obtained for dt=1·10^{-3} and the calculations have been performed up to t_{max}=500. For curve (a), marked with empty triangles, a uniform grid with n=400 has been used. Curve (b), marked with empty diamonds, indicates the results for a uniform grid with n=800. The passive gap has been located between n_1=180 and n_2=189 for n=400, n_1=360 and n_2=377 for n=800. In case of curves (c) - filled circles and (d) - empty circles, adaptive grids with n=800 (c) or n=870 (d) respectively have been applied. The value of dl_b in these calculations depends on system's length l and the number of grid points used. The signals at indicators i_1 and i_2, located at approximately constant distance of l_i=0.6 (in the dimensionless units of distance) before and behind the passive barrier have been analyzed (cf. the bottom part of Fig. 15).

Results presented in Fig. 21 show a rich structure of different filtering ratios, which is much more complex than the one shown in Fig. 0C for

http://rcin.org.pl

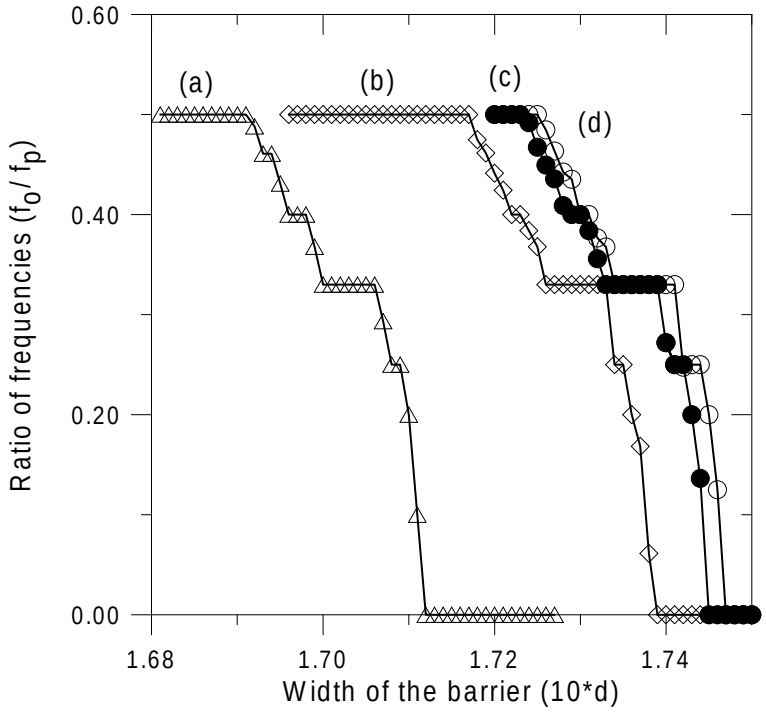

Figure 21. Results for the FitzHugh - Nagumo model. Filtering ratio f_o/f_p for fixed t_p=3.10 (f_p=0.323) and d changing within the presented range. All results have been obtained for dt=1·10^{-3}, t_{max}=500, but for each of the curves (a) - (d) different grids have been used. This figure illustrates the dependence of the results on computational parameters. **Curve (a)** - marked with empty triangles - uniform grid with n=400. **Curve (b)** - marked with empty diamonds - uniform grid with n=800. **Curve (c)** - marked with filled circles - adaptive grid with n=800. **Curve (d)** - marked with empty circles - adaptive grid with n=870.

http://rcin.org.pl

the "naive" model of an excitable system. Of course, one can observe some similarities: the region of d for which f_o/f_p=1/2 is the dominant one, and the second most important is f_o/f_p=1/3. But there are also filtering ratios between 1/3 and 1/2, which are absent in the "naive" model (see Section 1.2.2). The calculations show that although f_o/f_p as a function of d looks very similar for different values of parameters of integration, it shifts towards greater values of d when more accurate integration techniques are applied. A significant shift between curves (a) and (b) in Fig. 21 indicates that for the uniform grids the results strongly depend on the grid size. It is worth noticing that the behavior of the filtering ratio as a function of d does not change, but the function as a whole is just shifted towards wider barriers. It is expected that for yet finer grid one should obtain results which are numerically stable, but a finer grid means that more grid points should be used to describe a system of the same size. However, in the implicit method of solving parabolic reaction-diffusion equations the solution at each time step is obtained via iterations. In case of the FH-N model the roundup errors lead to instabilities when few thousands of grid points are used. The adaptive grids (Fig. 16) allow one to obtain more accurate numerical solutions. For such grids the fine resolution within the most important area of the investigated system may be achieved without using large number of grid points, which provides both accuracy and stability of computations. As already mentioned, curve (c) in Fig. 21 has been obtained for the adaptive grid with n=800. The resolution in the neighborhood of the passive gap for this grid is $dl_b=dl/8\approx0.06$ (for $l\approx25.72$), which is four times smaller than dl for the finest uniform grid. For curve (d) this resolution is twice higher, but $f_o/f_p(d)$ obtained for both grids (curves (c) and (d) in Fig. 21) are almost identical. Therefore, the adaptive grid with n=800 seems to be sufficient for the calculations and it has been

http://rcin.org.pl

used to obtain results given below.

Several values of the time step of integration (dt=5·10^{-3}, 1·10^{-3} and 1·10^{-4}) have been used to verify the consistency of the results. Although the implicit algorithms should be in general stable for all values of time and space integration steps, it has been observed that numerical instabilities may appear for dt=5·10^{-3} and large n. On the other hand, the results for dt=1·10^{-3} and dt=1·10^{-4} have been regular and consistent. Consequently, dt=1·10^{-3} has been used to study the complex frequency transforming patterns, described in the next section.

2.4.4 Complex patterns of output signals.

The results presented in this section have been obtained for the adaptive grid with n=800. The passive area has been located between n_1=400 and n_2=431 (30 grid points inside the passive barrier). The incoming and outgoing pulses have been monitored at grid points i_1=390 and i_2=441 respectively. The computations have been carried out with the time step dt=1·10^{-3} up to t_{max}=500, if not explicitly stated otherwise. Circa 150 pulses arrive at the barrier within the selected time t_{max}.

A special notation has been introduced to describe the output signal [124]. The incident pulses observed at i_1 introduce a natural time scale in the system. One writes "1" if a pulse gets successfully through the passive barrier and is observed at i_2 or "0" otherwise. Thus the output signal may be coded as a sequence of "0" and "1". In such notation a common case in which every second pulse passes (filtering ratio f_o/f_p=1/2) is coded as *(01)* and the mode "1/3", is described as *(001)*. It is understood that the given sequence repeats periodically. A pattern coded as $(abc...)^p(def...)^q$ (where p and q are positive integer numbers) means, that behind the barrier first the sequence

http://rcin.org.pl

(abc...) is observed p times, and next the sequence *(def...)* appears q times. In this notation non-periodic modes correspond to an infinite sequence of *(abcde...)*. If pattern's sequence is finite, then it is very easy to calculate the corresponding filtering ratio f_o/f_p because it equals to the sum of the symbols in the sequence divided by the number of symbols. For non-periodic modes one can estimate the filtering ratio using a finite part of the sequence and of course the more pulses is taken into account, the better approximation is achieved.

Figure 22 presents the filtering ratio for t_p=3.10 (f_p=0.323) as a function of the width of the passive barrier changing from 0.171 to 0.176 with increment of 0.0001 (this has been achieved by changing the total length of the system l from 27.49 to 28.19 with increment of 0.016). This value of t_p corresponds to line (a) in Fig. 18. The results coming from our computations are marked with filled circles. In Fig. 22 one may notice several plateaus, which correspond to simple patterns of frequency transforming and are labeled with appropriate filtering ratios. Looking from left to right there are modes: "1/2" with the sequence *(01)*, "2/5" with *(01)(001)*, "1/3" - *(001)*, "1/4" - *(0001)* and finally "0" with the sequence *(0)*. It is remarkable that a "simple" frequency transformation occurs within a wider range of barrier's width than complex ones. Other interesting transmission patterns, located between those plateaus, have also been observed, but the ranges of values of d within which those patterns appear are so narrow that they have been detected just for a single width of the barrier. The unique patterns have been labeled with letters a - k in Fig. 22. Probably the most complicated transmission pattern is associated with point a, located just below the plateau "1/2". In this case the sequence of pulses behind the barrier is: $(01)^{14}(001)(01)^{13}(001)$ and the corresponding filtering ratio f_o/f_p=29/60. For point b in Fig. 22

http://rcin.org.pl

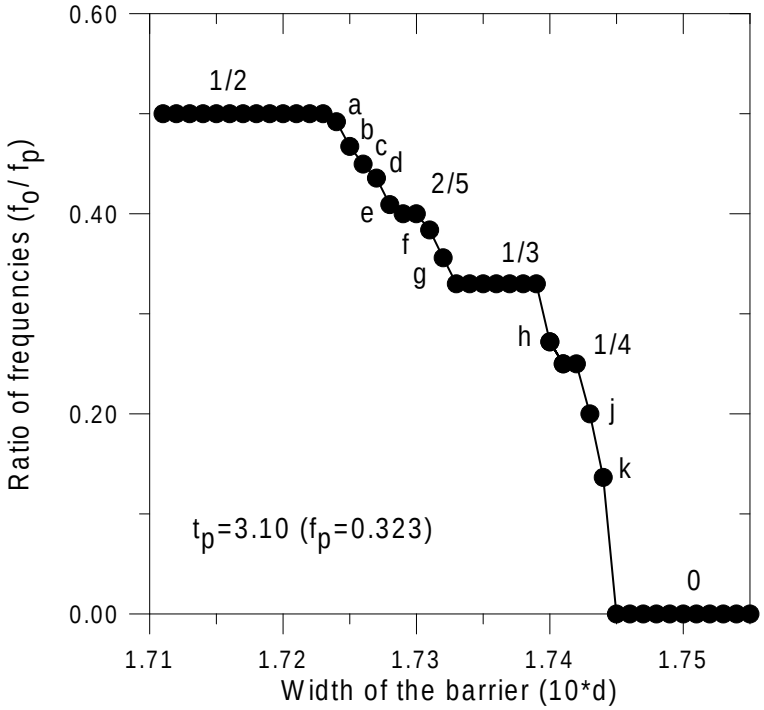

Figure 22. Results for the FitzHugh - Nagumo model. Filtering ratio f_o/f_p for fixed t_p=3.10 (f_p=0.323) and d changing within the presented range. The filled circles correspond to computational points. The curve forms several plateaus, which are labeled with corresponding values of the filtering ratio (1/2, 2/5, 1/3, 1/4 and 0). At points labeled a - k the following values of f_o/f_p (and transmission patterns) have been observed: a - 29/60, *(01)*^{14}*(001)(01)*^{13}*(001)*; b - 11/24, *(01)*^{4}*(001)(01)*^{5}*(001)*; c - 4/9, *(01)*^{3}*(001)*; d - 3/7, *(01)*^{2}*(001)*; e - 9/22, *(01001)*^{3}*(0101001)*; f - 3/8, *(01)(001)*^{2}; g - 7/20, *(01)(001)*^{6}; h - 2/7, *(001)(0001)*; j - 1/5, *(00001)* and k - 1/7, *(0000001)*.

http://rcin.org.pl

the corresponding pattern is *(01)*^{4}*(001)(01)*^{5}*(001)* resulting in f_o/f_p=11/24, point *c* - *(01)*^{3}*(001)*, f_o/f_p=4/9; point *d* - *(01)*^{2}*(001)*, f_o/f_p=3/7; point *e* - *(01001)*^{3}*(0101001)*, f_o/f_p=9/22; point *f* - *(01)(001)*^{2}, f_o/f_p=3/8; point *g* - *(01)(001)*^{6}, f_o/f_p=7/20; point *h* - *(001)(0001)*, f_o/f_p=2/7; point *j* - *(00001)*, f_o/f_p=1/5 and point *k* - *(0000001)*, f_o/f_p=1/7.

Figure 18 suggests that transmission patterns corresponding to filtering ratios greater than 1/2 are also present. Such patterns are absent in the "naive" model of excitable systems (Figs. 0B - 0C). To see them clearly the calculations for t_p=3.70 (f_p=0.270) have been performed for the barrier's width d changing from 0.130 to 0.171 with increment of 0.001 (l changing from 20.93 to 27.49 with increment of 0.16). This value of t_p corresponds to line (b) in Fig. 18. The results are plotted in Figure 23. Indeed, one may see here several plateaus, labeled with corresponding filtering ratios, which are greater than 1/2. From left to right there are: plateau "1" with the sequence *(1)*; plateau "6/7" - *(0111111)*; plateau "4/5" - *(01111)*; plateau "3/4" - *(0111)*; plateau "2/3" - *(011)*; plateau "1/2" - *(01)* and plateau "0" with the trivial transmission pattern *(0)*. Even more complex output signals have been observed. The points labeled with letters correspond to the following patterns and filtering ratios: point *a* - *(0)(1)*^{35}, f_o/f_p=35/36; point *b* - *(0)(1)*^{14}, f_o/f_p=14/15; point *c* - *(0)(1)*^{10}, f_o/f_p=10/11; point *d* - *(0)(1)*^{8}, f_o/f_p=8/9 and point *e* - *(011111)*, f_o/f_p=5/6. The output signals observed here are dual to those with filtering ratios smaller than 1/2.

Figure 24 presents the filtering ratio for d=0.160 (l=25.72) plotted versus the frequency of incident pulses $f_p \in [0.25, 0.28]$ (the time shift between consecutive pulses changing from 3.57 to 4.00 with increment of 0.02; approximate values of t_p are given on the top axis of Fig. 24). These values of d are placed on the line (c) in Fig. 18. The numerical labels in Fig. 24 give the filtering

http://rcin.org.pl

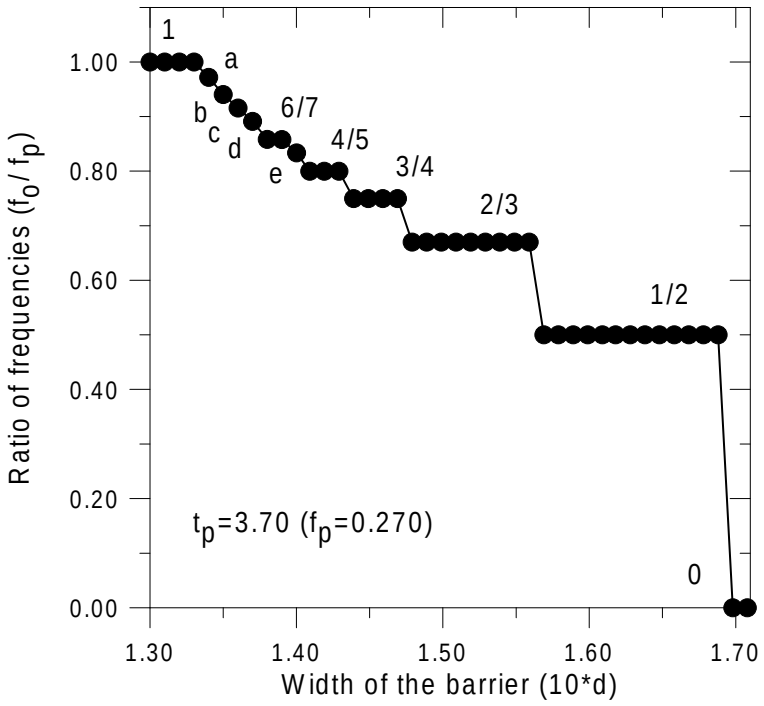

Figure 23. Results for the FitzHugh - Nagumo model. Filtering ratio f_o/f_p for fixed t_p=3.70 (f_p=0.270) and d changing within the presented range. The filled circles correspond to computational points. The plateaus are labeled with corresponding values of the filtering ratio (1, 6/7, 4/5, 3/4, 2/3, 1/2 and 0). At points labeled a - e the following values of f_o/f_p (and transmission patterns) have been observed: a - 35/36, *(0)(1)*^{35}; b - 14/15, *(0)(1)*^{14}; c - 10/11, *(0)(1)*^{10}; d - 8/9, *(0)(1)*^{8} and e - 5/6, *(011111)*.

http://rcin.org.pl

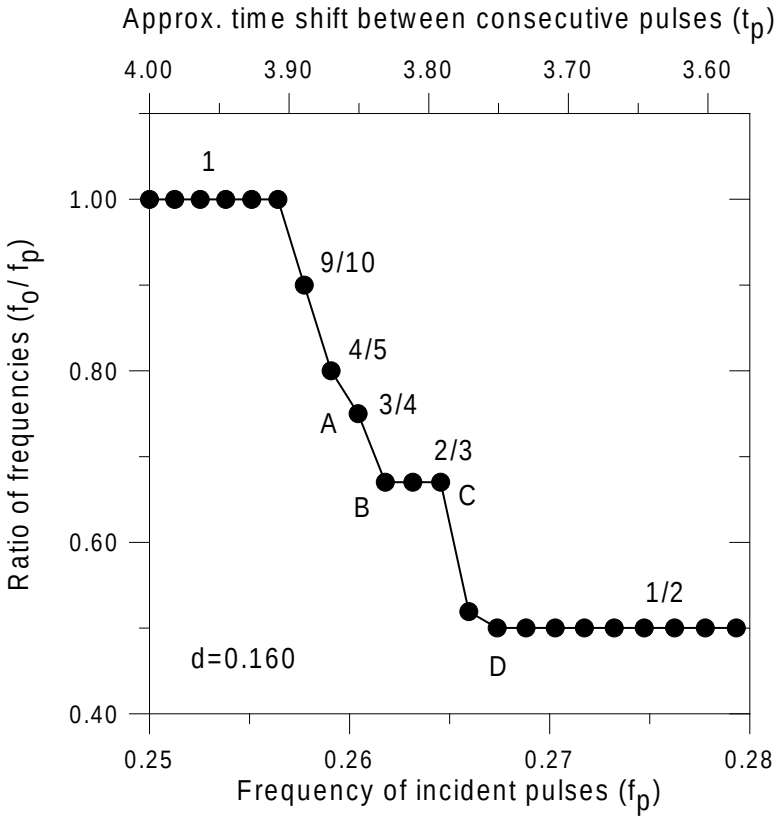

Figure 24. Results for the FitzHugh - Nagumo model. Filtering ratio f_o/f_p for fixed d=0.160 and f_p changing from 0.25 to 0.28 (see the bottom axis), which corresponds to t_p decreasing from 4.00 to 3.57 (see the approximate top axis). The filled circles correspond to computational points. The plateaus as well as single points are labeled with corresponding values of f_o/f_p (1, 9/10, 4/5, 3/4, 2/3 and 1/2). The letters A, B, C and D mark the intervals of the diagram which have been studied with a higher resolution. The results for the interval AB are presented in Fig. 25 and for the interval CD in Fig. 26.

http://rcin.org.pl

ratios observed for corresponding plateaus or points. In Fig. 24 from left to right there are: plateau "1" with the sequence *(1)*; point "9/10" with the sequence *(0)(1)*^{9}; point "4/5" - *(01111)*; point "3/4" - *(0111)*; plateau "2/3" - *(011)* and plateau "1/2" with *(01)*. In order to check whether the filtering ratio is a monotonic function of f_p, a number of calculations for $f_p \in [0.2604, 0.2618]$ and for $f_p \in [0.2646, 0.2674]$ have been performed. The ends of these intervals correspond to f_p for points A, B, C, D in Fig. 24. The system's behavior has been probed using $\delta t_p = 0.002$ (corresponding to $\delta f_p = 0.00014$). In the interval AB the behavior is trivial, which means that studied systems splits into two classes corresponding to *(0111)* and *(011)* modes (cf. Figure 25).

Similar calculations have been performed for systems located between points C and D in Fig. 24 (this interval corresponds to $f_p \in [0.2646, 0.2674]$). In this case two patterns (α and β in Figure 26) have been observed between the plateaus corresponding to filtering ratios 2/3 (*(011)* mode) and 1/2 (*(01)* mode). One of these patterns (β) describes quite simple transformation of the original signal to *(01)(011)* mode, which is just 1:1 mixture of the neighboring modes. The other point (α) corresponds to more interesting behavior. Using the same dt and dl_b as for the other points shown in Fig. 26 (filled circles) the filtering ratio $f_o/f_p = 0.51917$ has been observed. The decrease in time step dt increases the filtering ratio as follows: $dt = 1 \cdot 10^{-4}$ gives $f_o/f_p = 0.55602$ (empty circle), $dt = 2 \cdot 10^{-5}$ gives $f_o/f_p = 0.57594$ (empty triangle), $dt = 1 \cdot 10^{-5}$ gives $f_o/f_p = 0.57895$ (cross). Moreover it has been observed that time intervals between transmitted pulses are not always a multiplicity of t_p. In order to explain it the time evolution *u(t)* at the points i_1 and i_2 has been examined. Figure 27 shows the relevant part of it. One can notice that in some cases the transmitted signal does not develop into a pulse, *u(t)* slightly decreases

http://rcin.org.pl

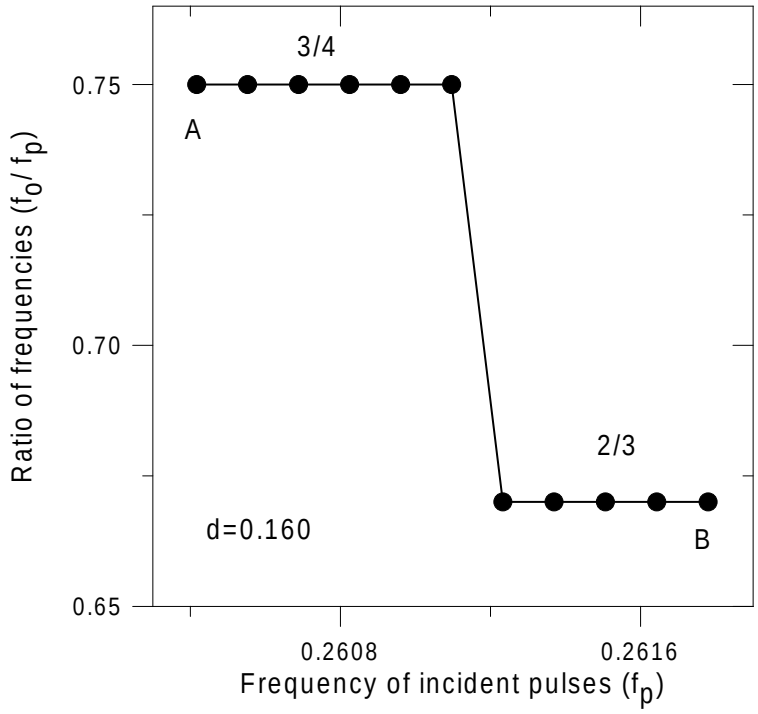

Figure 25. Results of a more detailed examination of the interval AB from Fig. 24. Filtering ratio f_o/f_p for fixed d=0.160 and f_p changing from 0.2604 to 0.2618. Points A and B in this figure correspond exactly to points A and B in Fig. 24. No filtering ratios different from 3/4 or 2/3 have been observed.

http://rcin.org.pl

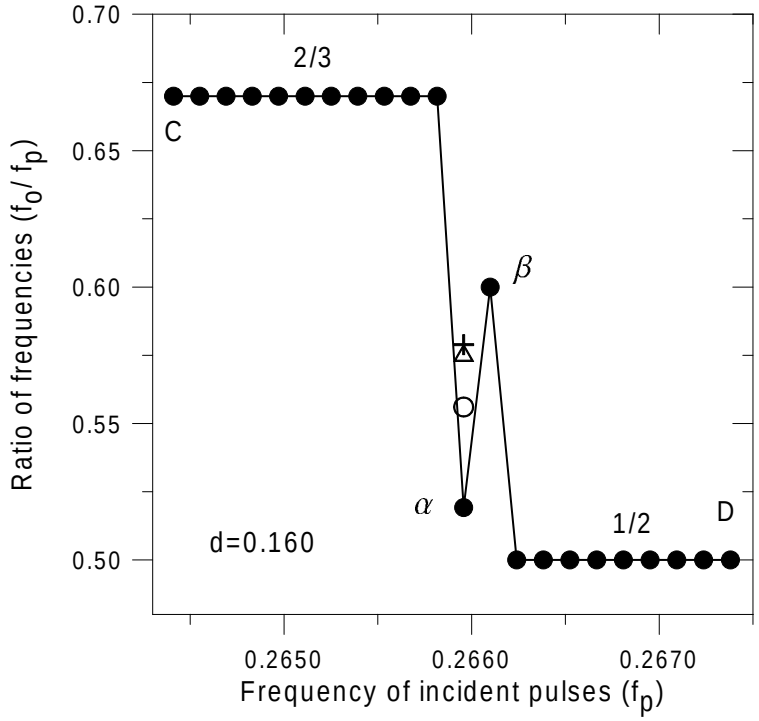

Figure 26. Results of a more detailed examination of the interval CD from Fig. 24. Filtering ratio f_o/f_p for fixed d=0.160 and f_p changing from 0.2646 to 0.2674. The filled circles mark the computational points. Points C and D in this figure correspond exactly to points C and D in Fig. 24. A "strange" point α has been found between plateaus 2/3 and 1/2 (labeled with values of the filtering ratio), for which the value of f_o/f_p depends on the time step of integration. Different symbols mark the values of the filtering ratio obtained for: dt=1·10^{-3} (filled circle), dt=1·10^{-4} (empty circle), dt=2·10^{-5} (empty triangle), dt=1·10^{-5} (cross). In the studied region the point β has been observed, which is regular and corresponds to the transmission pattern *(01)(011)* (thus f_o/f_p=3/5).

http://rcin.org.pl

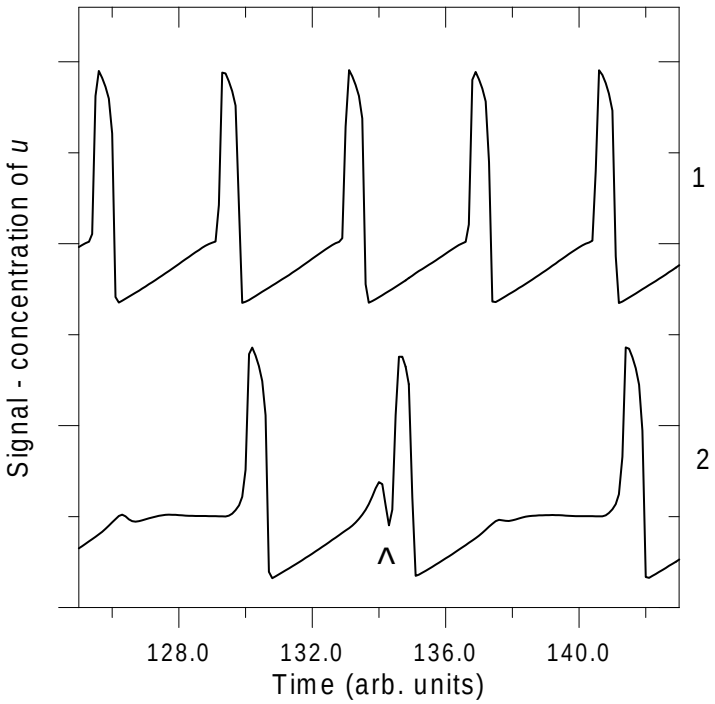

Figure 27. Results for the FitzHugh - Nagumo model. A part of the time evolution of the value of u at the grid point i_1 (input signal - the upper curve 1) and at the grid point i_2 (output signal - curve 2) observed for d=0.160, f_p=0.2660 with dt=1·10^{-5} (point α - the cross in Fig. 26). The arrow marks the position of the "strange excitation" in the output signal.

http://rcin.org.pl

and then it starts to increase again, forming a pulse shifted with respect to the forcing signal. Such strange behavior for f_p=0.2660 (t_p=3.76) does not disappear when decreasing dt and dl_b. The moment it appears first and the time intervals between successive strange excitations depend on dt, but no regularities have been noticed. The presence of irregular "strange excitations" makes the filtering ratio at the point α dependent on dt. The value of f_o/f_p at this point still remains smaller than 0.6, so one cannot exclude a non-monotonic dependence of the filtering ratio on f_o/f_p. Moreover, such strange excitations have been observed for the whole range of time integration steps used, so one is unable to blame numerical instabilities for their presence. The time evolution of the output signal between the strange excitations is a mixture of *(01)* and *(011)* modes with different proportions.

2.4.5 Results for the R-Z model.

In the calculations for the Rovinsky - Zhabotinsky model a uniform grid with n=320, n_1=150, n_2=155 has been used as well as the dimensionless time integration step $d\tau$=1·10^{-3}. The pulses have been initiated at the left end of the interval by increasing the value of x to 0.1.

Figure 28 presents a typical signal (value of x) observed at the first and second indicators (grid points i_1=148 and i_2=157) for dl=0.814 and τ_p=30.0 (255sec). For these values of parameters the excitation at the boundary gives a regular and stable train of pulses. In calculations, the results of which are shown in Fig. 28, n_2 is changed to obtain barriers of different widths. The upper curve (1) corresponds to incident pulses (reference signal at indicator 1). For n_2=151 (no passive barrier - curve 2) the same signal (shifted in time) is observed at indicator 2. The same behavior is observed for a thin, fully transparent passive barrier (n_2=153 - curve 3). All incident pulses observed

http://rcin.org.pl

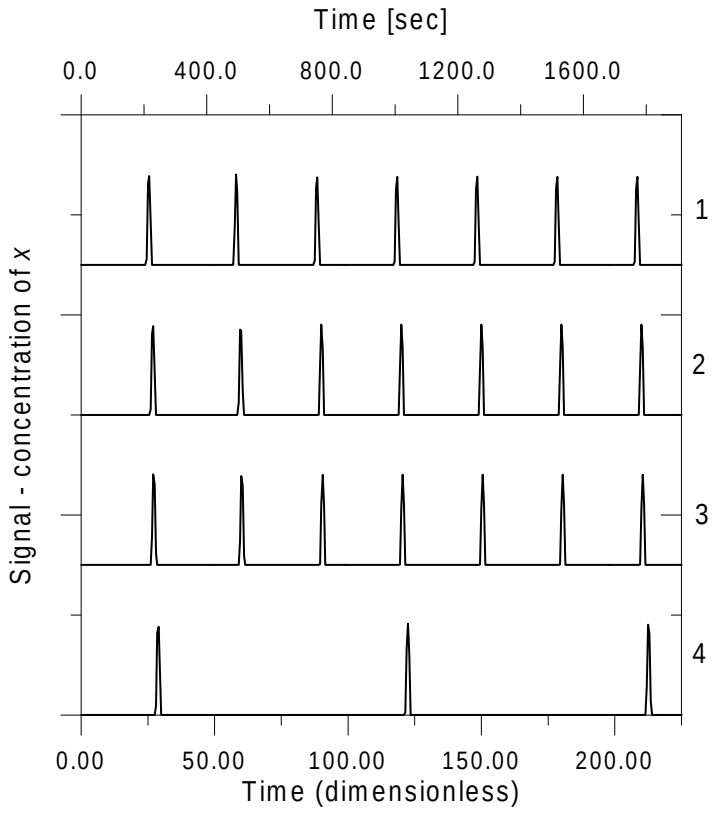

Figure 28. The time evolution of activator's concentration at the grid point i_1 (the upper curve 1) and at the grid point i_2 (curves 2-4). The evolutions at i_2 correspond to no barrier (curve 2), a narrow transparent barrier (curve 3) and a barrier for which frequency transformation occurs (curve 4). Results for the Rovinsky - Zhabotinsky model (Eqs. (2.5-2.8)), τ_p=30 (f_p=0.033)), d=1.628 ($0.0150 \cdot \sqrt{\frac{D_X}{D_{X_0}}} cm$) (curve 3), d=3.256 ($0.0300 \cdot \sqrt{\frac{D_X}{D_{X_0}}} cm$) (curve 4). τ_p=30 corresponds to $255 sec$.

http://rcin.org.pl

at indicator 1 get through the barrier and are also observed at indicator 2. For n_2=155 every third of the incident pulses is transmitted through the barrier as observed at indicator 2 (curve 4). In this case the width of the passive barrier is 3.256 ($0.0300 \cdot \sqrt{\frac{D_X}{D_{X_0}}} cm$).

It has been found that for the R-Z model the minimal time necessary to initiate a new pulse after the first pulse has been produced in the system is $\tau_{p,min,R-Z} \approx 5.8$ ($49 sec$) but one has to use much higher values of τ_p to obtain a stable, regular train of pulses. The range of τ_p from 30 ($255 sec$) to 60 ($510 sec$) with increment of 2 ($17 sec$) and the range of d changing from 3.188 ($0.02939 \cdot \sqrt{\frac{D_X}{D_{X_0}}} cm$) to 3.295 ($0.03037 \cdot \sqrt{\frac{D_X}{D_{X_0}}} cm$) have been studied. τ_{max}=2000 ($17000 sec$) has been used, so during the evolution from 33 to 66 pulses may appear in the system for each combination of τ_p and d.

The results are shown in Figure 29. For all the examined values of d and τ_p every excitation creates a pulse. The filtering ratio f_o/f_p presented in Fig. 29 reveals areas of parameters' values for which every second or every third of the incident pulses is transmitted (these regions are labeled with "1/2" and "1/3" respectively). Label "0" in Fig. 29 indicates the area in which no pulse can cross the passive barrier. The gray regions between the white, labeled areas in Fig. 29 correspond to more complex transmission patterns. Unlike for the FH-N model, the transformation of frequency occurs only for barriers which are narrower than the penetration depth for a single pulse given in Section 2.2 $d_{c,R-Z} \approx 3.295$ ($0.03037 \cdot \sqrt{\frac{D_X}{D_{X_0}}} cm$).

Figure 30 presents the filtering ratio f_o/f_p plotted versus the frequency of incident pulses f_p for a selected barrier's width d=3.2375 ($0.0298 \cdot \sqrt{\frac{D_X}{D_{X_0}}} cm$). This value of d corresponds to the dashed vertical line in Fig. 29. Here the frequencies f_p and f_o are dimensionless frequencies, calculated as the inverse of dimensionless time τ. For $f_p \in [0.0167,\ 0.0278]$ every second of incident

http://rcin.org.pl

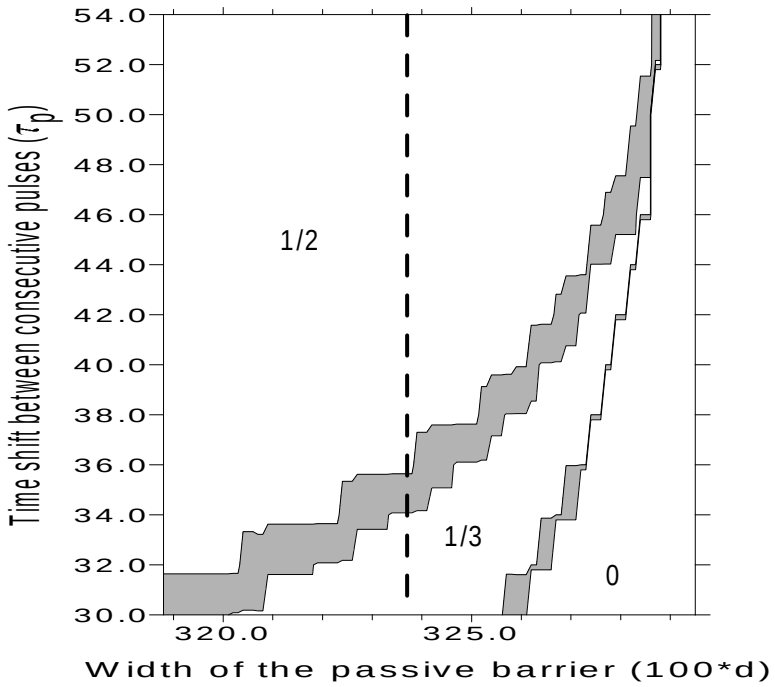

Figure 29. Filtering ratio (f_o/f_p) for the Rovinsky - Zhabotinsky model as a function of the barrier's width (dimensionless - d) and the time shift between consecutive pulses (dimensionless - τ_p). The white, labeled areas correspond to the situation when f_o is the fraction of f_p given in the picture. Gray color marks more complicated transformations of frequency. The dashed line indicates d=3.2375.

http://rcin.org.pl

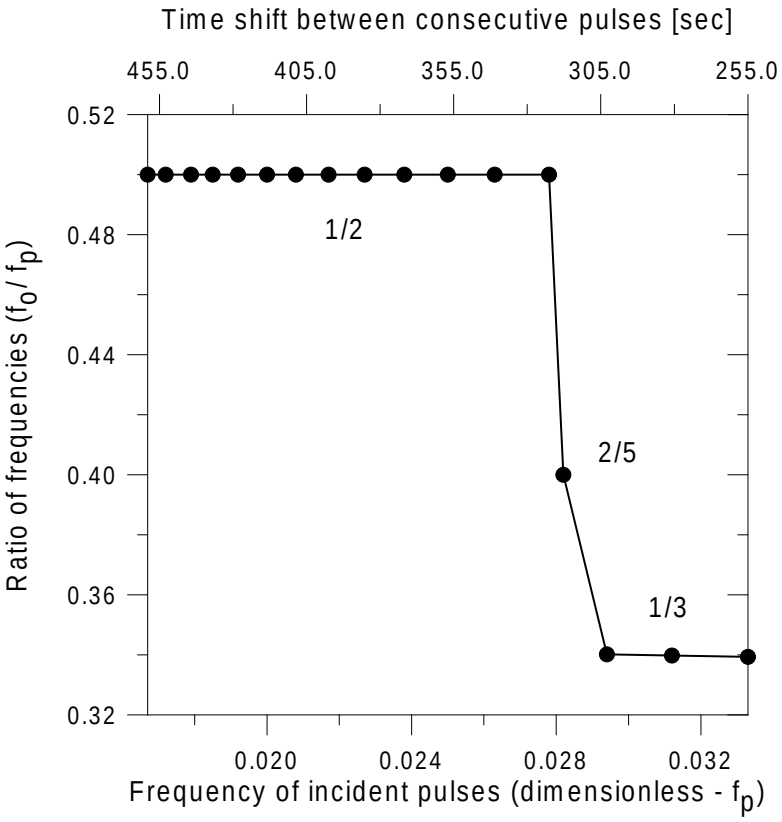

Figure 30. Filtering ratio in the Rovinsky - Zhabotinsky model for a selected barrier's width d=3.2375 ($0.0298 \cdot \sqrt{\frac{D_X}{D_{X_0}}} cm$). This value of d corresponds to the dashed vertical line in Fig. 29. f_o/f_p is presented as a function of the dimensionless frequency of incident pulses (f_p - bottom axis) or the (approximate) physical time shift between consecutive incident pulses (t_p [sec] - top axis). Labels give the filtering ratio (f_o/f_p).

http://rcin.org.pl

pulses gets through the barrier. For $f_p \geq 0.0294$ only one out of three incident pulses gets through the barrier (thus the filtering ratio is $f_o/f_p = 1/3$).

2.4.6 Results for the Oregonator model.

In order to check whether the frequency transforming is a typical feature of a passive barrier in an excitable medium calculations for the Oregonator model [126, 127, 128] have been performed. The form of the model presented in [127] with diffusion of the activator added has been used. In the Oregonator model the active field is described by the following reaction - diffusion equations (2.17-2.18):

$$\frac{\partial u}{\partial t} = \frac{1}{\epsilon}[u(1-u) - f \cdot v \cdot \frac{u-q}{u+q}] + D\nabla^2 u \tag{2.17}$$

$$\frac{\partial v}{\partial t} = u - v \tag{2.18}$$

where u corresponds to the scaled concentration of activator ($HBrO_2$) and v - to the scaled concentration of catalyst (Ce^{4+}) [127]. In the passive regions, without catalyst, the concentrations of u and v evolve according to Eqs. (2.19-2.20):

$$\frac{\partial u}{\partial t} = -\frac{1}{\epsilon} \cdot u^2 + D\nabla^2 u \tag{2.19}$$

$$v = 0 = const. \tag{2.20}$$

In Eqs. (2.17-2.20) t denotes the scaled time and ϵ (a time scale parameter) is small [127]. Another small parameter q is connected to the rate constants of the reactions involved in the Oregonator model. The stoichiometric parameter f is proportional to the average number of bromide ions released per metal ion reduced by organic matter. The details of scaling are described in [127].

In the calculations the following values of parameters have been used: ϵ=0.05 [128], f=3 [127], q=0.0002 [127] and D=1.0. For these values of

http://rcin.org.pl

parameters the stationary state of the system within the active areas corresponds to

$$u_{sa} = v_{sa} = 3.9988 \cdot 10^{-4} \tag{2.21}$$

and it is excitable. In the passive areas the stationary solution is given by

$$u_{sp} = v_{sp} \equiv 0 \tag{2.22}$$

In the calculations for this model a uniform grid with dl=0.3733, (n=400), n_1=200, dt=1·10^{-4} and t_p=10.4. The pulses have been initiated on the left end of the interval by decreasing v to v_{ini}=0.0. The evolution of this system has been studied up to t_{max}=1000 (so that over 95 pulses has been involved in each experiment). It has been observed that a passive barrier in the Oregonator model also reveals frequency transforming properties. Figure 31 presents a sample signal (the value of u) observed at the first and second indicators (grid points i_1=198 and i_2=213 respectively). As mentioned above, n_1=200 while n_2 is changed to obtain barriers of different width. The upper curve (1) corresponds to incident pulses (reference signal at indicator 1). For n_2=201 (no passive barrier - curve 2) the same signal (shifted in time) is observed at indicator 2. The same behavior is observed for a narrow, fully transparent passive barrier (n_2=206 - curve 3). All incident pulses observed at indicator i_1 get through the barrier and are also observed at indicator i_1. For a wider barrier (n_2=211) every second of the arriving pulses is transmitted through the barrier and may be observed at indicator 2 (curve 4). For curve 4 the width of the passive barrier is 3.733. In this case, as for R-Z (BZ) system, the frequency transforming occurs for barriers narrower than the penetration depth for a single pulse, because the first transmitted pulse makes the barrier impenetrable for the subsequent ones (note that in Fig. 31 the first of incident pulses gets through the barrier).

http://rcin.org.pl

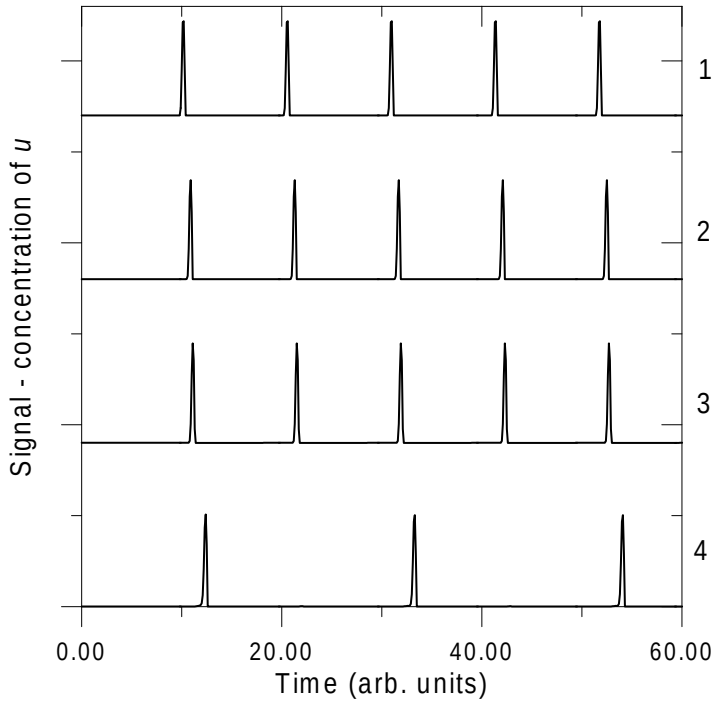

Figure 31. The time evolution of activator's concentration at the grid point i_1 (the upper curve 1) and at the grid point i_2 (curves 2-4). The evolutions at i_2 correspond to no barrier (curve 2), a narrow transparent barrier (curve 3) and a barrier for which frequency transformation occurs (curve 4). Results for the Oregonator model (Eqs. (2.17-2.20)), t_p=10.4 (f_p=0.096), d=1.867 (curve 3), d=3.733 (curve 4).

http://rcin.org.pl

2.4.7 Implications of frequency transforming for selected signal processing reactors.

Having in mind the results of previous sections one may expect that the properties of signal processing reactors which include a passive barrier should depend on input signal frequency. In this chapter the effect of frequency of input signal on two of such devices is discussed.

A chemical diode is an asymmetric junction of two active areas, which transmits pulses of excitation coming from one direction and stops those arriving from the other one. The structure of the diode, as proposed by I. Motoike and K. Yoshikawa in [86] is shown schematically in Figure 32, where the darker area stands for the passive medium and the brighter areas correspond to the active one. The left edge of the passive region is a straight line, while the lines bounding of the active region on the right are perpendicular and form a tip. The shortest distance between the active areas is $d_n > 0$. No flux boundary conditions at all borders of the structure presented in Fig. 32 and free flow of mobile reagents between active and passive areas are assumed. Plain pulses of excitation may be initiated at the left hand side border and travel to the right or they can be excited on the right hand side border and travel to the left. The dashed lines on both sides of the junction, denoted by i_1 and i_2, mark the indicators. The propagation of pulses through the junction is studied by measuring the mean value of the concentration of the activator (u or x) along these lines. Indicators i_1 and i_2 are located symmetrically with respect to the longitudinal axis of the junction and their length is about half of the width of the whole device. A travelling pulse of excitation may get from one active area to the other one through the passive gap, provided that the gap is not too wide.

As already mentioned (Section 2.2), I. Motoike and K. Yoshikawa found

http://rcin.org.pl

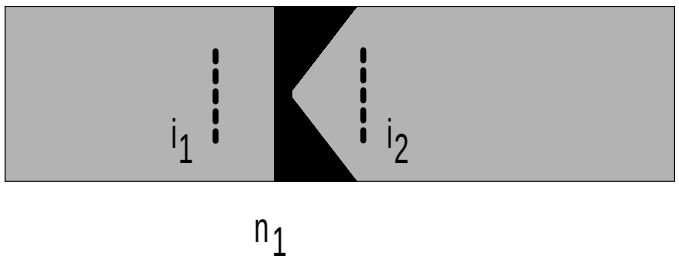

Figure 32. The scheme of a chemical diode. Brighter areas correspond to active regions, darker ones show the passive gap. The gap starts to the right from line n_1 of the grid (excluding n_1). Two dashed lines on both sides of the junction show the position of "indicators", at which the mean values of u (for the FH-N model) or x (for the R-Z model) as functions of time are recorded. For such geometry of the diode a single pulse of excitation may travel through the junction from left to right, but not in the opposite direction.

http://rcin.org.pl

[86] that the penetration depth strongly depends on the geometry of the boundary between active and passive media. They used the FH-N model (Eqs. (2.1-2.4)) and studied the propagation of pulses in a junction shown in Fig. 32. According to their results [86], if the penetration depth for a pulse propagating to the right is denoted by d_c, then the penetration depth for a pulse travelling in the opposite direction is only $0.63 \cdot d_c$. Results obtained for the passive barrier within the FH-N model (Section 2.2) give $d_{c,FH-N} \approx 0.163$. Now building a diode is very easy, because it is sufficient to separate the active areas by a passive field characterized by appropriate d_n, such that $0.63 \cdot d_{c,FH-N} < d_{n,FH-N} < d_{c,FH-N}$. For the purpose of tis work $d_{n,FH-N}=0.1152$ has been selected. A similar geometry of the reactor, which works as a signal diode, may be used in the case of Rovinsky - Zhabotinsky model. Here $d_{n,R-Z}=3.0$ ($0.02765 \cdot \sqrt{\frac{D_X}{D_{X_0}}} cm$) has been used. This is slightly smaller than the penetration depth $d_{c,R-Z}=3.295$ ($0.03037 \cdot \sqrt{\frac{D_X}{D_{X_0}}} cm$).

The work of a chemical diode is illustrated in Figure 33 (for the FH-N model) and Figure 34 (for the R-Z model). In both figures two upper curves (no. 1 and 2) correspond to a single plain pulse, excited on the left hand side boundary of the system and travelling to the right. The mean values of activator (u or x) along i_1 (curve 1) and i_2 (curve 2) are plotted as functions of time given at the top axis. The pulse which arrives first at i_1, gets through the passive gap and a moment later it is observed at i_2 (curve 2). The two lower curves (no. 3 and 4) illustrate the propagation of a pulse initiated on the right hand side boundary and travelling to the left. The mean values of u (or x) along i_2 (curve 3) and i_1 (curve 4) are plotted as functions of time shown on the bottom axis. In this case the pulse is first observed at i_2 (curve 3), but then it "dies out" within the passive area (curve 4 is just a straight line). The arrows mark the direction of propagation of the pulses,

http://rcin.org.pl

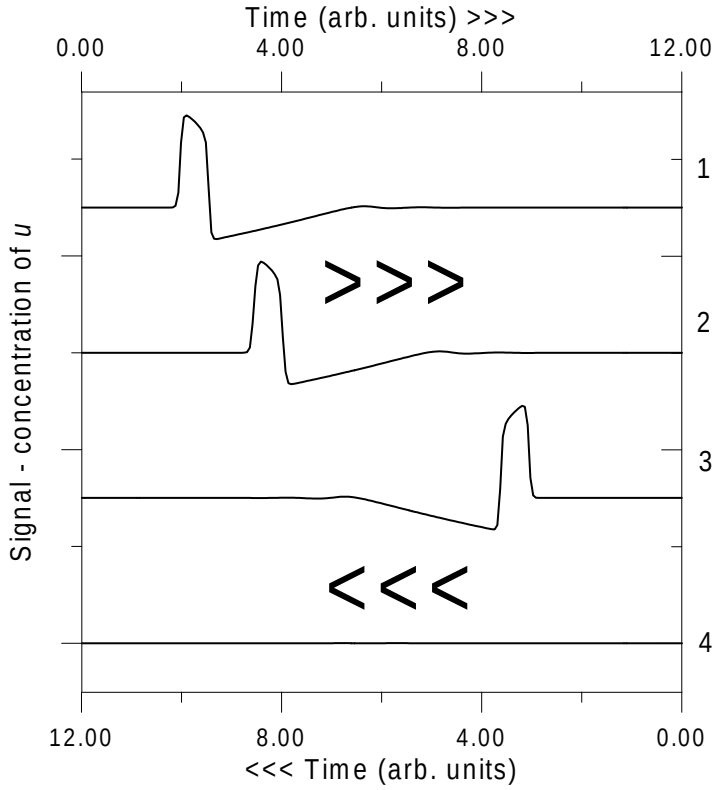

Figure 33. The time evolution of the value of u at the indicators i_1 (curves 1 and 4) and i_2 (curves 2 and 3). The two upper curves (no. 1 and 2) correspond to a pulse propagating from left to right (orientation defined by Fig. 32) and the corresponding time scale is at the top axis. In this case the diode transmits the pulse. The two lower curves (no. 3 and 4) correspond to a pulse propagating from right to left (cf. Fig. 32). In this case the pulse is stopped. The arrows mark the direction of propagation. Results for the FitzHugh - Nagumo model, $d_{n,FH-N}$=0.1152.

http://rcin.org.pl

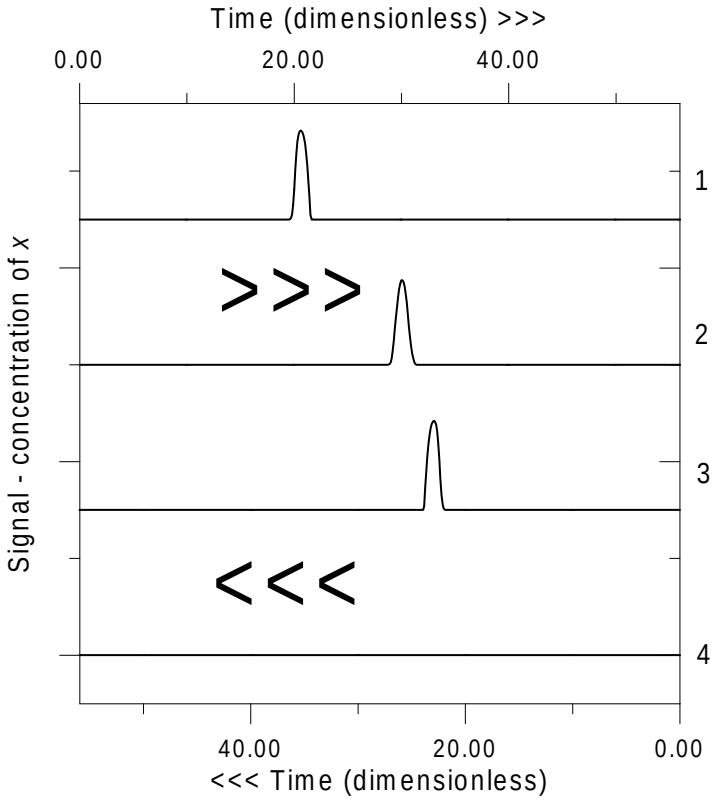

Figure 34. The time evolution of activator's concentration at the indicators i_1 (curves 1 and 4) and i_2 (curves 2 and 3). The two upper curves (no. 1 and 2) correspond to a pulse propagating from left to right (orientation defined by Fig. 32) and the corresponding time scale is at the top axis. In this case the diode transmits the pulse. The two lower curves (no. 3 and 4) correspond to a pulse propagating from right to left (cf. Fig. 32). In this case the pulse is stopped. The arrows mark the direction of propagation. Results for the Rovinsky - Zhabotinsky model, $d_{n,R-Z}$=3.0 ($0.02765 \cdot \sqrt{\frac{D_X}{D_{X_0}}} cm$).

http://rcin.org.pl

where the orientation is defined by Fig. 32. In Fig. 34 the mean values of x at the indicators are plotted versus dimensionless time τ (τ=1 corresponds to $8.5sec$).[15]

The results presented in Figs. 33 - 34 have been calculated using the implicit method already mentioned. For the FH-N model a rectangular area of 4.80x0.9792 covered with a square grid of 251x52 points has been considered (including borders, thus dl=0.0192). Indexing the vertical lines of the grid from 0 (left hand side border) to 250 (right hand side one) it may be specified that indicators are placed along i_1=80 and i_2=126. Both of them include 25 nodes. The passive area starts to the right from line n_1=100 (this line of the grid is still characterized by the active dynamics). The shortest distance between active areas is $d_{n,FH-N}$=0.1152, which is covered by six nodes. Time integration step dt=$5\cdot10^{-3}$ has been used. For the R-Z model the area of 240x38.25 has been covered with a square grid of 321x52 points, hence dl=0.75. The other parameters are respectively: i_1=130, i_2=175, n_1=150 and $d_{n,R-Z}$=3.0 ($0.02765\cdot\sqrt{\frac{D_X}{D_{X_0}}}cm$ - four nodes included). In this case the time integration step dt=$1\cdot10^{-3}$.

For the same values of parameters, calculations for a regular train of pulses arriving at a diode have been performed. The results are presented in Figures 35 - 37, which have exactly the same structure and symbols as Figs. 33 - 34.

For the FH-N model the input signal with frequency f_p=0.278 (corresponding to the time shift between consecutive pulses t_p=3.6) has been cho-

[15]The animated illustrations to Figures 33 - 34, showing the propagation of single pulses through the chemical diode, can be found on the CD-ROM (folder *Figures*). Fig_33a.htm - FH-N model, pulse propagating to the right; Fig_33b.htm - FH-N model, pulse propagating to the left (stopped by the diode); Fig_34a.htm - R-Z model, pulse propagating to the right; Fig_34b.htm - R-Z model, pulse propagating to the left (stopped by the diode).

http://rcin.org.pl

sen. The time evolution of the values of u at i_1 and i_2 are plotted in Fig. 35. As expected, the diode is transparent to all pulses travelling to the right (in the forward direction) - curves 1 and 2. However, for the chosen values of parameters the junction becomes transparent to some of the pulses travelling in the reverse direction (to the left - curves 3 and 4) . Therefore, the diode works as a transformer of chemical signal frequency.[16] It is easy to explain this observation. In this case the barrier ($d_{n,FH-N}$=0.1152) is narrower than the penetration depth in the forward direction ($d_{c,FH-N}$=0.163), therefore each pulse coming from this direction is transmitted. On the other hand it has been selected as being only slightly wider than the penetration depth in the reverse direction: $0.63 \cdot d_{c,FH-N}$=0.1027. Consequently, the gap demonstrates the same type of frequency transforming as the passive barrier discussed previously (see Section 2.4.2).

For the R-Z model the input signal with dimensionless frequency f_p=0.023 has been used (this corresponds to the time shift between consecutive pulses τ_p=44, ie. $374 sec$). The results are plotted in Figure 36. Comparing curves 3 and 4 (in Fig. 36) one can see that in this case the diode stops all the pulses propagating in the reverse direction. As shown in Fig. 34, $d_{n,R-Z}$=3.0 is larger than the penetration depth in this direction. The results of Section 2.4.5 for the R-Z model (Fig. 29) indicate that such system becomes less "transparent" at higher signal frequencies. Therefore, it is natural that all pulses propagating in the reverse direction are stopped. However, the diode fails to transmit some pulses propagating in the forward direction (here: the 2nd and 4th ones, see curves 1 and 2). This result can be easily explained

[16]The animated illustrations to Figure 35, showing the propagation of this short train of pulses through the chemical diode, can be found on the CD-ROM (folder *Figures*). Fig_35a.htm - FH-N model, pulses propagating to the right; Fig_35b.htm - FH-N model, pulses propagating to the left (note that not all of them are stopped by the diode).

http://rcin.org.pl

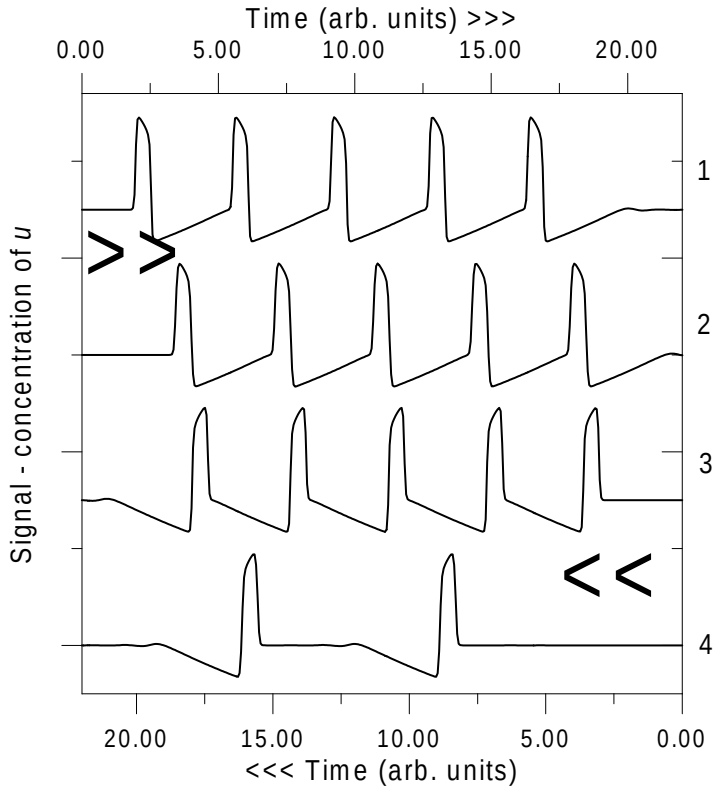

Figure 35. The time evolution of the value of u at the indicators i_1 (curves 1 and 4) and i_2 (curves 2 and 3). The two upper curves (no. 1 and 2) correspond to a train of pulses propagating from left to right (orientation defined by Fig. 32) and the corresponding time scale is at the top. The two lower curves (no. 3 and 4) correspond to a train of pulses propagating from right to left (cf. Fig. 32). The arrows mark the direction of propagation. Results for the FitzHugh - Nagumo model, $d_{n,FH-N}$=0.1152, t_p=3.60 (f_p=0.278). Although the diode works still properly in the forward direction (curves 1 and 2), some pulses may cross it also in the reverse direction (curves 3 and 4).

http://rcin.org.pl

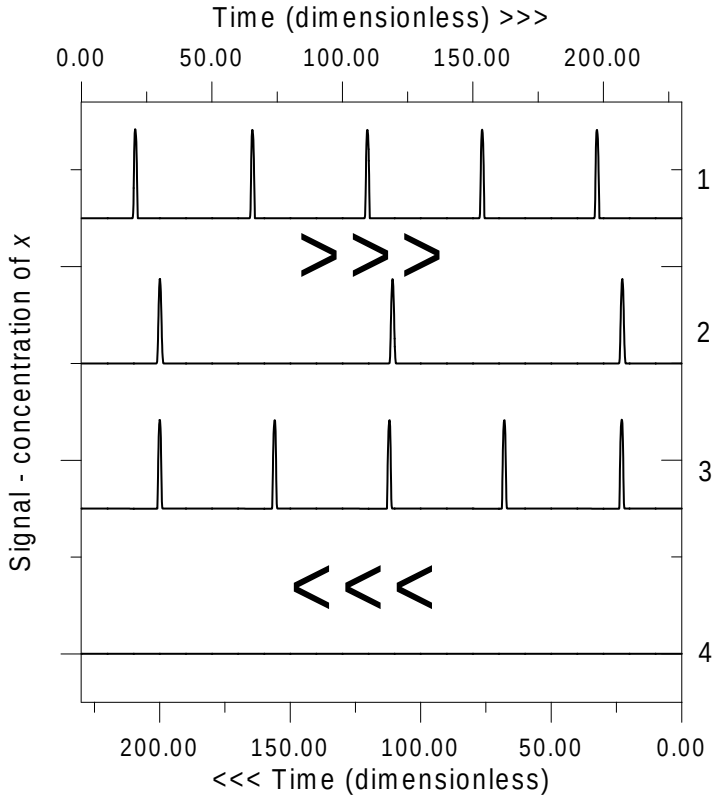

Figure 36. The time evolution of activator's concentration at the indicators i_1 (curves 1 and 4) and i_2 (curves 2 and 3). The two upper curves (no. 1 and 2) correspond to a train of pulses propagating from left to right (orientation defined by Fig. 32) and the corresponding time scale is at the top. The two lower curves (no. 3 and 4) correspond to a train of pulses propagating from right to left (cf. Fig. 32). The arrows mark the direction of propagation. Results for the Rovinsky - Zhabotinsky model, $d_{n,R-Z}$=3.0 ($0.02765 \cdot \sqrt{\frac{D_X}{D_{X_0}}} cm$), τ_p=44 (f_p=0.023). τ_p=44 corresponds to $374 sec$. In this case the diode stops every second pulse travelling in the forward direction (curves 1 and 2), while it works correctly in the reverse direction (curves 3 and 4).

http://rcin.org.pl

by what is already known from Section 2.4.5. Although $d_{n,R-Z} < d_{c,R-Z}$ (as 3.0<3.295), the gap is still in the region for which the frequency transforming in the R-Z model occurs.[17]

When the frequency of the input signal is increased - only the first pulse of the train is able to get through the diode in the forward direction and all subsequent pulses are stopped. This situation is shown in Figure 37, where the frequency of the incoming signal f_p=0.05 has been used (τ_p=20, corresponding to $170 sec$).[18]

The response of the cross junction (Section 2.3, Fig. 3) to a train of pulses travelling inside a channel has also been studied. It has been found that if the time shift between consecutive pulses in a train is small, the characteristics of the junction changes (with respect to the results given in Sections 2.3.1 - 2.3.2, concerning single pulses). A part of the cross junction has been studied, for the FH-N model with the inner width of the channel equal to 1.02 and the width of the passive stripes of 0.16 (exactly as in Section 2.3.1), using the implicit method with dl=0.02 and dt=$5 \cdot 10^{-3}$. The pulses inside one of the signal channels have been initiated with the time shift equal to t_p=3.6. The result of calculations is presented in Figure 38, where brighter colors correspond to higher values of u. The first pulse behaves exactly as expected: it remains within the channel (as the width of the passive stripes is just above

[17]The animated illustrations to Figure 36, showing the propagation of this short train of pulses through the chemical diode, can be found on the CD-ROM (folder *Figures*). Fig_36a.htm - R-Z model, pulses propagating to the right (note that the second and fourth of them are stopped by the diode); Fig_36b.htm - FH-N model, pulses propagating to the left.

[18]The animated illustrations to Figure 37, showing the propagation of this short train of pulses through the chemical diode, can be found on the CD-ROM (folder *Figures*). Fig_37a.htm - R-Z model, pulses propagating to the right (note that all but the first one are stopped by the diode); Fig_37b.htm - FH-N model, pulses propagating to the left.

http://rcin.org.pl

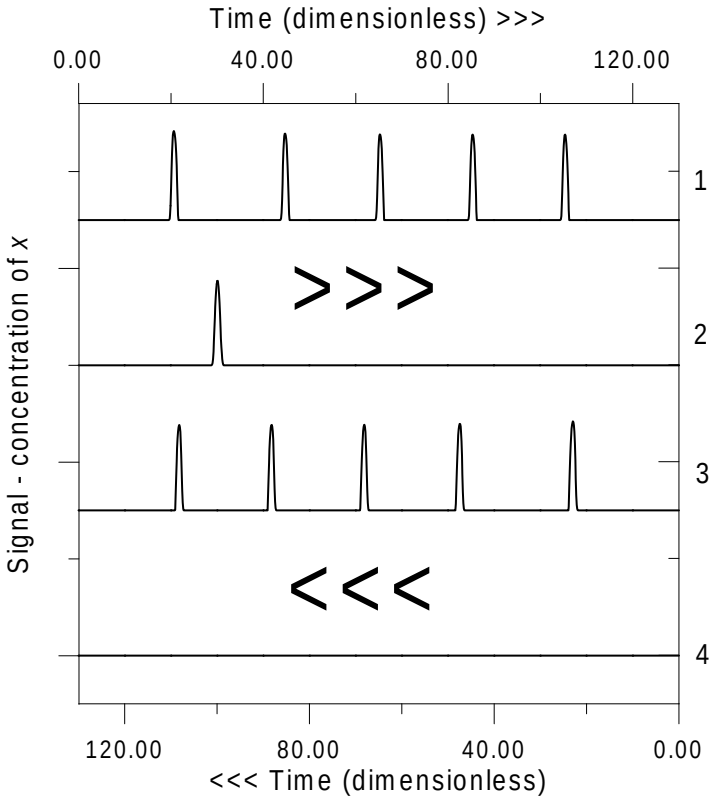

Figure 37. The time evolution of activator's concentration at the indicators i_1 (curves 1 and 4) and i_2 (curves 2 and 3). The two upper curves (no. 1 and 2) correspond to a train of pulses propagating from left to right (orientation defined by Fig. 32) and the corresponding time scale is at the top. The two lower curves (no. 3 and 4) correspond to a train of pulses propagating from right to left (cf. Fig. 32). The arrows mark the direction of propagation. Results for the Rovinsky - Zhabotinsky model, $d_{n,R-Z}$=3.0 ($0.02765 \cdot \sqrt{\frac{D_X}{D_{X_0}}} cm$), τ_p=20 (f_p=0.05). τ_p=20 corresponds to $170 sec$. In this case the diode stops all pulses but the first one from the train in the forward direction (curves 1 and 2). It works properly in the reverse direction (curves 3 and 4).

http://rcin.org.pl

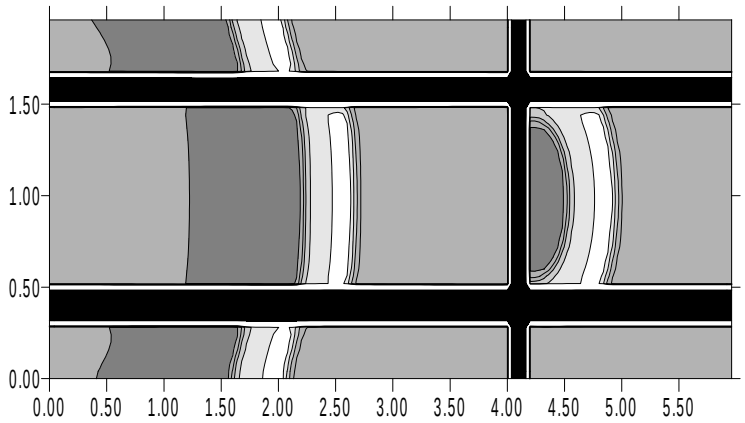

Figure 38. A snapshot showing the propagation of two consecutive pulses in a fragment of the cross junction structure. Brighter colors correspond to higher concentration of activator (u) The picture has been obtained for the FitzHugh - Nagumo model. The width of the passive stripes is 0.16 and the width of the active medium inside the channel equals to 1.02. The time shift between the pulses is t_p=3.60 (f_p=0.278).

http://rcin.org.pl

the penetration depth for a pulse travelling along the stripes), but it is able to get through the perpendicular "obstacle" (as the penetration depth in this direction is greater that the width of the passive stripes). However, the first pulse "opens" the stripes which bound the channel for the following pulses. One can see that the next pulse "leaks out" of the channel and excites the neighboring areas (cf. the second pulse in Fig. 38). Of course, for the FH-N model all the pulses in a train are able to cross the passive stripe perpendicular to the direction of motion.

Similar computations have been carried out for the R-Z model with the width of the passive stripes of 3.291 ($0.03034 \cdot \sqrt{\frac{D_X}{D_{X_0}}} cm$) and the inner width of the active channel equal to 50.192 ($0.4627 \cdot \sqrt{\frac{D_X}{D_{X_0}}} cm$). They have shown that for signals of high frequency (eg. for τ_p=20, corresponding to $170 sec$) the individual pulses propagate within the signal channel, but some of them may be stopped by the perpendicular passive stripe. Thus, the cross junctions described by both FH-N and R-Z types of dynamics are sensitive to the frequency of input signals.

2.4.8 Discussion.

This part of the work is concerned with the signals obtained after a regular train of pulses crosses a barrier of a passive medium. The most thorough calculations have been performed for the excitable medium described by the FH-N model, but qualitatively similar results may be obtained for the models of the BZ reaction (eg. the R-Z model and the Oregonator model considered here).

Two facts are obvious: if the barrier is narrow - it is transparent to the pulses, if it is wide - it is impenetrable. However, it has been found that between these two limiting cases there is a range of barrier's widths for which

http://rcin.org.pl

it works as a transformer of signal frequency. It means that every second, third etc. pulse from the incoming signal is transmitted and all the others are stopped at the barrier. The number of transmitted pulses decreases with the barrier's width. More complex examples of signal transformation have also been observed, like eg. a selection of two pulses out of every five arriving, shown in Fig. 20. Unfortunately, such interesting, complex behavior occurs in a narrow range of barrier's width and it is not as robust as the simple division of the number of input pulses by two or three.

The calculations have been performed for the FH-N model of an excitable system as well as for the R-Z and Oregonator models of the ferroin/cerium catalyzed BZ reaction. For all these models an interval of barrier's width has been found in which the barrier works as a transformer of frequency of the input signal. The filtering ratio equal to 1/2 is dominant among the nontrivial filtering. It corresponds to elimination of every second pulse from the train by the barrier. In case of the FH-N model, this process may occur for barriers which are narrower or wider than the penetration depth for a single pulse ($d_{c,FH-N}$=0.163). The "scenario" of such elimination for barriers wider than $d_{c,FH-N}$ in the FitzHugh - Nagumo model is shown in Fig. 17. In this case the first incident pulse "dies" at the barrier, but the next one is transmitted, another one dies etc. Apparently a pulse stopped at the barrier increases the value of u inside the barrier for a short period of time, so the "activator" is accumulated within the passive area. This helps the next incident pulse to get through the barrier. This mechanism is absent in the models of Belousov - Zhabotinsky reaction considered, where the frequency transforming has only been observed for barriers which are narrower than the penetration depth for a single pulse. In this case the stable elimination of every second pulse from a train means that the first incident pulse crosses the barrier, the next

http://rcin.org.pl

one "dies" etc. For division by 3 - the first pulse gets through and then two pulses "die" etc. (cf. Figs. 28 and 31).[19]

A family of transmitted signals has been found in which one signal out of n arriving gets through the barrier ($(0)^{n-1}(1)$ mode) . These signals, characterized by the firing number $1/n$, contribute to the devil's-staircase-like behavior of the firing number, expected on the basis of the "naive" model of a perturbed excitable system (Section 1.2.2). However, less trivial patterns of the transmitted signal have also been observed. Another interesting family of transmitted signals, which can be described as $(0)(1)^{n-1}$, corresponds to the case when only one signal is not transmitted out of every n arriving. Such behavior cannot be described by the "naive" model, but comes out quite naturally, if one assumes that an excitable system which has not reached its stationary state may be re-excited by a perturbation which is strong enough (see discussion in [69]). Finally, many complex structures of the output signal have been observed. They follow the structure of the Farey tree [130, 131] (take for example points a - h in Fig. 22).

From the point of view of numerical integration techniques, it is important to stress that the results concerning the complex transformations of chemical signals passing through a passive barrier are quite sensitive with respect to the time and space integration steps used. The exact position of plateaus in

[19]It has been suggested [129], that the different behavior of the FH-N and R-Z models may be the result of different scales, within which the values of variables change in these models. Looking at Figs. 1 - 2 one may notice, that in case of the FH-N model the scale is the same for its both variables (u and v), while for the R-Z model the relative change of one of the variables (x) during the excitation cycle is several orders of magnitude larger than for the other variable (z). The author of this work has tried to adjust the parameters of the FH-N model to make its nullclines qualitatively similar to those of the R-Z model. Unfortunately, all attempts have been unsuccessful, so this hypothesis still needs to be verified.

http://rcin.org.pl

the cross-sections like those presented in Figs. 22 - 24 depends on dt and dl, although the overall structure of the cross-section remains unchanged. In general, more exact results are obtained by means of more accurate algorithms (eg. adaptive grids), but even such algorithms seem to fail at the boundaries of plateaus (cf. Figs. 26 and 27)

As a consequence of the frequency transforming phenomenon, it has been found that two dimensional reactors composed of active and passive regions, designed for direct processing of chemical signal, are sensitive to the input signal frequency. The operations performed on high frequency trains of pulses may differ from those performed on pulses which are well separated in time. This effect has been shown on two examples of such reactors: the chemical diode ([83, 85, 86, 102]) and the cross junction ([111, 112, 115]), but one should expect that the other signal processing devices (logical gates [86], memory device [87]) would also exhibit nontrivial dependence on the input signal frequency. Malfunction of the chemical diode, qualitatively identical with the results of calculations for the R-Z model presented in Fig. 36, has been observed experimentally by Y. Igarashi, K. Yoshikawa and J. Górecki at the Department of Physics, Kyoto University, Kyoto, Japan in spring 2002 [132].[20]

Transformation of chemical signal frequency on a passive barrier in the ferroin catalyzed BZ reaction has been recently reported by K. Suzuki, T. Yoshinobu and H. Iwasaki [70]. The diagram which relates the filtering ratio seen in their experiments with the barrier's width and the period of excitations (Figure 10 in [70]) is in a qualitative agreement with the results shown in Fig. 29. Moreover, individual examples of frequency transforming (in the

[20]Thanks to courtesy of the Authors, the film showing their experiment is included on the CD-ROM (diode_12.avi, folder *Experiments*)

http://rcin.org.pl

ferroin catalyzed BZ system, too), have been observed experimentally by the author of this work. They correspond to several values of the filtering ratio (0, 1/2, 2/3, 1); please refer to Section 2.7 for details.

The authors of [69] pointed out that the resonant patterns of transmitted waves may be important in biological systems. They postulated that narrow excitable gaps in an unexcitable tissue may be responsible for transformation in the frequency of a biological signal. The results presented in this work show that such gaps are not necessary and the phenomenon may occur if some reagents responsible for signal propagation can diffuse through the unexcitable tissue.

http://rcin.org.pl

2.5 Excitable pulses on a ring.

Unidirectional waves on rings, described by FitzHugh-Nagumo equations, were used to study so called circumnutation of plants in their quest for a support [133]. A circular excitable medium with radial input and output channels can be used as a memory device [86, 87]. Thus, the features of excitable pulses propagating on a ring are important for applications of chemical systems to information processing, but also for the biologists.

At first, a single travelling pulse on an interval $[0,L]$ with the periodic boundary conditions has been considered. It has been found [125] that the velocity, width and amplitude of the pulse in its stationary shape depend on L. The velocity and width grow remarkably with increasing L, reaching their maximum values, corresponding to propagation on an infinite interval. As an example, the results obtained for the FitzHugh - Nagumo model are presented in Figures 39 (velocity) and 40 (width). Here the width of the pulse is defined as the length of the interval in which the value of u is greater than 0.1 (cf. Figure 41). Changes in the amplitude of the pulse are not so remarkable. The amplitude increases together with L by several percent only and quickly stabilizes. Real chemical systems are characterized by qualitatively the same dependencies between velocity or width of pulses and the space available for individual pulse. Consequently, several pulses initiated on a ring tend to arrange themselves in a symmetrical way, using the whole space available. This property of travelling waves was observed in real chemical experiments [89].

Once a pulse has passed through a part of the interval $[0,L]$ then a certain amount of time (called the recovery time) is needed before it would be able to propagate in this region again. If the pulse arrives earlier it cannot propagate and disappears. Thus, there exists a minimal length L_{min}, below

http://rcin.org.pl

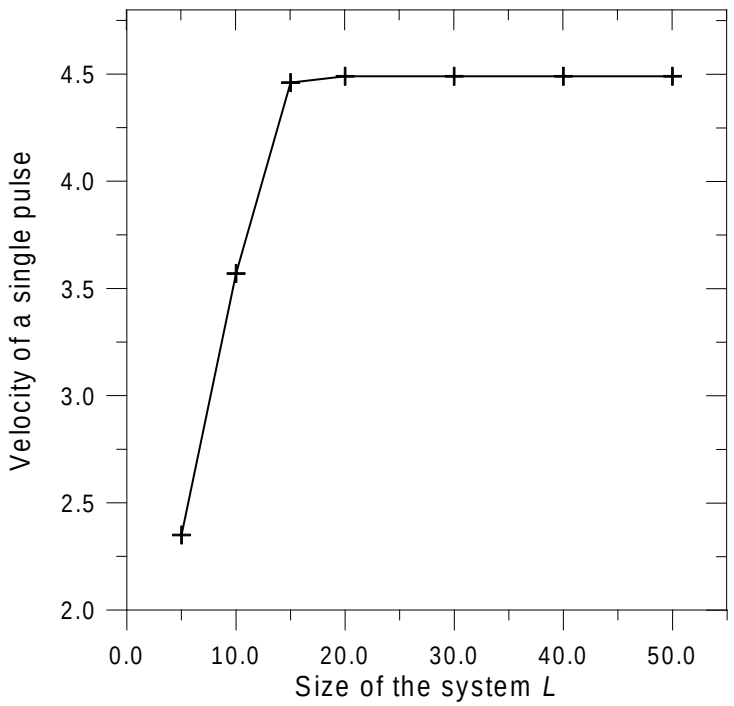

Figure 39. The velocity of a single pulse in the FitzHugh-Nagumo model for various length L of a one dimensional system with periodic boundary conditions. Symbols mark the computational results.

http://rcin.org.pl

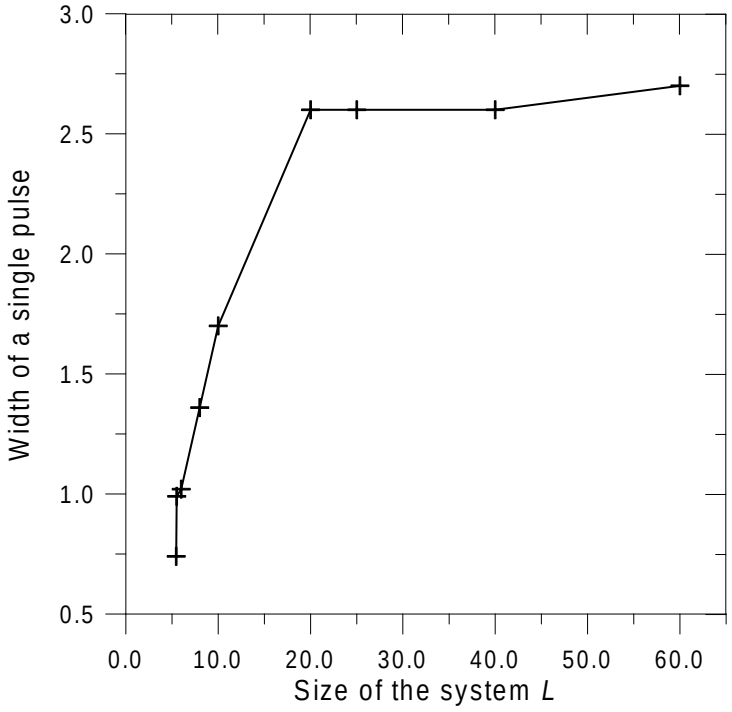

Figure 40. The width of a single pulse in the FitzHugh-Nagumo model for various length L of a one dimensional system with periodic boundary conditions. Symbols mark the computational results.

http://rcin.org.pl

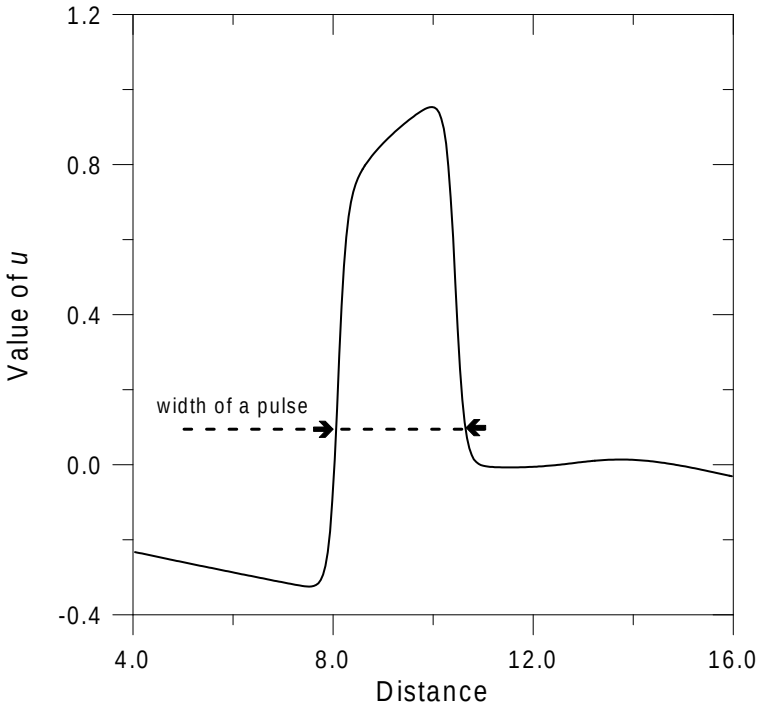

Figure 41. The stationary shape of a pulse of u ("activator") obtained for the FitzHugh - Nagumo model on an interval of length L=20. The width of the pulse is defined as the length of the interval in which the value of u is greater than 0.1.

http://rcin.org.pl

which the time, that the pulse needs to pass through the whole interval, is shorter than the recovery time of the medium. Consequently, for $L<L_{min}$ no stable travelling pulse can exist. After initiation the pulse on such a ring dies out. The critical length L_{min} for one pulse has been found by numerical calculations. Then it has been confirmed that the critical length for two, three etc. pulses is just the corresponding multiplicity of L_{min}.

Using the implicit method with n=200, dt=5·10^{-3} and t_{max}=10000 it has been found that for the FitzHugh - Nagumo model

$$L_{min,FH-N} \approx 3.529 \tag{2.23}$$

Similar calculations for the Rovinsky - Zhabotinsky model (n=200, dt=1·10^{-3}, τ_{max}=500) have shown that

$$L_{min,R-Z} \approx 5.79 \ (0.0534 \cdot \sqrt{\frac{D_X}{D_{X_0}}} cm) \tag{2.24}$$

The value of L_{min} can be easily transformed into the critical radius of a ring, supporting one stable pulse (called a "1-pulse" ring for simplicity):

$$r_{min} = \frac{L_{min}}{2\pi} \tag{2.25}$$

The critical radii of rings, supporting two, three and more stable pulses are just corresponding multiplicities of r_{min}. As a consequence of Eqs. (2.23 - 2.24) and Eq. (2.25) the critical radii of "1-pulse" rings for the FitzHugh - Nagumo ($r_{min,FH-N}$) and the Rovinsky - Zhabotinsky models ($r_{min,R-Z}$) are:

$$r_{min,FH-N} =\approx 0.562 \tag{2.26}$$

$$r_{min,R-Z} =\approx 0.922 \ (0.00850 \cdot \sqrt{\frac{D_X}{D_{X_0}}} cm) \tag{2.27}$$

Two dimensional ring characterized by its outer radius R and inner radius r - as presented in Figure 42 - has been considered. The propagation of a

http://rcin.org.pl

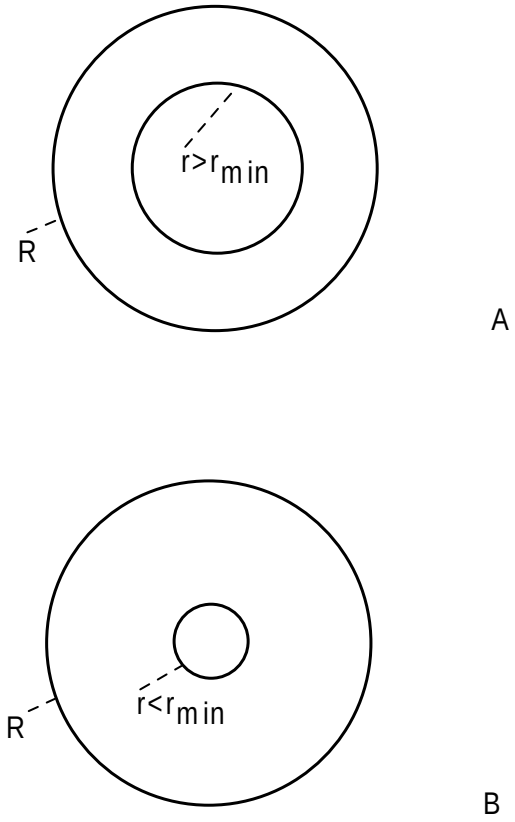

Figure 42. The types of rings considered. **A** - a ring with $R \gg r_{min}$ and $r > r_{min}$ enables stable propagation of a pulse around it. **B** - a ring with $R \gg r_{min}$ and $r < r_{min}$ maker a rotating pulse change its shape during propagation, because the pulse cannot constantly propagate along the inner boundary of the ring.

http://rcin.org.pl

single pulse of excitation around the ring has been studied for various values of r and R. It is expected, that for $r \gg r_{min}$, $R \gg r_{min}$ and R not much larger than r the pulse should just travels around the ring in a stable way, because in this case on the whole width of the ring the medium has enough time to relax before the excitable pulse reappears (cf. Fig. 42A). Consequently, one should use this kind of rings as memory devices, as proposed by I. Motoike and K. Yoshikawa [86, 87]. However, it is also expected, that for $R \gg r_{min}$ and $r < r_{min}$ the pulse cannot constantly propagate along the inner boundary of the ring, because then the time of one cycle for a pulse travelling around the inner boundary is shorter than the refractory time of the medium (cf. Fig. 42B). Thus, after one rotation the pulse has to "leave" the neighborhood of the inner boundary, while it can still propagate closer to the outer boundary. Later, when the medium in the inner part gets relaxed again, the pulse may re-enter this area. As the result, a pulse rotating on such a ring becomes unstable. It is constantly changing its shape, moving towards and away from the inner boundary of the ring.

The instabilities have been investigated for the FitzHugh - Nagumo model (Eqs. 2.1-2.2). The calculations have been carried out with the implicit method, adapted to use two dimensional polar coordinates. The grid consisting of 68 points in the radial direction and 512 points around the ring has been applied. In the calculations $dt = 5 \cdot 10^{-5}$ and $t_{max} = 130$. No flux boundary conditions have been assumed on both boundaries of the ring. Pulses have been introduced to the ring using a prerecorded file, containing the stationary shape of a pulse on a one dimensional interval with periodic boundary conditions. The mean values of u and v in the whole system (denoted by $\bar{u}$ and $\bar{v}$) have been recorded as the functions of time and plotted in coordinates ($\bar{u}$, $\bar{v}$). Initial part of such trajectory, corresponding to transient

http://rcin.org.pl

effects, has been ignored. The stable propagation of a pulse around the ring corresponds to a point on such a plot, as the values of $\bar{u}$ and $\bar{v}$ are constant in time.[21] Such stable propagation has been observed for $R>r>r_{min,FH-N}$ (in particular, R=3.0 or R=2.5 and r=0.57 have been used). On the other hand, when $r<r_{min,FH-N}$ the plot becomes complicated, because the rotating pulse is constantly changing its shape, moving towards and away from the inner boundary of the ring. Here I have used R=3.0 or R=2.5 and r=0.53. An example of such trajectory (obtained for R=3.0 and r=0.53) is shown in Figure 43.[22] For R=3.0 or R=2.5 and r=0.55 stable propagation of pulses around the ring has been observed. However, this is probably a transient effect, as the evolution of pulses on (two dimensional) rings has been studied up to t_{max}=130, while the value of $r_{min,FH-N}$ has been established in calculations carried out up to t_{max}=10000. Moreover, it has been observed that for R=2.0 pulses collapse after about two rotations, independently of the inner radius of the ring (r=0.53, 0.55 or 0.57).

[21] To be very precise, this is in fact not a point, but rather a very small circle, because the rotating pulse in its stationary form is moving with respect to the grid used in the calculations; the diameter of this circle becomes smaller if a finer grid is used.

[22] An animation illustrating part of the evolution for which Fig. 43 has been obtained can be found on the CD-ROM (Fig_43a.htm, folder *Figures*). For comparison, stable propagation of a pulse around a ring with r=0.57 and R=3.0 is illustrated in Fig_43b.htm (folder *Figures*).

http://rcin.org.pl

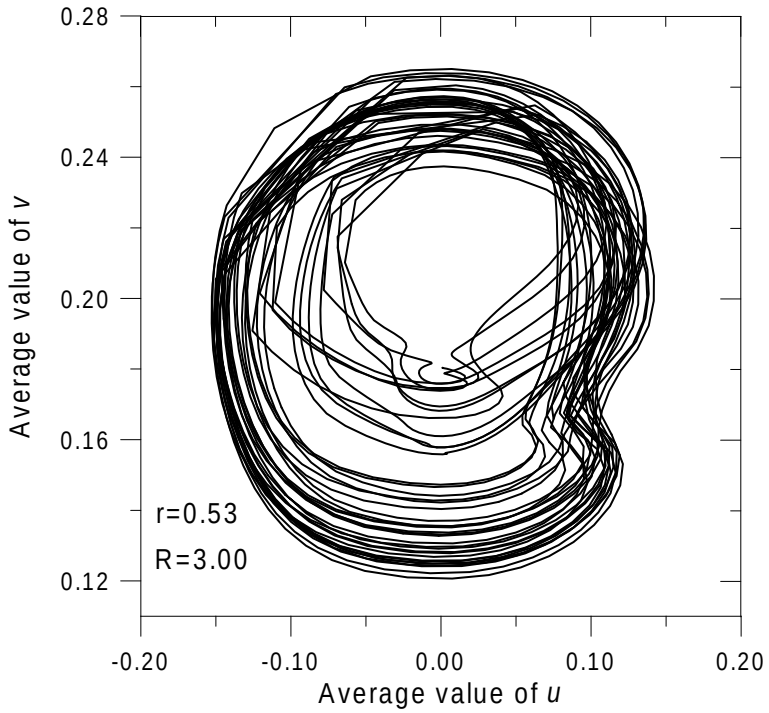

Figure 43. Average values of u and v (denoted by $\bar{u}$ and $\bar{v}$ in text) observed for a single pulse rotating on a ring with r=0.53 and R=3.0. The curve shown corresponds to $t\in$[30, 130]. The values of $\bar{u}$ and $\bar{v}$ are changing, because the pulse is constantly changing its shape while rotating. The result has been obtained for the FitzHugh - Nagumo model.

http://rcin.org.pl

To sum up, the instabilities appear for $r \approx r_{min,FH-N}$, as expected. On the other hand, they also seem to depend on R. The detailed mechanism leading to instabilities and the analytical condition for stable propagation of a single pulse on a ring are not known yet. This problem is still under investigation.[23]

[23]Even more interesting phenomena have been observed for a sphere with both "poles" symmetrically cut off, so that the circumference along the "equator" is much larger than L_{min}, while the circumference along the "parallels", which remain after cutting off the poles, is smaller than L_{min}. However, it has only been checked so far that there are several "modes" of changing shape for a pulse rotating around such a sphere. The modes are characterized by different symmetry. The problem has not been investigated any further yet.

http://rcin.org.pl

2.6 When two excitable pulses meet.

Another very interesting type of complex evolution has been observed in the system composed of two active semiplanes separated by a passive stripe for the FitzHugh - Nagumo model [112]. It is presented in Figure 44, for which he same color convention as for Figs. 5 - 11 is used. The horizontal stripe of passive medium is transparent for a pulse propagating perpendicularly, but impenetrable for a pulse propagating parallel to it (cf. Fig. 44a). The first excitable pulse propagates along the passive stripe, to the right. The second pulse, initially located in the bottom part of the system, crosses the barrier and starts its propagation on the more relaxed side of the upper part, spreading to the right (following the first pulse) and upwards (cf. Fig. 44b). On its way to the right it propagates along the passive stripe which has just been disturbed by the incident pulse. There is some activator left within the passive stripe, because the activator does not decompose there due to chemical reactions and it can only diffuse out of the stripe. The second pulse, propagating along the stripe to the right (cf. Fig. 44b), adds even more activator to the passive area (compare the "whiskers" sticking out of the passive stripe, described in Section 2.3.1). Meanwhile, the active medium on the other side of the stripe becomes relaxed and ready for a new excitation. Because of that at some point the second pulse gets through the parallel barrier once again and starts spinning around (cf. Fig. 44c). While spinning, it is able to cross the passive barrier again and again (Figs. 44d-f), due to the mechanism just described. Numerically the structure is stable. It persists in calculations lasting twenty times longer than a pulse needs to get through the whole square. No change in the position of the center of the pinwheel has been observed in the calculations carried out. This phenomenon has to be taken into account for cross junctions with very

http://rcin.org.pl

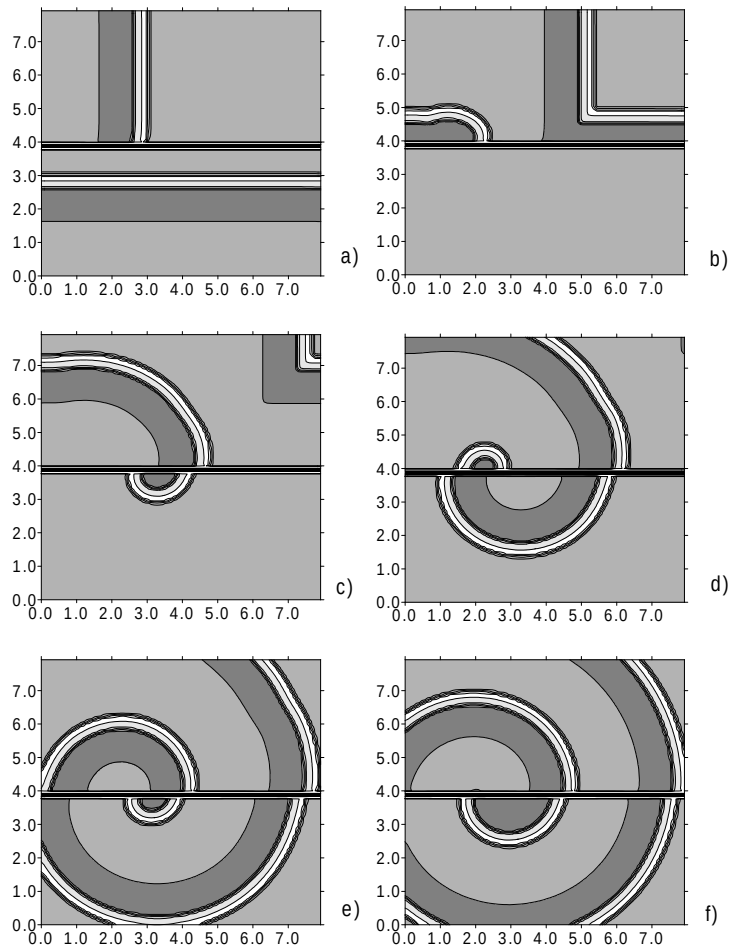

Figure 44. The "pinwheel" on a plane with a single stripe of diffusion field, obtained within the FitzHugh - Nagumo model. Gray areas correspond to the excitable field and the black stripe - to the diffusion one. Brighter colors correspond to higher values of u. The consecutive snapshots present the value of u at moments: a) t=4.0, b) t=7.0, c) t=10.0, d) t=12.0, e) t=14.0, f) t=200.0.

http://rcin.org.pl

wide signal channels.

The result illustrated in Fig. 44 has been obtained with the implicit method, on a 8x8 square covered with 400x400 grid. The width of the diffusion stripe here has been the same as for the cross junction described in Section 2.3.1 (d_{FH-N}=0.16). The time integration step dt=0.005 has been used.[24]

[24]The animated version of Fig. 44 can be found on the CD-ROM (Fig_44a.htm, folder *Figures*).

http://rcin.org.pl

2.7 The experiments on frequency transforming.

The numerical results concerning the propagation of trains of pulses through a passive gap presented in Section 2.4 have been checked in experiments, run by the author of this work in the Institute of Physical Chemistry of the Wuerzburg University in Wuerzburg, Germany, in March 2002. The experiments were made in a system based on the ferroin catalyzed BZ reaction.

Polysulfone membranes (PALL Corp., $47mm$ in diameter, $0.45\mu m$ in width) were covered with ferroin (bathophenantroline, Fluka) exactly according to the recipe given by Lazar, Noszticzius, Forsterling and Nagy-Ungvarai in [89] (Sol3 and Sol4 in Section 2.1.2 of their article). At start, the BZ solution providing the oscillatory regime for the reaction was prepared, according to [134] ($[H_2SO_4]$=1.25M, $[NaBrO_3]$=0.07M, $[CH_2(COOH)_2]$=0.375M). The rest of the experiment was carried out within the excitable regime, using the BZ solution described by Suzuki, Yoshinobu and Iwasaki in [70] ($[H_2SO_4]$=0.50M, $[NaBrO_3]$=0.4M, $[CH_2(COOH)_2]$=0.40M, $[NaBr]$=0.08M). The results presented here were obtained for the excitable regime.

In order to obtain two dimensional structures composed of active areas (with ferroin) and passive ones (without it) the elements of desired shape were first cut out of a ferroin covered membrane with scissors. The elements were then arranged on the adhesive tape and fixed. Alternatively, a piece of a ferroin covered membrane was first stick to an adhesive tape and later it was cut in two parts with a lancet or a razor blade (both techniques enabled to obtain very narrow passive stripes - of the order of $0.01mm$ - separating the active areas). Once built, the structures were fixed to the bottom of a Petri dish with the adhesive tape and immersed in the BZ solution. Usually

http://rcin.org.pl

the experimental setup had the form of a "comb", providing several active (excitable) paths, along which pulses could propagate; on each path there was one passive barrier, ie. a slit between two pieces of a ferroin covered membrane.[25] Pulses of excitation were initiated by touching the membrane with a silver wire and they were destroyed or broken by pouring distilled water (water purified with Millipore Milli-Q filtering system was used for this purpose, as well as for preparing solutions; the resistivity of the water was $18.2 M\Omega \cdot cm$). This way it was eventually possible to obtain a rotating spiral in a desired place of the system. The spiral was the source of a stable, regular train of pulses arriving at the passive barrier. The experiments were recorded with a CCD camera connected to a PC.[26]

The method of building the investigated systems did not allow to control precisely the width of passive gaps. However, once a device was constructed, it was possible to measure the distance between the active areas precisely under a microscope. Building a cross junction (as described in Section 2.3) was impossible with such a crude method of constructing the systems, so only the propagation of trains of pulses through a passive gap was investigated. The experimental observations are in qualitative agreement with the results presented in this work (Section 2.4): the frequency transforming effect has been observed.[27] For example, filtering ratio f_o/f_p=2/3 was found for pulses of excitation arriving in about $60 sec$ intervals at a passive barrier which was $0.016 mm$ wide. It corresponds to elimination of every third of arriving

[25] A picture showing one of such structures as an example can be found on the CD-ROM (Example.htm, folder *Experiments*)

[26] In such experiments the pulses are visible as blue stripes moving on a pink background. Blue and pink colors correspond to oxidized and reduced form of the catalyst ($Fe(phen)_3^{3+}$ and $Fe(phen)_3^{2+}$ respectively), compare [3] p. 183 or [4] p. 337.

[27] Note that the concentrations of reagents used in these experiments were different from those assumed in the calculations for the R-Z model (Section 2.3.2).

http://rcin.org.pl

pulses by the barrier.[28] The "classical" division of the original frequency of incident pulses by 2 (f_o/f_p=1/2) was observed for pulses arriving every $46sec$ at a barrier $0.065mm$ in width.[29] Trivial examples of f_o/f_p=1 (all pulses get through the barrier) and f_o/f_p=0 (no pulse can cross the barrier) were observed for t_p=$26sec$, d=$0.016mm$ and t_p=$32sec$, d=$0.258mm$ respectively.[30]

Moreover, the velocity of free propagation of a single pulse of excitation on a plain ferroin covered membrane was measured, giving $9.4mm/min$. It is of the same order of magnitude as the value obtained from the calculations for the R-Z model ($2.686mm/min$ for D_X=$10^{-5}cm^2/sec$, see Section 2.3.2), although the values of parameters used in computations (fixed concentrations, diffusion coefficients) were different from experimental ones.

[28]The recording of this experiment can be found on the CD-ROM (2_3.bat, folder *Experiments*)

[29]1_2.bat, folder *Experiments* on the CD-ROM.

[30]1_1.bat and 0.bat respectively in folder *Experiments* on the CD-ROM.

http://rcin.org.pl

Chapter 3

Possible applications of described devices to direct information processing.

This section contains some ideas on potential future applications of reactors composed of active and passive areas to direct information processing. First, the advantages of simple structures of the cross junction and the passive barrier (Sections 2.3 and 2.4) are described. These two simple elements, together with the chemical diode, a logical OR gate and a memory cell (as proposed by I. Motoike and K. Yoshikawa - see Figures 2, 3 and 7 in [86] respectively) are combined together to build two more sophisticated devices. The first one is an "adding machine", which is able to add two numbers given in binary representation. Second one is a counter of number of pulses that propagated in a signal channel. Both devices produce results in binary representation. Although some of the structures presented in this section may be hard to deploy, the author thinks that all of them can be constructed and applied in practice.

http://rcin.org.pl

The cross junction with an extra channel, diagonal to the signal channels (cf. Figure 45A), may be easily used as a logical AND gate. One should concern paths i_1 and i_2 (Fig. 45A) as input channels and paths o_1, o_2 and o_3 as output channels. If and only if two pulses appear simultaneously in i_1 and i_2, then an output signal is produced in o_3 (Fig. 5 is helpful to imagine what happens). If a single signal appears in i_1 or i_2 only - it propagates through the junction and goes out through o_1 or o_2 respectively (and no signal is initiated in o_3). Of course, there are no output signals at all if input signals do not appear in i_1 nor i_2. Thus, a logical AND gate has been constructed.

The advantages of a simple passive barrier are even easier to show. First, a barrier of a fixed width d may be used as a filter of frequency of a chemical signal. If the frequency of the incoming signal f_p is greater than a certain critical frequency f_{crit} (where f_{crit} depends on d - cf. Fig. 29), then no pulse can cross the barrier. Thus, only signals with frequency $f_p<f_{crit}$ may be observed behind the barrier. The passive barrier may also be used to divide the number of pulses in the incoming train by a desired integer number. Knowing the frequency of pulses in the incoming train, it is enough to adjust the barrier's width d appropriately (cf. Figs. 18, 19 and 29). The division by 2 seems especially useful (it is used later in this section to build the counter of pulses), so it is very convenient that it appears in a wide range of parameters (d, f_p). Last but not least, a ring "equipped" with input and output channels may be used to regularize a train of pulses in which the time shift between consecutive pulses is random or unknown. First the whole train has to be "collected" on such a ring, then one should wait until the pulses arrange themselves symmetrically (this phenomenon is described in Section 2.5) and finally a regular train of pulses can be read from the ring. This procedure is limited by the "capacity" of the ring used (so the longer trains are to be

http://rcin.org.pl

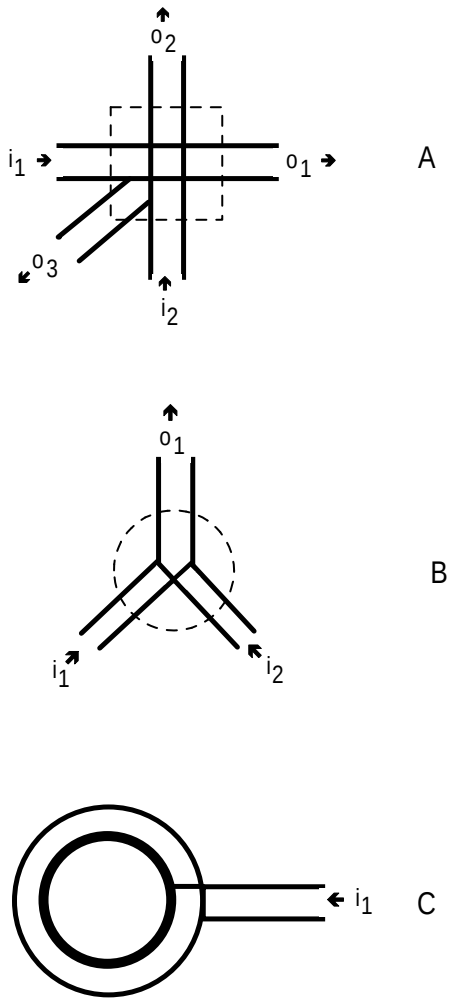

Figure 45. Simple signal processing elements. A - the logical AND gate based on the cross junction. B - the logical OR gate. C - a memory cell (pulse storage ring). Thick black lines in the picture correspond to passive stripes of properly chosen width. Thin dotted lines in Figs. 45A and 45B resemble the symbols used to indicate the corresponding elements in the schemes of more advanced devices shown in Fig. 46.

http://rcin.org.pl

regularized, the larger rings should be used). On the other hand, if a "N-pulse" ring is used, then the frequency of the regularized train of pulses has to be within a certain (known) range.

For the following I use two elements already built and tested. The logical OR gate (shown schematically in Fig. 45B) produces an output signal in o_1 if an input signal appears in i_1 or i_2. The interference between the output signal and the input channels is eliminated with a diode-like structure present at the junction of i_1, i_2 and o_1. This shape of the logical OR gate was proposed and confirmed to work in [86]. One more "ready-to-wear" element which is needed is a memory cell (shown in Fig. 45C). It can be used to memorize and regularize a train of up to N pulses if a "N-pulse" ring is applied. The pulses may later be read and/or erased. The structure presented in Fig. 45C was proposed and proven to work in model calculations as well as in real experiments in [87].

A scheme of a single segment of the adding machine is presented in Figure 46A, in which the AND gates based on the cross junction (Fig. 45A) are indicated with squares, while circles stand for the OR gates (Fig. 45B). The structure shown in Fig. 46A is able to add the "numbers" ("0" or "1") appearing in the input channels a_0 and b_0 and memorize the result (in the form of a single pulse) in the memory cell M_0 (thus, a "1-pulse" ring is enough to serve as the cell). If a pulse appears in the input channel a_0 (for simplicity let us write a_0=1), it goes through the cross junction C_1, then the OR gate R_1 and arrives at the cross junction C_2. Here it may meet a pulse coming from b_0. If it happens - both pulses annihilate within C_2 (so no output signal is produced in output channels o_1 and o_2 of C_2 - cf. Fig. 45A). Consequently no input signal appears on the OR gate R_2 and no signal ("0") is memorized in M_0. However, an output signal is initiated in the output channel o_3 of C_2

http://rcin.org.pl

(here the mechanism shown in Fig. 5 is used). This signal goes out of the device through the OR gate R_3 and may by used as an extra input signal for the next segment of the adding machine (e_1). The extra input channel e_0 is not really necessary in the first segment of the adding machine. However, its presence is crucial in all the other segments. An input signal appearing in this channel means that there was an "overflow" when adding the numbers in the previous segment. Such "overflow" signal should be added to a and b input signals in the next segment. The sum between a and e channels is performed in C_1 in exactly the same way as the sum between a_0 and b_0 in C_2. The sum of a and e is then used as one of input signals for C_2, where it is added to b. Using N segments like the one presented in Fig. 46A one is able to calculate the sum of two numbers given in binary representation:

$$a = a_0 + 2 \cdot a_1 + 4 \cdot a_2 + ... + 2^{N-1} \cdot a_{N-1} \tag{3.1}$$

plus

$$b = b_0 + 2 \cdot b_1 + 4 \cdot b_2 + ... + 2^{N-1} \cdot b_{N-1} \tag{3.2}$$

gives

$$M = M_0 + 2 \cdot M_1 + 4 \cdot M_2 + ... + 2^{N-1} \cdot M_{N-1} + 2^N \cdot e_N \tag{3.3}$$

where all the a_i, b_i, $M_i \in \{0, 1\}$.

A single segment of the counter of pulses propagating in a signal channel is presented in Fig. 46B. Before counting the original train of pulses should be collected on a "N-pulse" storage ring (like the one shown in Fig. 45C). Thus, the counter is able to count up to N pulses. Once the train is regularized, it may be read from the ring and put as the input signal i_0 to the first segment of the counter. The signal travels through the OR gate R_1 and arrives at the passive barrier B. The width of the barrier should be properly adjusted to eliminate every second of the incoming pulses from the train (it is possible

http://rcin.org.pl

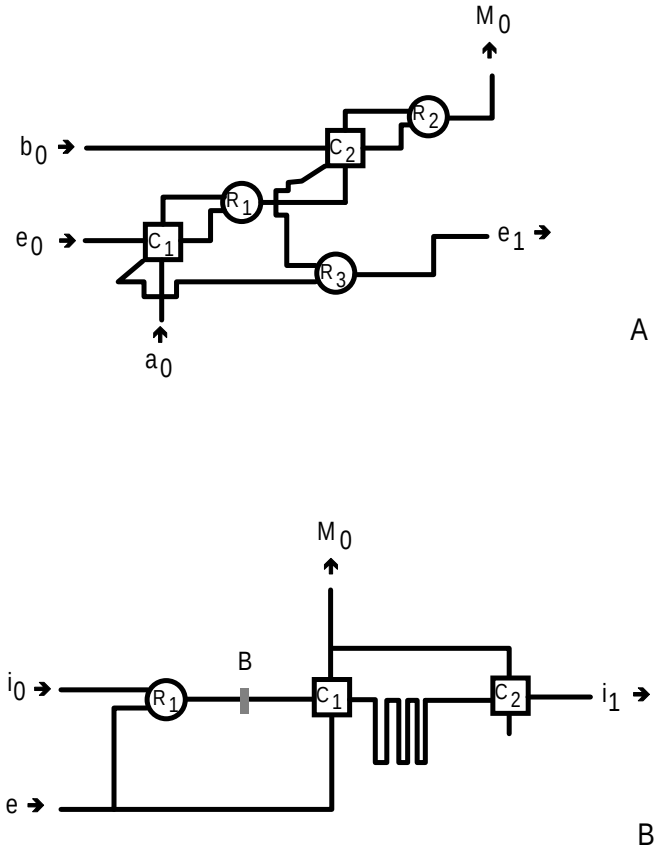

Figure 46. Advanced direct information processing reactors. A - a single segment of the adding machine. B - a single segment of the counter. Squares symbolize logical AND gates based on the cross junction (cf. Fig. 45A), circles stand for the logical OR gates (cf. Fig. 45B). Lines mark the signal paths and arrows indicate the direction of propagation of pulses. The gray vertical interval in Fig. 46B marks the passive barrier.

http://rcin.org.pl

because one is able to specify the range of frequencies of the regularized input signal). Let us also assume that the barrier's width is set below the penetration depth for a single pulse, so that the first pulse from the incoming train is always able to cross the barrier. If there were K pulses in the initial train, then one would get $[K/2]+1$ pulses behind the barrier (where $[p]$ stands for the "floor" function, ie. the greatest integer number not greater than p). It is very important to check whether the initial number of pulses K was odd or even. This may be achieved by putting one more pulse of excitation in the channel e, just after the last pulse from the incoming train has arrived at the barrier B. The pulse from e is duplicated. First of its copies goes directly into the cross junction C_1 and the second one goes through the OR gate R_1 and arrives at the barrier B. If K was odd, then the second copy would "die" at the barrier. The first copy would then arrive at C_1 and go through it (in the vertical direction in Fig. 46B). Consequently a pulse would be memorized in the memory cell M_0, indicating that K was odd. Before memorizing, a copy of this signal is produced. This copy is directed to the cross junction C_2, where it should be used to "kill" the *first* of the pulses which previously passed through the barrier B (this is achievable if a proper difference in lengths of signal paths is provided). If K was even, then the second copy of e would cross the barrier and annihilate together with the first copy at the junction C_1 (again, a proper difference of lengths of signal paths has to be provided). In this case no pulse would be memorized in the memory cell M_0, indicating that K was even and none of the pulses which previously passed through the barrier would be "killed" at C_2. Anyway, the train of pulses going out of C_2 (in the horizontal direction), should be regularized (with a storage ring) and used as the input train for the next segment of the counter (i_1). The procedure should be iterated until all the pulses from the *original*

http://rcin.org.pl

train (i_0) are eliminated. At his moment one gets the binary representation of K in the memory cells M_0, M_1, M_2 etc.

$$K = M_0 + 2 \cdot M_1 + 4 \cdot M_2 + ... \tag{3.4}$$

In case of the counter, we are not interested in the output signals which may appear in the diagonal channels of C_1 or C_2 (cf. Fig. 45A) when two pulses coming from perpendicular directions annihilate within the junction. Last but not least, it is worth mentioning that alternative structures of counters of pulses have already been proposed by J. Górecki, K. Yoshikawa and Y. Igarashi [135].

The adding machine and the counter would work properly if lengths of signal paths between their elements are chosen properly (so that the pulses would coincide in desired places at desired moments).

http://rcin.org.pl

Chapter 4

Conclusions.

The main purpose of this work was to study chemical reactors, composed of active and passive areas, from the point of view of their applications to direct processing of information in the form of chemical signals.

Several types of two dimensional reactors have been studied. They include the cross junction (Section 2.3), the passive barrier (Section 2.4) and the ring (Section 2.5). All these structures have turned out to be useful in direct processing of chemical signals and thus the information that these signals may carry. The junction can be applied as a logical AND gate (coincidence detector of two pulses) or as a switch of the direction of propagation of a single pulse. It works for both FitzHugh - Nagumo and Rovinsky - Zhabotinsky models.

Propagation of single excitable pulses as well as trains of such pulses through a passive barrier has been studied. It has been found that the barrier is able to systematically eliminate pulses from a train. Consequently, it can be used to divide the number of pulses in the train by a desired integer number. The mechanisms of elimination have been discovered to be different in the FitzHugh - Nagumo model and the Rovinsky - Zhabotinsky model,

http://rcin.org.pl

in their forms and for the values of parameters used in this work (Eqs. (2.1 - 2.4) and (2.5 - 2.8) respectively). However, it is not certain whether the observed differences come as the result of different parameters used, or is there a generic difference between the models. On the other hand, the fact that the elimination has been observed for three different models (FH-N, R-Z and the Oregonator) suggests that the phenomenon might be typical for all excitable systems, especially because it appears in the "naive" model presented in Section 1.2.2. The phenomenon of systematical elimination of pulses from a train has turned out to be crucial for several signal processing devices (such as the chemical diode, logical gates etc.) previously proposed by other researchers, as well as for the cross junction proposed here (Section 2.4.7). The results concerning stability of pulses on a ring may be important when such rings are used as memory cells.

The numerical results concerning frequency transformations of regular trains of pulses by a passive barrier (Section 2.4) have been confirmed experimentally. The results of experiments described in Section 2.7 are in excellent qualitative agreement with the numerical predictions. In particular, frequency transformations corresponding to f_o/f_p=1, 2/3, 1/2 and 0 have been observed. These experimental observations are only some examples confirming the numerical results obtained. They imply that the Rovinsky - Zhabotinsky model used in this work describes pretty well systems based on the ferroin catalyzed BZ reaction. This conclusion is further supported by results of other experiments with chemical diodes (mentioned in Section 2.4.7) and with passive barriers (eg. [70]).

Two complex devices performing nontrivial operations, ie. adding two numbers or counting the pulses in a channel, have been proposed (Chapter 3). Both of them utilize the basic signal processing elements, like the cross

http://rcin.org.pl

junction and the passive barrier (discussed in this work) or the memory cell and the logical OR gate (known from the literature). The construction of the adding machine and the counter seems feasible, although it does not have to be easy.

One final word of conclusion, coming from the last two paragraphs, is that once quite advanced information processing devices have been proposed and the model, within which these devices were "born", properly describes real chemical reactors (as the experiments suggest), we should expect to find such systems applied, for example in new generations of "intelligent" materials or medicaments. Maybe in not so distant future.

http://rcin.org.pl

Bibliography

[1] J. D. Murray, *Mathematical Biology* (Springer Verlag, New York, USA, 1993).

[2] T. Tlaczala, Wiadomosci Chemiczne **38** 219 (1984) (in Polish).

[3] A. L. Kawczynski, *Reakcje chemiczne - od rownowagi przez struktury dyssypatywne do chaosu* (Wydawnictwa Naukowo - Techniczne, Warsaw, Poland, 1990) (in Polish).

[4] M. Orlik, *Reakcje oscylacyjne - porzadek i chaos* (Wydawnictwa Naukowo - Techniczne, Warsaw, Poland, 1996) (in Polish).

[5] A. L. Lehninger, *Biochemie* (Verlag Chemie, Weinheim, Germany, 1979) (in German).

[6] O. Gurel and D. Gurel, *Types of Oscillations in Chemical Reactions* (Akademie - Verlag, Berlin, Germany, 1984).

[7] D. Gurel and O. Gurel, *Recent Developments in Chemical Oscillations* (Akademie - Verlag, Berlin, Germany, 1984).

[8] W. C. Bray, J. Am. Chem. Soc. **43**, 1262 (1921).

[9] B. P. Belousov, *Sbornik referatov po radiacjonnoj medicynie za 1958 g.* (Medgiz, Moscow, USSR, 1959), p. 145 (in Russian).

http://rcin.org.pl

[10] A. Zaikin and A. M. Zhabotinsky, Nature **225**, 535 (1970).

[11] A. M. Zhabotinsky, *Koncentracjonnyje avtokolebanija* (Nauka, Moscow, USSR, 1974) (in Russian).

[12] A. M. Turing, Phil. Trans. Roy. Soc. London **B237**, 37 (1952).

[13] B. Rudovics, J.-J. Perraud, P. De Kepper and E. Dulos, *Turing Structures and Wave Patterns in The Cima Reaction* in *Far-from-equilibrium Dynamics of Chemical Systems - Proceedings of The Third Interantional Symposium*, J. Górecki, A. S. Cukrowski, A. L. Kawczynski and B. Nowakowski, Ed. (World Scientific, Singapore 1994), p. 101.

[14] G. Dewel, P. Brockmans and A. De Wit, *Interaction of Hopf and Turing Instabilities in Chemical Systems* in *Far-from-equilibrium Dynamics of Chemical Systems - Proceedings of The Third Interantional Symposium*, J. Górecki, A. S. Cukrowski, A. L. Kawczynski and B. Nowakowski, Ed. (World Scientific, Singapore 1994), p. 95.

[15] A. T. Winfree and S. H. Strogatz, Nature **311**, 611 (1984).

[16] V. S. Zykov, *Modelirovanije volnovych processov v vozbudimych sredach* (Nauka, Moscow, USSR, 1984) (in Russian).

[17] V. N. Biktashev, Physica D **36**, 167 (1989).

[18] V. N. Biktashev, Physica D **40**, 83 (1989).

[19] T. Yamaguchi and S. C. Mueller, Physica D **49**, 40 (1991).

[20] V. S. Zykov and S. C. Mueller, Physica D **97**, 322 (1996).

[21] R. R. Aliev, T. Amemiya and T. Yamaguchi, Chem. Phys. Lett. **257**, 552 (1996).

http://rcin.org.pl

[22] M. Vinson, S. Mironov, S. Mulvey and A. Pertsov, Nature **386**, 477 (1997).

[23] O. Steinbock, Phys. Rev. Lett. **78**, 745 (1997).

[24] T. Amemiya, P. Kettunen, S. Kadar, T. Yamaguchi and K. Showalter, Chaos **8**, 872 (1998).

[25] M. Vinson and A. Pertsov, Phys. Rev. E **59**, 2764 (1999).

[26] H. Henry and V. Hakim, Phys. Rev. Lett. **85**, 5328 (2000).

[27] V. A. Davydov, N. Manz, O. Steinbock, V. S. Zykov and S. C. Mueller, Phys. Rev. Lett. **85**, 868 (2000).

[28] V. Perez-Munuzuri, F. Sagues and J. M. Sancho, Phys. Rev. E **62**, 94 (2000).

[29] A. L. Kawczynski and B. Legawiec, Phys. Rev. E **64**, 056202-1 (2001).

[30] A. Guderian, A. F. Muenster, M. Kraus and F. W. Schneider, J. Phys. Chem. A **102**, 5059 (1998).

[31] A. Guderian, A. F. Muenster, M. Jinguji, M. Kraus and F. W. Schneider, Chem. Phys. Lett. **312**, 440 (1999).

[32] R. Stoessel and A. F. Muenster, Chem. Phys. Lett. **263**, 789 (1996).

[33] A. P. Munuzuri, M. Dolnik, A. M. Zhabotinsky and I. R. Epstein, J. Am. Chem. Soc. **121**, 8065 (1999).

[34] A. K. Horvath, M. Dolnik, A. P. Munuzuri, A. M. Zhabotinsky and I. R. Epstein, Phys. Rev. Lett. **83**, 2950 (1999).

[35] S. Kadar, J. Wang and K. Showalter, Nature **391**, 770 (1998).

http://rcin.org.pl

[36] P. E. Strizhak, A. B. Basylchuk, I. Demjanchyk, F. Fecher, F. W. Schneider and A. F. Muenster, Phys. Chem. Chem. Phys. **2**, 4721 (2000).

[37] P. E. Strizhak, I. Demjanchyk, F. Fecher, F. W. Schneider and A. F. Muenster, Angew. Chem. Int. Ed. **39**, 4573 (2000).

[38] M. Baer, N. Gottschalk, M. Eiswirth and G. Ertl, J. Phys. Chem. **100**, 1202 (1994).

[39] M. Baer, A. K. Bangia, I. G. Kevrekidis, G. Haas, H. H. Rotermund and G. Ertl, J. Phys. Chem. **100**, 19106 (1996).

[40] N. Hartmann, M. Baer, I. G. Kevrekidis, K. Krischer and R. Imbihl, Phys. Rev. Lett. **76**, 1384 (1996).

[41] S. Trinh and D. Ramkrishna, Ind. Eng. Chem. Res. **37**, 2232 (1998).

[42] R. J. Field, E. Körös and R. M. Noyes, J. Am. Chem. Soc. **94**, 8649 (1972).

[43] R. J. Field and R. M. Noyes, J. Chem. Phys. **60**, 1877 (1974).

[44] A. B. Rovinsky and A. M. Zhabotinsky, J. Phys. Chem. **88**, 6081 (1984).

[45] A. B. Rovinsky, J. Phys. Chem. **90**, 217 (1986).

[46] R. R. Aliev and A. B. Rovinsky, J. Phys. Chem. **96**, 732 (1992).

[47] G. Nicolis and J. Portnow, Chem. Rev. **73**, 365 (1973).

[48] R. R. Aliev, Chaos, Solitons and Fractals, **5**, 567 (1995).

[49] V. N. Biktashev and A. V. Holden, Chaos **8**, 48 (1998).

http://rcin.org.pl

[50] F. Xie, Z. Qu and A. Garfinkel, Phys. Rev. E **58**, 6355 (1998).

[51] Z. Qu, J. N. Weiss and A. Garfinkel, Phys. Rev. E **61**, 727 (2000).

[52] Y. Nagai, H. Gonzalez, A. Shrier and L. Glass, Phys. Rev. Lett. **84**, 4248 (2000).

[53] P. Coullet, D. Daboussy and J. R. Tredicce, Phys. Rev. E **58**, 5347 (1998).

[54] R. FitzHugh, Biophysics J. **1**, 445 (1961).

[55] J. Nagumo, S. Arimoto and S. Yoshizawa, Proc. IRE **50**, 2061 (1962).

[56] A. L. Hodgkin and A. F. Huxley, J. Physiol. **117**, 500 (1952).

[57] R. J. Field and M. Burger, Eds. *Oscillations and Travelling Waves in Chemical Systems* (Wiley, New York, USA, 1985).

[58] A. Malevanets and R. Kapral, Phys. Rev. E **55**, 5657 (1997).

[59] L. Hegedus, N. Kirchner, M. Wittmann, P. Simon, Z. Noszticzius, T. Amemiya, T. Ohomori and T. Yamaguchi, Chaos **9**, 283 (1999).

[60] R. Yoshida, E. Kokufuta and T. Yamaguchi, Chaos, **9**, 260 (1999).

[61] K. Miyakawa, F. Sakamoto, R. Yoshida, E. Kokufuta and T. Yamaguchi, Phys. Rev. E **62**, 793 (2000).

[62] R. Yoshida, M. Tanaka, S. Onodera, T. Yamaguchi and E. Kokufuta, J. Phys. Chem. A **104**, 7549 (2000).

[63] R. Yoshida, G. Otoshi, T. Yamaguchi and E. Kokufuta, J. Phys. Chem. A **105**, 3667 (2001).

http://rcin.org.pl

[64] See eg. J. Wiersig and Kang-Hun Ahn, Phys. Rev. Lett. **87**, 026803-1 (2001); M. Brons, P. Gross and K. Bar-Eli, Int. J. Bif. Chaos **7**, 2621 (1997) or T. Gilbert and R. W. Gammon, Int. J. Bif. Chaos **10**, 155 (2001).

[65] M. Dolnik, I. Finkeova, I. Schreiber and M. Marek, J. Phys. Chem. **93**, 2764 (1989).

[66] I. Finkeova, M. Dolnik, B. Hrudka and M. Marek, J. Phys. Chem. **94**, 4110 (1990).

[67] M. Dolnik and M. Marek, J. Phys. Chem. **95**, 7267 (1991).

[68] M. Dolnik, M. Marek and I. R. Epstein, J. Phys. Chem. **96**, 3218 (1992).

[69] A. Toth, V. Gaspar and K. Showalter, J. Phys. Chem. **98**, 522 (1994).

[70] K. Suzuki, T. Yoshinobu and H. Iwasaki, J. Phys. Chem. A **104**, 5154 (2000).

[71] P. Parmananda, H. Mahara, T. Amemiya and T. Yamaguchi, Phys. Rev. Lett. **87**, 238302-1 (2001).

[72] P. Ball, Nature **406**, 118 (2000).

[73] A. Hjelmfelt, F. W. Schneider and J. Ross, Science **260**, 335 (1993).

[74] M. Okamoto, Y. Maki, T. Sekiguchi and S. Yoshida, Physica D **84**, 194 (1995).

[75] A. Hjelmfelt and J. Ross, J. Phys. Chem. **97**, 7988 (1993).

[76] A. Hjelmfelt and J. Ross, Physica D **84**, 180 (1995).

http://rcin.org.pl

[77] L. Kuhnert, K. I. Agladze and V. I. Krinsky, Nature **337**, 244 (1989).

[78] R. R. Aliev, J. Phys. Chem. **98**, 3999 (1994).

[79] N. G. Rambidi and A. V. Maximychev, BioSystems **41**, 195 (1997).

[80] N. G. Rambidi and D. Yakovenchuk, Phys. Rev. E **63**, 026607 (2001).

[81] A. Toth and K. Showalter, J. Chem. Phys. **103**, 2058 (1995).

[82] O. Steinbock, P. Kettunen and K. Showalter, J. Phys. Chem. **100**, 18970 (1996).

[83] K. Agladze, R. R. Aliev, T. Yamaguchi and K. Yoshikawa, J. Phys. Chem. **100**, 13895 (1996).

[84] T. Kusumi, T. Yamaguchi, R. R. Aliev, T. Amemiya, T. Ohmori, H. Hashimoto and K. Yoshikawa, Chem. Phys. Letters **271**, 355 (1997).

[85] K. Yoshikawa, I. Motoike and K. Kajiya, IEICE Trans. Electron. **E80-C**, 931 (1997).

[86] I. N. Motoike and K. Yoshikawa, Phys. Rev. E **59**, 5354 (1999).

[87] I. N. Motoike, K. Yoshikawa, Y. Iguchi and S. Nakata, Phys. Rev. E **63**, 036220 (2001).

[88] D. Winston, M. Arora, J. Maselko, V. Gaspar and K. Showalter, Nature **351**, 132 (1991).

[89] A. Lazar, Z. Noszticzius, H. D. Forsterling and Z. Nagy-Ungvarai, Physica D **84**, 112 (1995).

[90] A. Lazar, H. D. Forsterling, H. Farkas, P. Simon, A. Volford and Z. Noszticzius, Chaos **7**, 731 (1997).

http://rcin.org.pl

[91] A. Volford, Z. Noszticzius, V. Krinsky, C. Dupont, A. Lazar and H. D. Forsterling, J. Phys. Chem. A **102**, 8355 (1998).

[92] J. Ungvarai and Z. Nagy-Ungvarai, Acta Chimica Hungarica - Models in Chemistry **135**, 393 (1998).

[93] A. Volford, P. L. Simon, H. Farkas and Z. Noszticzius, Physica A **274**, 30 (1999).

[94] R. Toth, V. Gaspar, A. Belmonte, M. C. O'Connell, A. Taylor A and S. K. Scott, Phys. Chem. Chem. Phys. **2**, 413 (2000).

[95] M. Seipel, F. W. Schneider and A. F. Munster, Faraday Discussions 120, 395 (2001).

[96] A. P. Munuzuri and V. Perez-Villar, Phys. Rev. Lett. **79**, 1941 (1997).

[97] S. Kadar, T. Amemiya and K. Showalter, J. Phys. Chem. A **101**, 8200 (1997).

[98] A. Guderian, A. F. Munster, M. Jinguji, M. Kraus and F. W. Schneider, Chem. Phys. Lett. **312**, 440 (1999).

[99] K. Agladze, A. Toth, T. Ichino and K. Yoshikawa J. Phys. Chem. A **104**, 6677 (2000).

[100] I. Sendina-Nadal, S. Alonso, V. Perez-Munuzuri, M. Gomez-Gesteira, V. Perez-Villar, L. Ramirez-Piscina, J. Casademunt, J. M. Sancho and F. Sagues, Phys. Rev. Lett. **84**, 2734 (2000).

[101] O. Steinbock, P. Kettunen and K. Showalter, Science **269**, 1857 (1995).

[102] C. Dupont, K. Agladze and V. Krinsky, Physica A **249** 47 (1998).

http://rcin.org.pl

[103] K. Suzuki, T. Yoshinobu and H. Iwasaki, Jpn. J. Appl. Phys. 2 **38**, L345 (1999).

[104] K. Suzuki, T. Yoshinobu and H. Iwasaki, J. Phys. Chem. A **104**, 6602 (2000).

[105] K. Suzuki, T. Yoshinobu and H. Iwasaki, Chem. Phys. Lett. **349**, 437 (2001).

[106] O. Steinbock and P. Kettunen, Chem. Phys. Lett. **251**, 305 (1996).

[107] P. Shah, Y. Kevrekidis and J. Benziger, Langmuir **15**, 1584 (1999).

[108] H. Sevcikova, J. Kosek and M. Marek, J. Phys. Chem. **100**, 1666 (1996).

[109] F. Fecher, F. W. Schneider and A. F. Muenster, J. Phys. Chem. A **104**, 8715 (2000).

[110] B. Linares-Barranco, E. Sanchez-Sinencio, A. Rodriguez-Vazquez and J. L. Huertas, IEEE Journal of Solid-State Circuits **26**, 956 (1991).

[111] J. Sielewiesiuk and J. Górecki, Acta Phys. Pol. B **32**, 1589 (2001).

[112] J. Sielewiesiuk and J. Górecki, *On the numerical simulations of impulses in excitable media*, to appear in GAKUTO International Series on Mathematical Sciences and Applications **17** (2001).

[113] A. Lazar, H. D. Forsterling, A. Volford and Z. Noszticzius, J. Chem. Soc. - Faraday Transactions **92**, 2903 (1996).

[114] M. Woltering, R. Girnus and M. Markus, J. Phys. Chem. A **103**, 4034 (1999).

[115] J. Sielewiesiuk and J. Górecki, J. Phys. Chem. A **105**, 8189 (2001).

http://rcin.org.pl

[116] J. Sielewiesiuk and J. Górecki, J. Phys. Chem. A **106**, 4068 (2002).

[117] J. Sielewiesiuk and J. Górecki, Phys. Chem. Chem. Phys. **4**, 1326 (2002).

[118] M. Frankowicz, A. L. Kawczyński and J. Górecki, J. Phys. Chem. **95**, 1265 (1991).

[119] A. M. Zhabotinsky, F. Buchholtz, A. B. Kiyatkin and I. R. Epstein, J. Phys. Chem. **97**, 7578 (1993).

[120] L. P. Hammett, *Physical Organic Chemistry. Reaction Rates, Equilibria and Mechanisms* (McGraw-Hill, New York, USA, 1970).

[121] B. Legawiec, private communication. See also B. Legawiec and D. Ziolkowski, Inzynieria chemiczna i procesowa **2**, 293 (1988) (in Polish).

[122] A. P. Munuzuri, V. A. Davydov, M. Gomez-Gesteira, V. Perez-Munuzuri and V. Perez-Villar, Phys. Rev. E **54**, R5921 (1996).

[123] S. Fujieda, Y.Mori, A. Nakazawa and Y. Mogami, Adv. Space Res. **28**, 537 (2001).

[124] J. Sielewiesiuk and J. Górecki, *On complex transformation of chemical signals passing through a passive barrier*, Phys. Rev. E (2002), in press.

[125] J. Sielewiesiuk and J. Górecki, *Chemical Waves in an Excitable Medium: Their Features and Possible Applications in Information Processing* in *Attractors, Signals and Synergetics. Proceedings of the 1st European Interdisciplinary School on Nonlinear Dynamics for System and Signal Analysis Euroattractor 2000, Warsaw, June 2000*, Wlodzimierz Klonowski, Ed. (Pabst Science Publishers, Lengerich, Germany 2002), p. 448-460.

http://rcin.org.pl

[126] J. J. Tyson and P. C. Fife, J. Chem. Phys. **73**, 2224 (1980).

[127] J. D. Dockery, J. P. Keener and J. J. Tyson, Physica D **30**, 177 (1988).

[128] R. Toth, A. Papp, V. Gaspar, J. H. Merkin, S. K. Scott and A. F. Taylor, Phys. Chem. Chem. Phys. **3**, 957 (2001).

[129] A. L. Kawczynski, private communication.

[130] J. Farey, Philos. Mag. J. **47**, 385 (1816). This article may be hardly accessible, but a pretty good summary of it can be found at `http://www-groups.dcs.st-andrews.ac.uk/~history/Mathematicians/Farey.html`.

[131] `http://www.cut-the-knot.com/blue/Farey.html` contains a nice explanation of the idea of the Farey tree and Farey series.

[132] Y. Igarashi, K. Yoshikawa and J. Górecki, unpublished results of experiments performed for the Ru-catalyzed BZ reaction at Physics Department, Kyoto University, Kyoto, Japan (2002).

[133] S. Lubkin, Bulletin of Math. Biology **56**, 795 (1994).

[134] B. Schroeder and J. Rudolph (ed.), *Experimente aus der Chemie* (Verlag Chemie, Weinheim, Germany, 1978), p. 132 (*Eine oszillierende Reaktion* by R. J. Field) (in German).

[135] J. Górecki, K. Yoshikawa and Y. Igarashi, *On chemical reactors which can count*, submitted to Journal of Physical Chemistry A (2002).

[136] S. K. Scott, *Oscillations, Waves and Chaos in Chemical Kinetics* (Oxford University Press, Oxford, UK, 1994), p. 27-29.

http://rcin.org.pl

Appendix A

From the Field - Körös - Noyes mechanism of the BZ reaction to the Rovinsky - Zhabotinsky model.

The contents of this part of the dissertation has been published as the supporting material for our publication in the *Journal of Physical Chemistry A* [115]. It is available at `http://pubs.acs.org`.

When I prepared programs for numerical calculations I discovered that many papers which use the Rovinsky - Zhabotinsky model of the ferroin catalyzed Belousov - Zhabotinsky reaction contain simple mistakes in formulas, which may significantly affect the results. Here I provide a step-by-step derivation of the dimensionless Eqs. (2.5-2.8) from the Field - Körös - Noyes (FKN) reaction scheme and give the definitions of the scaling constants.

Let us start from the modified Field - Körös - Noyes [42, 136] mechanism of the Belousov - Zhabotinsky reaction [44] completed by reaction (R13) (in

http://rcin.org.pl

[45]):

$$H^+ + HBrO_3 + HBrO_2 \rightleftarrows HBrO_2^+ + BrO_2\cdot + H_2O \qquad (R1)$$

$$BrO_2\cdot + H^+ \rightleftarrows HBrO_2^+ \qquad (R2)$$

$$Fe(phen)_3^{2+} + HBrO_2^+ \rightleftarrows Fe(phen)_3^{3+} + HBrO_2 \qquad (R3)$$

$$2HBrO_2 \rightarrow HOBr + HBrO_3 \qquad (R4)$$

$$H^+ + Br^- + HBrO_2 \rightarrow 2HOBr \qquad (R5)$$

$$H^+ + Br^- + HOBr \rightleftarrows Br_2 + H_2O \qquad (R6)$$

$$H^+ + Br^- + HBrO_3 \rightarrow HBrO_2 + HOBr \qquad (R7)$$

$$Fe(phen)_3^{3+} + CHBr(COOH)_2 \rightleftarrows Fe(phen)_3^{2+} + H^+ + \cdot CBr(COOH)_2 \qquad (R8)$$

$$H_2O + \cdot CBr(COOH)_2 \rightarrow H^+ + Br^- + \cdot COH(COOH)_2 \qquad (R9)$$

$$HOBr + CHBr(COOH)_2 \rightleftarrows CBr_2(COOH)_2 + H_2O \qquad (R10)$$

$$Br_2 + CHBr(COOH)_2 \rightleftarrows CBr_2(COOH)_2 + H^+ + Br^- \qquad (R11)$$

$$CHBr(COOH)_2 + H_2O \rightarrow CHOH(COOH)_2 + H^+ + Br^- \qquad (R13)$$

We use the notation as in [44]: $A = [HBrO_3]$, $B = [CHBr(COOH)_2]$, $C = [Fe(phen)_3^{2+}] + [Fe(phen)_3^{3+}]$, $R = [\cdot CBr(COOH)_2]$, $U = [HBrO_2^+]$, $X = [HBrO_2]$, $Y = [Br^-]$, $Z = [Fe(phen)_3^{3+}]$, h_0 is the Hammett acidity function [119, 120] and q is the stoichiometric factor. The kinetic equations introduced in [44, 45] read:

$$\frac{\partial X}{\partial t} = -k_1 h_0 AX + k_{-1}U^2 + k_3 U(C-Z) - k_{-3}XZ - 2k_4 h_0 X^2 - k_5 h_0 XY + k_7 h_0 AY \qquad (A1)$$

$$\frac{\partial Y}{\partial t} = -k_5 h_0 XY - k_7 h_0 AY + qk_9 R + k_{13} B \qquad (A2)$$

$$\frac{\partial Z}{\partial t} = k_3 U(C-Z) - k_{-3}XZ - k_8 BZ + k_{-8} h_0 R(C-Z) \qquad (A3)$$

$$\frac{\partial U}{\partial t} = -2k_{-1}U^2 + 2k_1 h_0 AX - k_3 U(C-Z) + k_{-3}XZ \qquad (A4)$$

http://rcin.org.pl

$$\frac{\partial R}{\partial t} = k_8 BZ - k_{-8} h_0 R(C - Z) - k_9 R \qquad (A5)$$

where $k_{\pm i}$ are the rate constants of the corresponding reactions.

These kinetic equations can be simplified. First, let us neglect the term $k_{-1} \cdot U^2$ in Eqs. (A1, A4) (as U is small [44]). Next, assuming that U and R are rapid variables comparing to X, Y and Z, from Eq. (A4) we get:

$$U = \frac{2k_1 h_0 AX + k_{-3} XZ}{k_3(C - Z)} \qquad (A6)$$

and from Eq. (A5):

$$R = \frac{k_8 BZ}{k_{-8} h_0 (C - Z) + k_9} \qquad (A7)$$

In the denominator of the last formula we can neglect k_9, because $k_9 \ll k_{-8} h_0 (C\text{-}Z)$. All these approximations are based on experimental observations, quoted in [44].

Substituting (A6, A7) to (A1 - A3) one obtains:

$$\frac{\partial X}{\partial t} = k_1 h_0 AX - 2k_4 h_0 X^2 - k_5 h_0 XY + k_7 h_0 AY \qquad (A8)$$

$$\frac{\partial Y}{\partial t} = q \frac{K_8 BZ}{h_0(C - Z)} - k_5 h_0 XY - k_7 h_0 AY + k_{13} B \qquad (A9)$$

$$\frac{\partial Z}{\partial t} = 2k_1 h_0 AX - \frac{K_8 BZ}{h_0(C - Z)} \qquad (A10)$$

where

$$K_8 = \frac{k_8 k_9}{k_{-8}} \qquad (A11)$$

Up to this point the procedure presented here is identical as in [44]. Basing on Eqs. (A8 - A10) we derive the dimensionless reaction - diffusion equations for active and passive fields.

http://rcin.org.pl

For the active field we eliminate Y as a fast variable using Eq. (A9) (see [44]) and get:

$$Y = (q\frac{K_8BZ}{h_0(C-Z)} + k_{13}B) \cdot \frac{1}{k_5h_0X + k_7h_0A} \quad (A12)$$

which can be substituted to Eqs. (A8) and (A10). It follows that:

$$\frac{\partial X}{\partial t} = k_1h_0AX - 2k_4h_0X^2 - (\frac{k_5X - k_7A}{k_5X + k_7A}) \cdot (q\frac{K_8BZ}{h_0(C-Z)} + k_{13}B) \quad (A13)$$

$$\frac{\partial Z}{\partial t} = 2k_1h_0AX - \frac{K_8BZ}{h_0(C-Z)} \quad (A14)$$

In the passive field we have $Z{=}C{\equiv}0$ and so $R{\equiv}0$. This reduces Eqs. (A8 - A9) to:

$$\frac{\partial X}{\partial t} = -2k_4h_0X^2 - k_5h_0XY + k_7h_0AY \quad (A15)$$

$$\frac{\partial Y}{\partial t} = -k_5h_0XY - k_7h_0AY + k_{13}B \quad (A16)$$

Once again the fast variable Y is eliminated. From (A16) we receive:

$$Y = \frac{k_{13}B}{k_5h_0X + k_7h_0A} \quad (A17)$$

and after substitution to (A15) we end up with the following kinetics for the passive field:

$$\frac{\partial X}{\partial t} = -2k_4h_0X^2 - \frac{k_5X - k_7A}{k_5X + k_7A}k_{13}B \quad (A18)$$

$$Z \equiv 0 \quad (A19)$$

In our model the activator X diffuses, while the catalyst Z is immobilized. Thus, we add the diffusion of X to the kinetic equations (A13-A14) for the active and (A18 - A19) for the passive regions and get:

$$\frac{\partial X}{\partial t} = k_1h_0AX - 2k_4h_0X^2 - (\frac{k_5X - k_7A}{k_5X + k_7A}) \cdot (q\frac{K_8BZ}{h_0(C-Z)} + k_{13}B) + D_X\nabla_r^2X \quad (A20)$$

http://rcin.org.pl

$$\frac{\partial Z}{\partial t} = 2k_1 h_0 AX - \frac{K_8 BZ}{h_0(C-Z)} \tag{A21}$$

for the active field and

$$\frac{\partial X}{\partial t} = -2k_4 h_0 X^2 - \frac{k_5 X - k_7 A}{k_5 X + k_7 A} k_{13} B + D_X \nabla_r^2 X \tag{A22}$$

$$Z \equiv 0 \tag{A23}$$

for the passive one.

If one introduces dimensionless variables x, z, τ and ρ, so that

$$X = \frac{k_1 A}{2k_4} x \tag{A24}$$

$$Z = Cz \tag{A25}$$

$$t = \frac{k_4 C}{k_1^2 A^2 h_0} \tau \tag{A26}$$

$$r = \sqrt{\frac{k_4 C}{h_0}} \cdot \frac{1}{k_1 A} \cdot \sqrt{D_X} \cdot \rho \tag{A27}$$

and coefficients:

$$\alpha = \frac{k_4 K_8 B}{k_1^2 A^2 h_0^2} \tag{A28}$$

$$\beta = \frac{2k_4 k_{13} B}{k_1^2 A^2 h_0} \tag{A29}$$

$$\mu = \frac{2k_4 k_7}{k_1 k_5} \tag{A30}$$

$$\epsilon = \frac{k_1 A}{k_4 C} \tag{A31}$$

then Eqs. (A20 - A21) and (A22 - A23) turn into:

$$\frac{\partial x}{\partial \tau} = \frac{1}{\epsilon}[x(1-x) - (2q\alpha \frac{z}{1-z} + \beta)\frac{x-\mu}{x+\mu}] + \nabla_\rho^2 x \tag{A32}$$

$$\frac{\partial z}{\partial \tau} = x - \alpha \frac{z}{1-z} \tag{A33}$$

for the active medium and

$$\frac{\partial x}{\partial \tau} = -\frac{1}{\epsilon}[x^2 + \beta \frac{x-\mu}{x+\mu}] + \nabla_\rho^2 x \tag{A34}$$

http://rcin.org.pl

$$z \equiv 0 \qquad (A35)$$

for the passive medium. Eqs. (A32 - A33) and (A34 - A35) are identical with Eqs. (2.5-2.6) and (2.7-2.8) in Section 2.1.2, respectively.

Now let me point out the differences between my results and the other papers. The scaling of time (Eq. (A27)) and definition of β (Eq. (A29)) differ from those given in [44, 45] by the factor h_0 in the denominator, although the remaining scaling constants (Eqs. (A24), (A25), (A28), (A30), (A31)) and the reaction - diffusion equations (A32 - A33) are identical with those given in [44, 45].

The Rovinsky - Zhabotinsky model was also used by Kusumi et. al. in [84]. Their kinetic equations for the active field are identical with (A32 - A33), however the definition of μ they give differs from (A30) by the factor of 2 and the scaling of ρ is different from (A27) by the factor $h_0^{1/2}$ in the denominator. The passive medium in [84] is described by kinetic equations simpler than (A34 - A35). The simpler equations were however not sufficient for my study, because for the values of parameters considered in this work they lead to excitations of active areas at the boundary of active and passive media.

http://rcin.org.pl

Appendix B

Integration schemes used.

Let us consider a reaction - diffusion equation in one dimension in the most general form (B1):

$$\frac{\partial c}{\partial t} = D\frac{\partial^2 c}{\partial x^2} + r(c) \qquad (B1)$$

where c is the concentration of a chemical reagent, t and x are the time and space variables respectively, D stands for the diffusion coefficient of the reagent and *r(c)* is the kinetic term, describing the chemical reaction.

Let us assume that the values of c are discretized on a grid. Let us denote the current value of c at the *i-th* grid point (i=0,1,...,n,n+*1*) by ${c_i}^0$ (known) and the corresponding value after time dt by ${c_i}^t$ (unknown). Let us assume that the grid is uniform and the distance between consecutive grid points is *dx*.

In general ${c_i}^t$ can be calculated as:

$$c_i^t = c_i^0 + \Delta c_i + dt \cdot D\frac{\partial^2 c}{\partial x^2}|_i \qquad (B2)$$

where Δc_i corresponds to the change of c at the *i-th* grid point due to the chemical reaction.

In the Euler explicit method the calculations of ${c_i}^t$ are fully based on the

http://rcin.org.pl

current state of the system ${c_i}^0$. Consequently:

$$c_i^t = c_i^0 + dt \cdot r(c_i^0) + dt \cdot D\frac{\partial^2 c}{\partial x^2}|_i \qquad (B3)$$

where:

$$\frac{\partial^2 c}{\partial x^2}|_i = \frac{c_{i+1}^0 + c_{i-1}^0 - 2 \cdot c_i^0}{(dx)^2} \qquad (B4)$$

In the Crank - Nicolson method the diffusion term is approximated as:

$$\frac{\partial^2 c}{\partial x^2}|_i = \frac{1}{2}[\frac{c_{i+1}^0 + c_{i-1}^0 - 2 \cdot c_i^0}{(dx)^2} + \frac{c_{i+1}^t + c_{i-1}^t - 2 \cdot c_i^t}{(dx)^2}] \qquad (B5)$$

This makes ${c_i}^t$ occur on both sides of Eq. (B2) and shows that the methods based on the Crank - Nicolson discretization of the Laplace operator are implicit methods.

Equation (B2) can be solved with respect to ${c_i}^t$ giving:

$$c_i^t = A_i \cdot c_{i+1}^t + B_i \qquad i = 0, 1, ..., n \qquad (B6)$$

where

$$A_i = \frac{\frac{Ddt}{2(dx)^2}}{1 - \frac{Ddt}{2(dx)^2}(A_{i-1} - 2)} \qquad (B7)$$

$$B_i = \frac{\frac{Ddt}{2(dx)^2}(B_{i-1} + c_{i+1}^0 + c_{i-1}^0 - 2c_i^0) + \Delta c_i + c_i^0}{1 - \frac{Ddt}{2(dx)^2}(A_{i-1} - 2)} \qquad (B8)$$

Additional constraints are imposed on the coefficients A_i, B_i by the boundary conditions used.

In case of no flux boundary conditions we have A_0=1 and B_0=0 (from Eq. (B6), because ${c_0}^t$=${c_1}^t$). Consequently, all the A_i, B_i up to A_n, B_n can be calculated using Eqs. (B7 - B8). At the other boundary of the system, according to Eq. (B6) we have:

$$c_n^t = A_n \cdot c_{n+1}^t + B_n \qquad (B9)$$

http://rcin.org.pl

but due to no flux boundary conditions ${c_n}^t = {c_{n+1}}^t$, so:

$$c_{n+1}^t = \frac{B_n}{1 - A_n} \qquad (B10)$$

Having ${c_{n+1}}^t$, the values of ${c_i}^t$ for i=n,n-*1*,...,1,0 can be calculated by back-substitution, using Eq. (B6).

In case of periodic boundary conditions, one has to solve a more complicated set of equations:

$$c_0^t = A_0 \cdot c_1^t + B_0 \qquad (B11a)$$

$$c_1^t = A_1 \cdot c_2^t + B_1 \qquad (B11b)$$

.....

$$c_{n-1}^t = A_{n-1} \cdot c_n^t + B_{n-1} \qquad (B11c)$$

$$c_n^t = c_0^t \qquad (B11d)$$

$$A_0 = A_1 = ... = A_{n-1} \qquad (B11e)$$

Equations (B11d - B11e) come directly as the consequence of the periodic boundary conditions (B11d) and the fact that in this case no grid point on the interval is distinguished (B11e).

In Section 2.4.1 a modification of the implicit method just described is mentioned. Instead of a uniform (equally spaced) grid, an adaptive grid is used. The adaptive grid is characterized by a smaller distance between consecutive grid points within and near the passive barrier and longer one far from the barrier. Let us denote the space step to the left from the *i-th* grid point (ie. the distance between nodes no. *i-1* and *i*) by dx_{i-1} and the space step to the right from the *i-th* grid point (ie. the distance between nodes *i* and *i+1*) by dx_i.

http://rcin.org.pl

Then the Laplace operator is given by Equation (B12):

$$\frac{\partial^2 c}{\partial x^2}|_i = \frac{1}{2}\cdot\frac{2}{dx_{i-1}+dx_i}[(\frac{c^0_{i-1}}{dx_{i-1}}+\frac{c^0_{i+1}}{dx_i}-\frac{dx_{i-1}+dx_i}{dx_{i-1}dx_i}c^0_i)+(\frac{c^t_{i-1}}{dx_{i-1}}+\frac{c^t_{i+1}}{dx_i}-\frac{dx_{i-1}+dx_i}{dx_{i-1}dx_i}c^t_i)] \quad (B12)$$

Equation (B6) holds and consequently the coefficients A_i, B_i have more complicated forms:

$$A_i = \frac{\frac{Ddt}{dx_{i-1}+dx_i}\cdot\frac{1}{dx_i}}{1-\frac{Ddt}{dx_{i-1}+dx_i}(\frac{A_{i-1}}{dx_{i-1}}-\frac{1}{dx_i}-\frac{1}{dx_{i-1}})} \quad (B13)$$

$$B_i = \frac{\frac{Ddt}{dx_{i-1}+dx_i}(\frac{c^0_{i+1}-c^0_i}{dx_i}+\frac{c^0_{i-1}-c^0_i}{dx_{i-1}}+\frac{B_{i-1}}{dx_{i-1}})+\Delta c_i + c^0_i}{1-\frac{Ddt}{dx_{i-1}+dx_i}(\frac{A_{i-1}}{dx_{i-1}}-\frac{1}{dx_i}-\frac{1}{dx_{i-1}})} \quad (B14)$$

The kinetic term Δc_i, present in Eqs. (B8, B14), can be calculated in many ways. For the purpose of this work, the well established Runge - Kutta method of the fourth order has been used. For computations in two dimensions (eg. the cross junction - Section 2.3, the rings - Section 2.5 and the pinwheels - Section 2.6) the implicit method presented here has been applied to individual rows of the two dimensional grid and then the procedure has been iterated to obtain self-consistency between the rows.

The explicit Euler method becomes unstable when $\frac{Ddt}{(dx)2} > \frac{1}{2}$, so for a fine grid a very short time integration step is required, whereas the implicit method is stable for all values of *dx* and *dt*.

http://rcin.org.pl

Appendix C

List of publications by the author.

The thesis is based on the following publications by the author:

1. J. Sielewiesiuk and J. Górecki, *Chemical impulses in the perpendicular junction of two channels*, Acta Physica Polonica B **32**, 1589 (2001).

2. J. Sielewiesiuk and J. Górecki, *On the logical function of a cross junction of excitable chemical media*, Journal of Physical Chemistry A **105**, 8189 (2001).

3. J. Sielewiesiuk and J. Górecki, *On the numerical simulations of impulses in excitable media*, to appear in GAKUTO International Series on Mathematical Sciences and Applications **17** (2001).

4. J. Sielewiesiuk and J. Górecki, *Chemical Waves in an Excitable Medium: Their Features and Possible Applications in Information Processing* in *Attractors, Signals and Synergetics. Proceedings of the 1st European Interdisciplinary School on Nonlinear Dynamics for System and*

http://rcin.org.pl

Signal Analysis Euroattractor 2000, Warsaw, June 2000, Wlodzimierz Klonowski, Ed. (Pabst Science Publishers, Lengerich, 2002), p. 448-460.

5. J. Sielewiesiuk and J. Górecki, *Passive barrier as a transformer of "chemical signal" frequency*, Journal of Physical Chemistry A **106**, 4068 (2002).

6. J. Sielewiesiuk and J. Górecki, *On the response of simple reactors to regular trains of pulses*, Physical Chemistry Chemical Physics **4**, 1326 (2002).

7. J. Sielewiesiuk and J. Górecki, *On complex transformation of chemical signals passing through a passive barrier*, Physical Review E (2002), in press.

http://rcin.org.pl

Appendix D

Conferences and seminars.

The material contributing to the thesis was presented during the following conferences and seminars:

1. International workshop *Reaction-diffusion equations and travelling waves*, Stefan Banach International Mathematical Center, Warsaw, Poland, 15-26.05.2000; presentation: J. Górecki and J. Sielewiesiuk, *Chemical waves on a ring.*

2. 1st European Interdisciplinary School on Nonlinear Dynamics for System and Signal Analysis *Euroattractor 2000*, Institute of Biocybernetics and Biomedical Engineering, Polish Academy of Science, Warsaw, Poland, 09-16.06.2000; presentation: J. Sielewiesiuk and J. Górecki, *Chemical waves in an excitable medium: their features and possible applications in information processing.*

3. Marian Smoluchowski International Symposium on Statistical Physics: Fundamentals and Applications, Zakopane, Poland, 10-17.09.2000; poster: J. Sielewiesiuk and J. Górecki, *Chemical impulses in the perpendicular junction of two channels formed of excitable and diffusion media.*

http://rcin.org.pl

4. Institute of Physical Chemisty, Polish Academy of Sciences, Warsaw, Poland, 09.11.2000. Condensed Matter Group Seminar: *Bezposrednie przetwarzanie informacji w nieliniowych ukladach chemicznych* (in Polish).

5. 2nd Polish-Japanese Days on Mathematical Aspects of Modelling Structure Formation Phenomena, Interdisciplinary Center for Mathematical and Computational Modelling, Warsaw University and Stefan Banach International Mathematical Center, Bedlewo, Poland, 19-26.11.2000; presentation: J. Sielewiesiuk and J. Górecki, *On an application of a chemical reactor for direct information processing.*

6. Institute of Physical Chemisty, Polish Academy of Sciences, Warsaw, Poland, 16.05.2001. PhD Student Seminar: *Przyklady zastosowania pobudliwych ukladow chemicznych do bezposredniego przetwarzania informacji* (in Polish).

7. Faraday Discussion 120, *Nonlinear Chemical Kinetics: Complex Dynamics and Spatiotemporal Patterns*, Royal Society of Chemistry, UMIST, Manchester, Great Britain, 10-12.09.2001; poster: J. Sielewiesiuk and J. Górecki, *On the Direct Processing of a Chemical Signal.*

8. Workshop of the European Science Foundation Programme REACTOR, Leeds, Great Britain, 07-09.09.2001; poster and presentation: J. Sielewiesiuk and J. Górecki, *On the switching properties in a cross junction of chemical excitable media*; poster: J. Sielewiesiuk and J. Górecki, *On the filtering properties of a passive gap in a chemical excitable medium.*

9. Institute of Physical Chemisty, Polish Academy of Sciences, Warsaw,

http://rcin.org.pl

Poland, 22.10.2001. Chemical Dynamics Group Seminar: *Odpowiedzi prostych reaktorow na periodyczne pobudzenia* (in Polish).

10. Institute of Physical Chemistry, University of Wuerzburg, Wuerzburg, Germany, 14.03.2002. Seminar: *On the direct processing of a chemical signal.*

11. Institute of Physical Chemisty, Polish Academy of Sciences, Warsaw, Poland, 22.04.2002. Chemical Dynamics Group Seminar: *Transformacje czestosci sygnalow chemicznych: teoria i eksperyment* (in Polish).

http://rcin.org.pl

Appendix E

Contents of the CD-ROM.

The CD-ROM contains supporting material for the PhD thesis. It has the following structure:

readme.htm - table of contents of the CD-ROM.

thesis.pdf - the full version of the PhD thesis in PDF format.

Experiments - films showing selected frequency transforming modes observed in experiments with the ferroin catalyzed Belousov - Zhabotinsky reaction. Double-click the **.BAT** files to see the corresponding films.[1] The file **diode_12.avi** shows malfunction of the chemical diode, observed experimentally by Yasuhiro Igarashi, Kenichi Yoshikawa and Jerzy Górecki at the Department of Physics, Kyoto University, Kyoto, Japan in spring 2002.[2]

Figures - animated extensions of selected figures from the thesis and some additional animations.

[1] Some computers with Windows NT 4.0 Workstation fail to display the films.

[2] Courtesy of the Authors of the experiment.

http://rcin.org.pl

\Extra

\Acrobat - Acrobat Reader 4.05 installation program for Microsoft Windows 95/98/NT/2000/XP. Acrobat Reader is a tool for viewing PDF files. To install it, double-click the **rs405eng.exe** file.

\Cross_junction - a complete web presentation about the cross junction within the FitzHugh - Nagumo model. To start browsing, double-click the **!START.htm** file.

* All documents on the CD-ROM are optimized for viewing with Microsoft Internet Explorer 4.0 or later, in 800x600 (256 colors) full screen display mode. In order to switch to the full screen mode start Internet Explorer and select View >>> Full Screen or just press F11. To switch off the full screen mode press F11 again.

B 347/02

Instytut Chemii Fizycznej Biblioteka P.A.N.

http://rcin.org.pl

Biblioteka Instytutu Chemii Fizycznej PAN
B.347/2002
00000000256605

http://rcin.org.pl